



The University of
Nottingham

UNITED KINGDOM • CHINA • MALAYSIA

**Profiling Autoantibodies in Chronic
Obstructive Pulmonary Disease
using Antigen Microarray
Technology**

By

Reham Shindi

BSc, MSc

Thesis submitted to the University of Nottingham
for the degree of Doctor of Philosophy (PhD)

February 2016

Abstract

Chronic obstructive pulmonary disease (COPD) encompasses the diseases of chronic bronchitis and emphysema, both of which can cause the main feature of this disease; airflow obstruction. COPD is the third leading cause of mortality in the world, and although cigarette smoking is the main risk factor of the disease, other environmental factors and genetic disorders can also play a role. The pathogenesis of COPD is currently still poorly documented, which results in poor diagnosis and treatment for the disease. The involvement of autoimmunity in the pathogenesis of the COPD is becoming more apparent; in recent studies, high levels of circulating autoantibodies have been detected in patients with COPD, suggesting that this lung disorder may have an autoimmune component. Therefore, research has focused on identifying a set of autoantigens known to be associated with other autoimmune disorders that may play a role in the pathogenesis of this disease.

The aim of this study was to develop antigen microarrays for profiling antigen specific-autoantibodies in the serum of patients with COPD, as a diagnostic tool at the early stage of the disease.

To achieve the project aim, we have employed antigen microarrays. Before applying this technique, quality control experiments were performed to optimize the procedure. This included testing different slide surface coatings, investigating numerous blocking buffers and methods to amplify the signal intensities, as well as a series of validity tests to determine if the assay was both accurate and reproducible.

The optimization results showed that a combination of amino-silane coated

slides with I Block buffer and Genisphere amplifier performed well due to the high signal detection and low background observed. Validation for optimized technique was achieved and showed no cross-reactivity occurred, an acceptable limit of the coefficient of variation (CV %), and a significant correlation between ELISA and the antigen microarray platform, with microarray giving a bigger dynamic range of signals. The results for the limit of detection (LOD) were applied and the cut off for a positive autoantibody response was taken from the 95 th percentile of the healthy non-smokers control group.

The results for the investigation of the different 39 autoantigens showed that there was a significant increase in reactivity for both the IgG and IgM autoantibodies in the COPD group compared to the control for CENP-B, collagen5, RNP/sm, La ssb, histone, ro-52 and SCL-70, which suggests these antigens have the potential to be used as diagnostic biomarkers for the detection of COPD. These results also showed that a number of healthy smokers produced an increased reactivity to the same autoantigens as the COPD patients, which suggests there is potential susceptibility of these smokers to develop COPD.

In conclusion, this thesis developed a rapid, inexpensive, broad-spectrum antigen microarray technology, which could have a pivotal future role in the early diagnosis of COPD.

Declaration

The work presented in this thesis was performed between 2012 and the end of 2015 in the School of Life Sciences, University of Nottingham, UK. The work described here is totally my own. This thesis has not been previously submitted for any other degrees.

Reham Shindi February 2016

Acknowledgments

I would like to express my gratitude to my main supervisor Dr. Lucy Fairclough whose expertise, understanding, and patience added considerably to my experience and knowledge. She provided me all her best to find my feet quickly from the first day when I joined the group. My thanks also goes out to my second and third supervisors Dr. Patrick Tighe and Dr. Ian Todd for continued help and guidance. I appreciate their vast knowledge and skills in many areas and their assistance in writing my thesis.

In addition, I would like to thank Dr. Ola Negm for being a good friend and teacher during my study. Also I would like to thank all of the technicians and my colleagues from PhD students especially, my friend Amna Al-mehari, for their help and support.

My huge thanks go to my mum and dad for their continuous encouragement and support, without their love I would not have made it through.

Also I would like to thank my sisters and spirit of my brother who always looking forward to see me the best. My thanks also go to my husband for his support and never forget my lovely children for their patience and their love, which made me strong during my study.

Finally, I would like to thank my government the Kingdom of Saudi Arabia for giving me this opportunity of education and funding my project.

I hope that I made all of you proud of me.

Table of contents

Abstract.....	ii
Declaration	iv
Acknowledgments	v
Table of contents	vi
Table of figures.....	ix
Table of tables	xiii
Abbreviations	xiv
1. General introduction	18
1.1 Chronic obstructive pulmonary disease (COPD)	18
1.1.1. Definition.....	18
1.1.2. Pathogenesis of COPD	19
1.1.3. Smoking risk factors.....	22
1.1.4. Diagnoses and treatment.....	25
1.1.5. Systemic effects of COPD.....	26
1.2 Inflammatory cells and mediators in COPD	28
1.2.1 Innate immune cells.....	28
1.2.1.1 Epithelial cells	28
1.2.1.2 Eosinophils	29
1.2.1.3 Neutrophils	29
1.2.1.4 Macrophages.....	31
1.2.1.5 NK and NKT cells	32
1.2.1.6 Dendritic cells.....	33
1.2.2 Adaptive immune response in COPD.....	33
1.2.2.1 CD8 ⁺ T lymphocytes	33
1.2.2.2 CD4 ⁺ T cells	34
1.2.2.3 B lymphocytes	36
1.3 Autoimmunity in COPD.....	37
1.3.1 Autoantibodies.....	42
1.3.2 Autoantigens in COPD	44
1.4 Enzyme-linked immunosorbent assay (ELISA).....	45
1.5 Microarray Technology	46
1.5.1 Microarray slide surfaces and immobilization	50
1.5.2 Spot size and morphology	52
1.5.3 Signal detection and generation.....	52
1.6 Assay validation	55
1.7 Hypothesis of study	56
1.8 Aims and objectives	56
1.8.1 Aims	56
1.8.2 Objectives.....	56
2. Materials and Methods	57
2.1 Materials:	57
2.1.1 Printing buffer	57
2.1.2 Coating buffer for ELISA.....	57
2.1.3 Blocking buffers	57
2.1.4 Wash buffer (PBS-Tween 0.05 %).....	57
2.1.5 Serum diluent.....	58
2.1.6 Streptavidin CY5	58
2.1.7 Streptavidin infrared dye	58

2.1.8	Streptavidin –HRP conjugated for ELISA	58
2.1.9	Substrate solution for ELISA	58
2.1.10	Sephadex G-25	58
2.1.11	Amplification reagents (Ultrap TM 40-Oyster-650)	58
2.1.12	Slide surfaces for microarray.....	59
2.1.13	Candidate antigens.....	59
2.1.13.1	Antigens for optimisation and validation tests	59
2.1.13.2	Antigens for application	59
2.2	Methods:.....	62
2.2.1	Study population for microarray	62
2.2.2	Study population for ELISA.....	63
2.2.3	Buffer exchange.....	63
2.2.4	Biotinylation method.....	63
2.2.5	The investigation of the binding of patient autoantibodies to candidate antigens	64
2.2.6	Protocol for printing antigens on the slide surface.....	64
2.2.6.1	Process of printed slides	65
2.2.7	Data Analysis.....	66
2.2.8	ELISA Protocol	68
2.2.9	Generating microarray standard curves.....	70
2.2.10	Microarray validation	70
2.2.11	Statistical analysis	70
3.	Optimisation of an Antigen Microarray Platform	72
3.1	Introduction:	72
3.2	Materials and methods:.....	73
3.3	Results:	74
3.3.1	Amino-silane slides	74
3.3.2	Epoxy-silane slides.....	78
3.3.3	Thin film 3D polymer slides (Hydrogel):.....	81
3.3.4	Aldehyde slides	84
3.3.5	Summary of optimisation using the different slide types.....	87
3.3.6	Amplification.....	87
3.3.7	Testing different concentrations of 3DNA amplyfier	87
3.3.8	Measuring the concentration of control antigens at different dilutions of Genisphere amplifier.....	91
3.4	Discussion:	94
3.5	Conclusions:	96
4.	Validation of an Antigen Microarray Platform.....	97
4.1	Introduction:	97
4.2	Materials and methods:.....	99
4.3	Results:	101
4.3.1	Limits of detection.....	101
4.3.2	Reproducibility	103
4.3.3	Assay precision.....	105
4.3.4	Cross-reactivity.....	107
4.3.5	Comparison of microarray technology with ELISA	111
4.3.6	Biotinylation of proteins results	113
4.3.7	Investigation of the binding of patient autoantibodies to the candidate antigens	114
4.4	Discussion:	115

5.	Application of an antigen microarray as a diagnostic platform for COPD	118
5.1	Introduction:	118
5.2	Materials and methods:.....	119
5.3	Results:	122
5.3.1	Age and gender differences between study groups	122
5.3.2	Antigen microarray quality control	122
5.3.3	Levels of IgG-autoantibodies in sera of COPD individuals, non-smoking controls and smoking controls	124
5.3.4	The correlation between IgG autoantibodies levels and FEV-1 % in those with COPD.....	139
5.3.5	Antigen microarray quality control for IgM antibody responses	145
5.3.6	The levels of IgM autoantibodies in sera of COPD individuals, non-smoking controls and smoking controls.....	146
5.3.7	The correlation between IgM autoantibody concentrations and FEV-1 % in those with COPD.....	157
5.3.8	Investigation of potential autoantibodies associations and disease states within the microarray data	163
5.4	Discussion:	173
6.	General Discussion, future work and conclusions	179
6.1	General Discussion	179
6.2	Future work & conclusions	185
6.2.1	Concluding remarks.....	186
7.	References	188

Table of figures

Figure 1. 1: Airflow limitation in COPD.....	19
Figure 1. 2: The pathogenesis of COPD.....	22
Figure 1. 3: The Fletcher-Peto Graph showing the outcomes of smoking cessation.	24
Figure 1. 4: Systemic effects of COPD.	27
Figure 1. 5: Principle of antigen microarray	48
Figure 1. 6: Diagrams show a schematic representation of four different types of the commercial NEXTERION slides.....	51
Figure 1. 7: Methods of detection and signal generation in microarray.....	54
Figure 2. 1: Illustration of the procedure of printing antigens on a slide surface	65
Figure 2. 2: Example of GPR file produced.....	67
Figure 2. 3: Illustrated ELISA method.....	69
Figure 3. 1: Testing Amino-silane slide with different blocking buffers.	76
Figure 3. 2: Analysis results of amino-silane slide:	77
Figure 3. 3: Scanned image of epoxy-silane slide surface with different blocking buffers:.....	79
Figure 3. 4: analysis results of epoxy-silane slide surface:	80
Figure 3. 5: A scanned image of hydrogel slide surface with different blocking buffers:.....	82
Figure 3. 6: Data analysis of thin film 3D slide surface.....	83
Figure 3. 7: Spots morphology of aldehyde- slides with different blocking buffers:.....	85
Figure 3. 8: Data analysis of aldehyde slides surface.....	86
Figure 3. 9: Spots morphology of testing different concentrations of Genisphere amplifier with amino-silane slide:	88
Figure 3. 10: Data analysis of scanned arrays of aminosilane slide for IgG dilution curve at eight dilutions of Genispher amplifier.....	89
Figure 3. 11: Data analysis of scanned arrays of amino-silane slide for control antigens at differen dilutions of Genisphere.....	90

Figure 3. 12: illustrated the interpolation of control antigens on HIgG standard curve at eight dilutions of Genisphere.....	92
Figure 3. 13: concentration of autoantibodies -specific control antigen at eight different dilutions of Genisphere.....	93
Figure 4. 1: Assay limit of detection.	102
Figure 4. 2: Reproducibility of signal detection for antigen microarray	104
Figure 4. 3: precision of three positive control antigens	106
Figure 4. 4: Investigation of cross-reactivity for anti-IgG detection antibody (test 1).....	108
Figure 4. 5: cross-reactivity test with anti-IgG at different dilutions	109
Figure 4. 6: cross-reactivity test of the detection antibodies with and without amplification.....	110
Figure 4. 7: correlation between ELISA and microarray methods.....	112
Figure 4. 8: Image of an array printed on an amino-silane slide with biotinylated autoantigens.....	113
Figure 4. 9: Diagram representing the interaction between patient sample and autoantigens on amino-silane slide.....	114
Figure 5. 1: Total IgG levels in sera against three control antigens.	123
Figure 5. 2: The reactivity of IgG-autoantibodies against different antigens between patients with COPD, healthy non-smokers and healthy smoker controls.	128
Figure 5. 3: The reactivity of IgG-autoantibodies against different antigens between patients with COPD, healthy non-smokers and healthy smoker controls.	129
Figure 5. 4: The reactivity of IgG-autoantibodies against different antigens between patients with COPD, healthy non-smokers and healthy smoker controls.	130
Figure 5. 5: The reactivity of IgG-autoantibodies against different antigens between patients with COPD, healthy non-smokers and healthy smoker controls.	131

Figure 5. 6: The reactivity of IgG-autoantibodies against different antigens between patients with COPD, healthy non-smokers and healthy smoker controls.	132
Figure 5. 7: The reactivity of IgG-autoantibodies against different antigens between patients with COPD, healthy non-smokers and healthy smoker controls.	133
Figure 5. 8: Correlation between predicted FEV-1 and control antibody concentrations for <i>Candida</i> , Tetanus and <i>H. Influenza</i>	140
Figure 5. 9: Correlation between predicted FEV-1 and autoantibody concentration: citrullinated forms of collagen2 - collagen5, fibronectin, keratin and collagen1-3 (A-I, respectively).....	141
Figure 5. 10: Correlation between predicted FEV-1 and autoantibodies concentration: collagen4, collagen5, cytochrome c, decorin, GBM, CENP-B, keratin18, keratin8 and La ssb.....	142
Figure 5. 11: Correlation between predicted FEV-1 and autoantibodies concentration; nucleosome, pANCA, PL-12, PL-7, ribosome, RNP 68ksm free, RNP/sm, RNP/sm free and ro-52.	143
Figure 5. 12: Correlation between predicted FEV-1 and autoantibodies concentration: SAA2, SCL-70, sm antigen, HNRD, histone, AGG1, azorocidin, cANCA and ro-ssa.....	144
Figure 5. 13: IgM concentration in sera of COPD, healthy smoking and non-smoking controls.	145
Figure 5. 14: Differences in the concentration of autoantibodies (IgM) against different autoantigens in sera of subjects with COPD, healthy smokers and non-smoker controls.	149
Figure 5. 15: Differences in the concentration of autoantibodies (IgM) against different autoantigens in sera of subjects with COPD, healthy smokers and non-smoker controls.	150
Figure 5. 16: Differences in the concentration of autoantibodies (IgM) against different autoantigens in sera of subjects with COPD, healthy smokers and non-smoker controls.	151
Figure 5. 17: Differences in the reactivity of autoantibodies (IgM) against different autoantigens in sera of subjects with COPD, healthy smokers and non-smokers controls.....	152

Figure 5. 18: Correlation between predicted FEV-1 % and IgM antibody concentration for the specific-control antigen: <i>Candida</i> , Tetanus and <i>H. Influenza</i>	158
Figure 5. 19: Correlation between predicted FEV-1 % and IgM autoantibody concentrations of the specific- autoantigens: AGG1, azorocidin, cANCA, CENP-B, cytochrome c, decorin, GBM, histone and HNRD.	159
Figure 5. 20: Correlation between predicted FEV-1 % and IgM autoantibody concentrations for the specific- autoantigens: citrullinated collagen2, citrullinated collagen3, citrullinated collagen4, citrullinated collagen5, citrullinated fibronectin, citrullinated keratin, collagen1, collagen2 and collagen3.....	160
Figure 5. 21: Correlation between predicted FEV-1 % and IgM autoantibody concentrations of the specific- autoantigens: collagen4, collagen5, keratin18, keratin8, La ssb, nucleosome, pANCA, PL-12 and pl-7.....	161
Figure 5. 22: Correlation between predicted FEV-1 % and IgM autoantibody concentrations of the specific- autoantigens: ribosome, RNP/sm, RNP/sm free, ro-52, ro-ssa, scl-70 and sm antigen.....	162
Figure 5. 23: Heat map of IgG autoantibodies	165
Figure 5. 24: Heat-map of IgM autoantibodies	168
Figure 5. 25: Hierarchical clustering of IgG autoantibody measurements using both antigen and sample distance measures.	170
Figure 5. 26: Hierarchical clustering of IgM autoantibody measurements using both antigen and sample distance measures.	172

Table of tables

Table 2. 1: A selection of blocking buffers investigated to identify the ideal buffer for printing antigen microarrays.	57
Table 2. 2: A list of all autoantigens used for running patient samples.	60
Table 2. 3: Demographic data of the study participants.	62
Table 5. 1: A panel of control antigens and autoantigens examined in this study and source obtained from.	120
Table 5. 2: Significant differences of IgG antibodies between study groups.	134
Table 5. 3: Details of samples and reactivity of IgG antibodies against the examined antigens from COPD patients using the 95 th percentile of the control group as a cutoff.	134
Table 5. 4: Details of samples and reactivity of IgG autoantibodies against the examined antigens from healthy controls.	136
Table 5. 5: Details of samples and reactivity of IgG autoantibodies in COPD patients that are above 95%percentile of healthy smokers control.	137
Table 5. 6: Significant differences between IgM antibodies between the study groups.	153
Table 5. 7: Details of samples and reactivity of IgM autoantibodies against the examined autoantigens from COPD.	153
Table 5. 8: Details of samples and reactivity of IgM autoantibodies against the examined antigens from healthy smokers and healthy non-smoker controls.	155
Table 5. 9: Details of samples and reactivity of IgM autoantibodies in COPD patients that are above 95 % percentile of healthy smokers control.	155

Abbreviations

6MWD	6-minute walking distance
A1AT	alpha 1-antitrypsin
AATD	A1AT deficiency
ABS	acrylonitrile butadiene styrene
ACPA	anti-citrullinated antibodies
AECOPD	acute exacerbations of COPD
AMs	alveolar macrophages
ANA	anti-nuclear antigens
ANCA	anti-neutrophil cytoplasmic antibodies
APCs	antigen presenting cells
AT	anti-tissues
aTregs	activated Tregs
B-1a (1b, 2)	subset of B lymphocytes
BALT	bronchus associated lymphoid tissue
B-cells	lymphocyte subtype
BMI	body mass index
BODE index	Body-mass index, airflow Obstruction, Dyspnea, and Exercise
c-ANCA	cytoplasmic ANCA
Candida	<i>Candida Albicans</i>
CD4 ⁺ T cells	helper T cells
CD54	Cluster of Differentiation 54 (ICAM-1)
CD56 ^{bright}	Subset of natural killer cells
CD56 ^{dim}	Subset of natural killer cells
CD8 ⁺ T cells	cytotoxic T cells
CENP-B	centromere protein B
cit	citrullinated
COPD	Chronic obstructive pulmonary disease
CS	cigarette smoke
CV %	coefficient of variation
CVD	Cardiovascular disease
Cy5	cyanine 5 fluorescent dye

cyt-c	Cytochrome c
DCs	Dendritic cells
DNA	deoxyribonucleic acid
<i>E. coli</i>	Escherichia coli
ECP	eosinophil cationic protein
ELISA	Enzyme-Linked Immuno-Sorbent Assay
ENA	Extractable nuclear antigens
EPO	eosinophil peroxidase
FASL	Fas ligand
FBHs	food-borne helminthiases
FDA	Food and Drug Administration
FEV-1 %	Percentage of forced expiratory volume in 1 second
FPR2	formyl peptide receptor 2
FPR ₂ /ALX	formyl peptide receptor
FrIII	subset of regulatory T cells
FVC	maximum exhaled air volume after a full intake of breath
GBM	glomerular basement membrane
GOLD	Global Initiative for Chronic Obstructive Lung Disease
<i>H. influenza</i>	<i>Haemophilus influenza B</i>
H ₂ SO ₄	sulfuric acid
hIgG	Human-IgG
HNS	healthy non-smokers
HRP	Horseradish peroxidase enzyme
HS	healthy smokers
HSP ₆₀	heat shock proteins
ICAM-1	Intercellular Adhesion Molecule 1
IFN- γ	interferon gamma
Ig	immunoglobulin
IL-	interleukin
IL-1 β	interleukin-1 beta
kD	kilo-Dalton
La/SSB	Sjögren's Syndrome related antigen type B
LLOQ	lower limit of quantification

LOD	limit of detection
LOQ	limit of quantification
MCP-1	macrophage chemotactic protein
MEV	MultiExperimentViewer
MIP-1B	macrophage inflammatory protein-1 beta
MMPs	matrix metalloproteinases
MPO	myeloperoxidase
MS	Multiple sclerosis
NF-kB	nuclear factor kappa-light-chain-enhancer of activated B cells
NH ₂	amino linkers
NHS	N-Hydroxysuccinimide
NIBSC	National institute for Biological standards and control
NK	Natural killer cells
NKT	Natural killer T cells (innate like lymphocytes)
O ₂ ⁻	superoxide radicals
OD	optical density
OSP	outer surface protein
PADs	peptidylarginine deiminase enzymes
PAM	pulmonary alveolar macrophages
P-ANCA	perinuclear staining pattern
PBS	phosphate buffered saline
PBSTrehTw	PBS-trehalose Tween
PL-12	alanyl-tRNA synthetase
PL-7	threonyl-tRNA synthetase
PLP	proteolipid proteins
PM	polymyositis
PMN	polymorphonuclear leukocytes
PR3	proteinase 3
PRRs	pattern recognition receptors
PVA	polyvinyl alcohol
PVDF	poly-vinylidene difluoride
RA	rheumatoid arthritis
Ro/SSA	Sjögren's Syndrome related antigen A

ROS	reactive oxygen species
rpm	revolutions per minute
RT	room temperature
SAA	serum amyloid A
Scl-70	scleroderma
SD	standard deviation
SLE	Systemic lupus erythematosus
sm	extractable nuclear antigen
SnRNPs	small nuclear rionucleoproteins
SPR	surface Plasmon resonance
SS	Sjögren's Syndrome
SSc	systemic sclerosis
Th17	subset of helper T cells
TLRs	Toll like receptors
TMB	tetramethylbenzidine
TNF- α	tumor necrosis factor-alfa
Tregs	regulatory-T cells
ULOQ	upper limit of quantification
UV	ultraviolet
VCAM-1	vascular adhesion molecule 1
WG	Wegener's granulmatosis

1. General introduction

1.1 Chronic obstructive pulmonary disease (COPD)

1.1.1. Definition

COPD is a chronic abnormal inflammatory response of the lungs that encompasses two different diseases; chronic bronchitis and emphysema. Both pathologies can lead to the main feature of the disease, progressive and not fully reversible airflow limitation (Figure 1. 1)[1]. Each type of the disease affects different parts of the lung, however, patients with COPD often have a combination of both conditions. There are many definitions for COPD which depends on the accurate diagnosis of the disease[1]. In chronic bronchitis, studies have shown that neutrophils are increased rapidly in the airways, which results in stimulation of the bronchial epithelium to secrete IL-8 in high levels[2, 3]. In addition, these cells contain a variety of inflammatory mediators and enzymes that can lead to many changes in the bronchial tubes, such as tightness and swelling, which can cause shortness of breath. In the case of emphysema, it is characterized by an aggressive enlargement of the terminal bronchioles and destruction of alveolar walls, which leads to the development of the inflammation and can result in lung destruction.

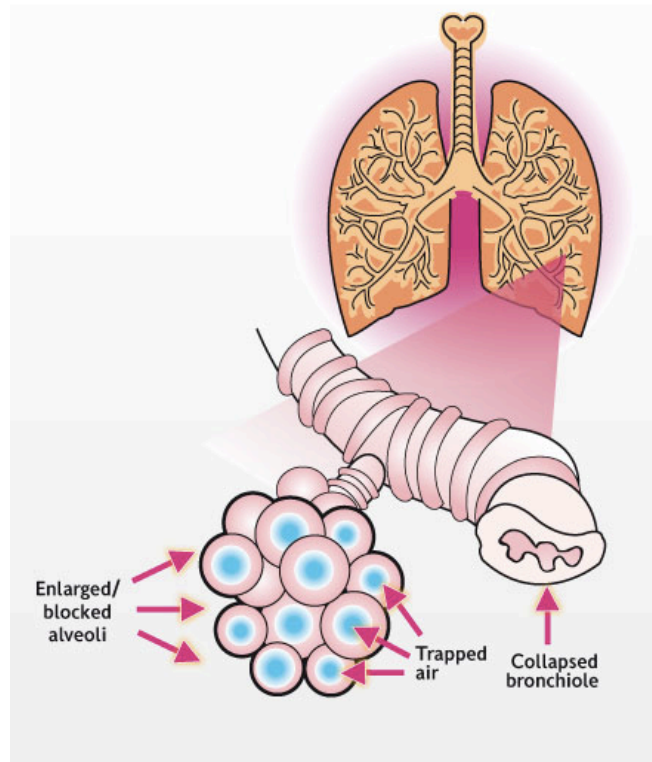


Figure 1. 1: Airflow limitation in COPD.

Parenchymal destruction occurs due to loss of lung tissue elasticity. Destruction of the alveolar walls leads to the development of emphysema. Inflammation of the bronchiole tubes leads to tightening, swelling and also collapsed bronchioles, which results in chronic bronchitis. Taken from[4].

1.1.2. Pathogenesis of COPD

COPD can result from several causes that can be divided into environmental factors or genetic susceptibility, with the major causes of COPD being the exposure to cigarette smoke (Figure 1.2). Other causes increase the risk for COPD, especially for non-smokers, such as childhood asthma and childhood respiratory infections[5, 6]. With regard to the environmental factors, occupational factors are supported in many studies, such as The American Thoracic Society, which demonstrated that 15 % of COPD might be associated with occupational exposure[7]. Since the nineteenth century, occupational factors such as the exposure to dust and fumes, have been linked to chronic bronchitis, and later, in the 1950s and early 1960s, emphysema was also observed to be increased among dust-exposed workers[8]. Since the 1970s,

many studies have investigated the relationship between occupational exposures and the prevalence of COPD by using different population samples. The results of these studies have varied widely depending on different factors, for instance the ages of patients, geographic area and level of cigarette smoking[8].

In terms of the influence of genetic factors on the development of COPD, there is a long history of genetic studies in COPD, but the main difficulty in these studies is to identify regions of chromosomes that are related to COPD[9]. The best-known example of a gene associated to COPD is alpha 1-antitrypsin (A1AT). A1AT is a serine protease inhibitor in the body, whose function is to inhibit neutrophil elastase in the human lung[10]. It has been demonstrated that most of the cases of A1AT deficiency are related to a genetic mutation which prevents A1AT from carrying out its important role in reducing host tissue injury by inhibiting proteases at sites of inflammation[11]. The use of Genome-wide association studies (GWAS) has allowed for the investigation into the molecular mechanisms of lung function and diseases. These types of studies can provide new insights and can be the basis for further research to investigate the exact mechanisms involved in lung disease[12, 13]. The investigation of genes associated with COPD susceptibility in smokers has highlighted several genomic regions that have a strong risk association; these include family with sequence similarity 13, hedgehog interacting protein, nicotinic, alpha 3 (neuronal)/cholinergic receptor, iron-responsive element binding protein 2 (FAM13A, HHIP, CHRNA3/ CHRNA5/IREB2), cholinergic receptor, nicotinic, alpha 5 (neuronal), a region on chromosome 19, and member A[14-16]. Despite all these potential candidates for genetic risk factors, currently the only genetically driven cause of COPD that has a potential for intervention is A1AT

deficiency as a result of SERPINA1 mutations[17].

There are three main theories that underline the pathogenesis of COPD; the first one is the protease-anti-protease theory that suggests there is an imbalance between proteases and anti-proteases, which leads to destruction of the elastin component and other components of the extra-cellular matrix. The source of this theory came from the patients with A1AT deficiency (AATD), as they develop early onset emphysema implicating a role for its target enzymes (neutrophil elastase and proteinase 3), and AATD animal models have many features of COPD. Further work has indicated other proteases are thought to be important, such as the matrix metalloproteinases (MMPs)[18], cathepsin B and collagenases, and thus they may also play a role in the protease/anti-protease theory.

The second theory is the oxidant-antioxidant theory, which states that variance between levels of harmful oxidants and protective antioxidants leads to oxidative stress. The oxidative stress in turn affects the actions of the anti-proteases and the expression of pro-inflammatory mediators.

The third theory observes that the state of inflammation is important in the pathogenesis of COPD, and this links to the previous theories[19]. Despite there being evidence that the inflammation in COPD patient's lungs can be triggered by cigarette smoke, it is still not clear why this inflammation still persists after smoking cessation. In addition, anti-inflammatory treatment is not a successful cure for the disease, it can only control the symptoms, which clearly shows that the link between the different pathological features are still unknown[20].

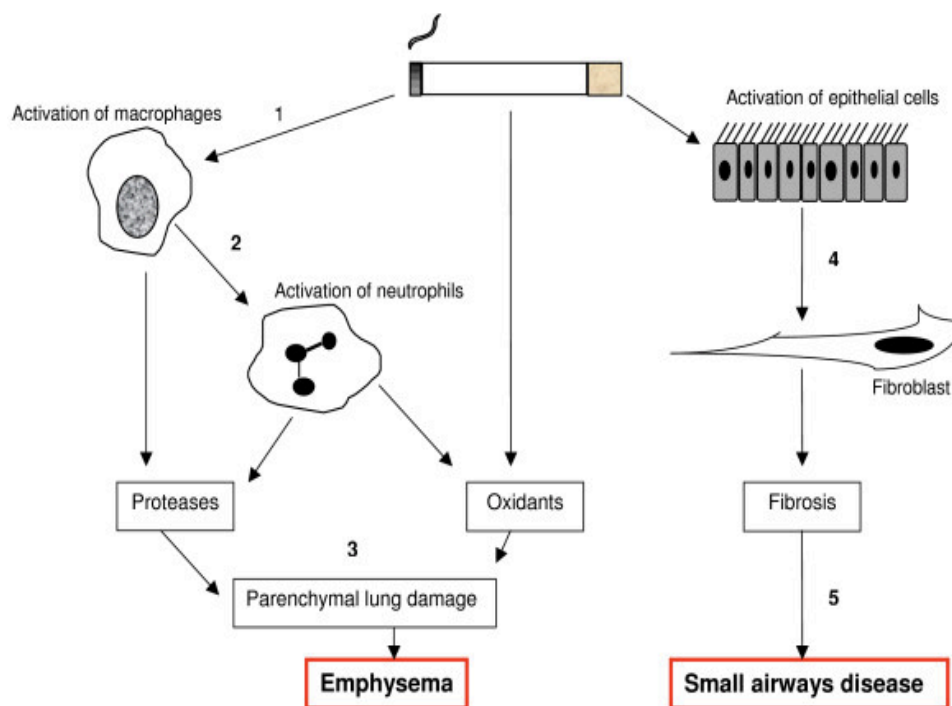


Figure 1. 2: The pathogenesis of COPD.

1) Cigarette smoking activates macrophages, 2) leading to release proteases or activation of neutrophil chemo attractants, 3) together with the release of oxidants leads to parenchymal lung damage and development of emphysema. 4) Activation of epithelial cells in the bronchial tubes leads to activation of the fibroblasts and development of chronic bronchitis. Adapted from[21].

1.1.3. Smoking risk factors

Smoking is the major leading cause of the development of COPD, however, only approximately 15-25 % of smokers develop COPD. It is thought to be associated with the changes in the lung morphology for COPD, which leads to the common symptoms of the disease, such as breathlessness[22]. Cigarette smoke contains thousands of chemical components including nicotine, toxins, carbon monoxide and many oxidants, and the inhalation of these chemicals can induce inflammation in the lung tissues[23, 24]. Once toxic substances in cigarette smoke are inhaled into the lungs they activate the epithelial cells, which secrete inflammatory mediators that induce inflammation in the airways and lung parenchyma[25]. The destruction

of lung tissues in COPD occurs from the action of polymorphonuclear leukocytes (PMNs) and pulmonary alveolar macrophages (PAM) that release proteinases and cause hyper secretion of mucus, which means the inflammation activity is an ongoing exacerbation [26]. The smoke of one cigarette contains thousands of oxidative free radicals and short-lived oxidants, such as superoxide radicals (O_2^-) and nitric oxide[27]. In addition, some of the oxidants, for example tarsemiqinone, can persist in the lung causing further damage. The increased oxidative stress in the lungs of patients with COPD can be due to elevated levels of inhaled oxidants, which play a serious role in the lung physiology and pathogenesis of COPD[28, 29]. Quitting smoking is the most effective intervention to slow down the symptoms of the disease, as well as improving the quality of life, and therefore it is highly recommended for individuals who are diagnosed with COPD. However, lung inflammation still persists in individuals despite smoking cessation[30, 31]. A study by Fletcher and Peto (Figure 1.3) showed the impact of smoking on lung function decline, and how cessation of smoking at any age can slow down this decline during the progress of the disease, but it cannot eliminate it [32, 33].

The Fletcher-Peto graph:

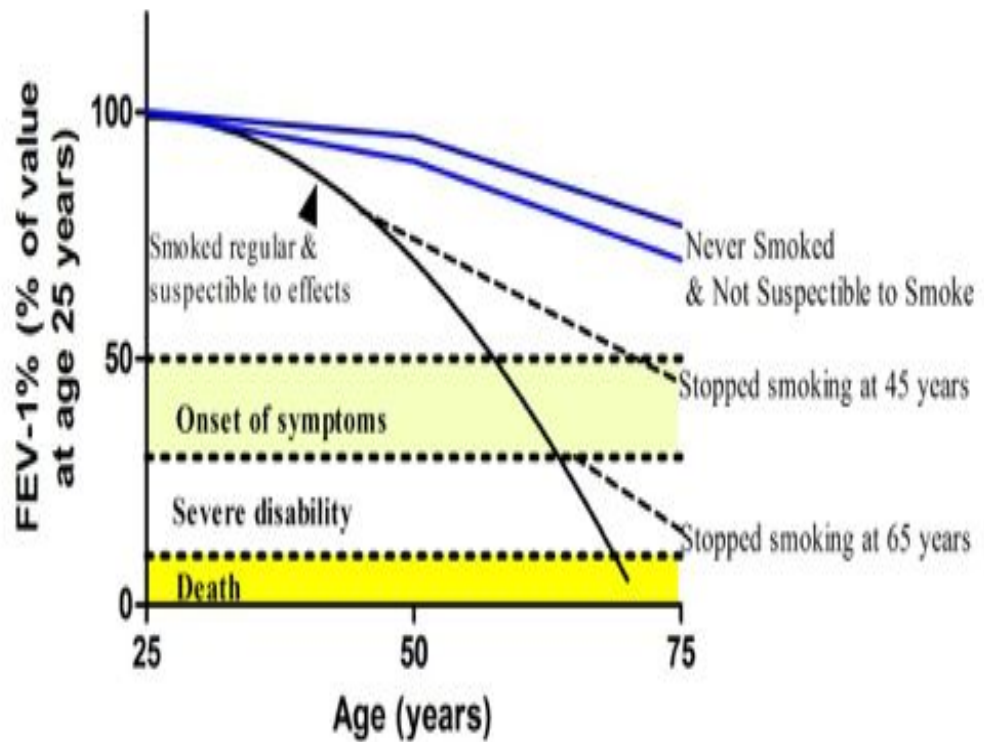


Figure 1. 3: The Fletcher-Peto Graph showing the outcomes of smoking cessation.

Diagram shows how cessation of smoking at any age can slow down the decline in lung function during the progresses of the disease but cannot eliminate it. FEV-1 % represents the forced expiratory volume in 1 second for patients with COPD. Adapted from [33].

1.1.4. Diagnoses and treatment

There are many different strategies in order to diagnose patients with COPD; spirometry is a very common test that should be used in all people who have one of the common symptoms of the disease, for example the exposure to any environmental pollution (such as cigarettes and occupational factors) or the presence of cough with increased sputum production[34]. Treatment for COPD is different for each patient and it is based on the severity of the disease. Smoking cessation is the most effective approach to treat COPD, or at least to reduce the decline in lung function in COPD patients. Bronchodilators are the most common therapy used among COPD patients as they can limit and control the symptoms. Another treatment that has shown to be effective in stable COPD patients is inhaled corticosteroids, as these can produce a small increase in post-bronchodilator FEV-1 % and a small reduction in bronchial reactivity, but no effect was observed on the rate of FEV-1 % in severe cases of COPD. Many studies have shown that a combination therapy can improve lung function compared to a monotherapy, for instance the combination of one or more long-acting bronchodilators and an inhaled corticosteroid[35][36]. Another approach to treatment of COPD is the inhibition of proteases and the use of inhibitors of neutrophil elastase, cathepsins, and MMPs, which is currently in clinical practice. Recently, new strategies have been developed, including the early detection of the disease by identifying markers in smokers who are at risk of COPD to encourage smoking cessation, and to monitor disease activity in order to develop new therapies[37] [38].

1.1.5. Systemic effects of COPD

There are several clinical systemic effects that are associated with COPD, such as oxidative stress and altered circulating levels of inflammatory proteins[39]. Indeed, weight loss, muscle wasting and tissue depletion are prevalent in patients with severe COPD, but can also be found in mild to moderate cases[40]. Cardiovascular disease (CVD) is considered to be one of the most important causes of death and hospitalization in patients with COPD, suggesting this needs to be monitored in patients with COPD[41]. The cause of these systemic effects are probably multifactorial and interrelated; currently the actual mechanisms are unknown, but they may be a result of many different factors, such as systemic inflammation, inactivity, oxidative stress, and tissue hypoxia. As these systemic effects can contribute to the respiratory morbidity observed in COPD, they should be included in the clinical assessment of patients and factored in to their treatment plan[42]. In COPD patients there is evidence that the increased levels of circulating inflammatory markers are due to the spill over hypothesis – the inflammatory mediators originate in the pulmonary compartment and they are responsible for producing the systemic inflammation. This suggests that systemic inflammation could be a common pathogenic mechanism not only in COPD but also its comorbidities, such as metabolic syndrome (Figure 1.4)[43].

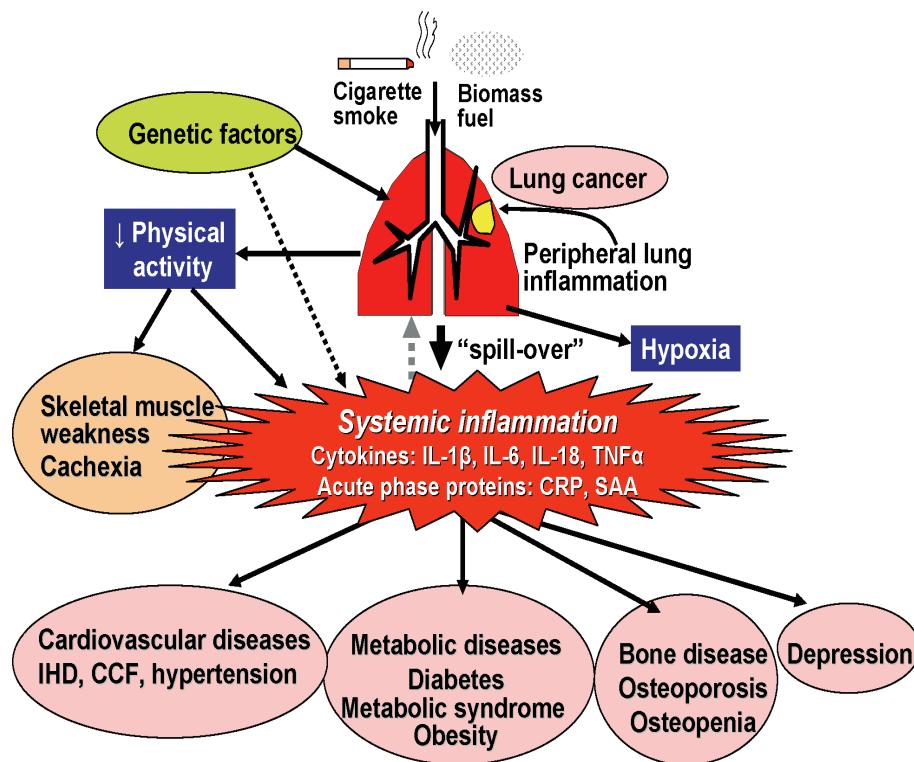


Figure 1. 4: Systemic effects of COPD.

The peripheral lung inflammation in COPD patients may spill over into the systemic circulation, resulting in different systemic diseases such as: skeletal muscle weakness and cachexia, and may cause an increased tendency to cardiovascular, metabolic, and bone diseases, and also depression. Adapted from[43].

1.2 Inflammatory cells and mediators in COPD

The role of inflammatory cells in the development of COPD is currently still under investigation due to the diverse nature of the diseases associated with COPD. Bronchitis, small airways disease and emphysema all display different forms and patterns of inflammation within the lungs. The cells thought to be most important in these inflammation processes are the neutrophils and macrophages as they release a variety of inflammatory proteins, which can cause tissue damage. The proteins released by these cells include proteolytic enzymes, generated oxidants, cytokines and chemokines, which all interplay and trigger an immune response[44]. Many studies have shown that there is an increase in the number of neutrophils and macrophages cells in the sputum and Broncho alveolar lavage fluid of patients with COPD, which supports the idea that these cells play a vital role[34]. Both innate and adaptive immune cells play key roles in the development and progression of COPD. Innate immune cells that involved in COPD are the epithelial cells, neutrophils, macrophages, dendritic cells, natural killer cells and eosinophils, and the adaptive immune cells include T-lymphocytes and B-lymphocytes[45].

1.2.1 Innate immune cells

1.2.1.1 Epithelial cells

A number of inflammatory diseases occur, in part, due to the activation of the innate immunity of airway epithelial cells; for example asthma and COPD are two lung diseases that have activation of airway epithelial cells implicated in their pathogenesis[46]. Airway epithelial cells can recognize microorganisms and pathogens through pattern recognition receptors (PRRs). These are present as a soluble form or as transmembrane receptors. Toll like receptors (TLRs) are one of the PRRs that are expressed by airway epithelial cells, as well as on most innate

immune cells. There are many types of (TLRs) and each one has a distinct ligand that binds with it. Many studies have shown that airway epithelial cells release pro-inflammatory mediators such as interleukin(IL)-6, IL-8 and TNF- α [47]. These mediators can lead to airway inflammation and epithelial damage. In addition, many investigations have demonstrated that pro-inflammatory cytokines released by these cells have a significant role in the pathogenesis of a variety of pulmonary diseases, including COPD[48].

1.2.1.2 Eosinophils

There is plenty of evidence that eosinophils play a central role in the pathogenesis of asthma, and there is increasing evidence that they also play a role in COPD[49]. The number of eosinophils is increased rapidly during exacerbations, and this can be detected in the sputum and biopsies of lung from patients with severe COPD[50]. Eosinophils release a variety of inflammatory proteins such as protein eosinophil cationic protein (ECP), eosinophil peroxidase (EPO) and many others, which are toxic to the bronchial epithelial cells. Indeed, eosinophils also secrete pro-inflammatory cytokines (e.g. TNF- α) that are believed to be important in the pathogenesis of lung diseases including COPD, yet the triggers of the secretion of these mediators are unclear[51].

1.2.1.3 Neutrophils

Neutrophils are thought to be involved in most of the inflammatory lung disorders, including COPD. They are recruited in high concentrations in the lung during an infection in order to fight infection. Although these cells have an important role in host defense against infection, they can also cause tissue damage; the increased number of neutrophils in the lungs correlates with the observed decline in lung

function, and an increase in neutrophilic inflammation is commonly observed in acute exacerbations of COPD. Further evidence of their importance in COPD comes from the correlation between the high levels of the indicators of peripheral airway dysfunction measured by high resolution computed tomography, and increased sputum neutrophil counts in smokers[26].

Several studies have reported that the increased numbers of neutrophils in the lung is associated with cigarette smoking[52]. The activation of neutrophils by producing protease and oxygen-derived free radicals has been implicated in the pathogenesis of COPD, and a major step in recruitment of these cells in the lung is a neutrophil chemoattractant signal that is generated locally in the endothelium and enables them to become adherent. The next step is the migration of the cells through intracellular pathways [53]. Neutrophils store a variety of inflammatory mediators in high levels such as serine proteinases (e.g., neutrophil elastase, cathepsin G) and MMPs. Once neutrophils are activated, all these enzymes can be released and become involved in the pathogenesis of COPD[54]. There are several studies to support the role of neutrophil serine proteinases in the development of COPD in animal models as well as patient studies; for example, the administration of neutrophil serine proteinases into rodent's lungs results in the development of emphysema in these rodents[55]. Neutrophil chemotactics are also considered as a major factor as they can cause tissue injury alongside their role in the migration of neutrophils from the blood into the lungs. These factors, including lipid mediators and chemokines, such as IL-8, which are thought to be play an important role in the lungs [56]. IL-8 is known to also be produced by other cells, such as macrophages, epithelial cells and fibroblasts, and it has been reported that IL-8 is important in the development of many human conditions other than COPD including wound repair and angiogenesis. In recent

studies it has been observed that there is a strong correlation between the levels of IL-8 in the sputum of patients with COPD and the severity of the disease[57, 58]. It has been shown that IL-8 can therefore be used as a marker in evaluating the severity of COPD[59]. This study has shown that by measuring the concentration of IL-8 in the sputum of patients with COPD, this can indicate the activation of neutrophils and eosinophils in these subjects. This is supported by other studies that have shown that IL-8 may have a role during the exacerbation of the disease, recruiting neutrophils and eosinophils into the airways[60].

1.2.1.4 Macrophages

In normal lung tissue, macrophages are the most prevalent of the immune cells and they play important roles in both innate and adaptive immune responses. In addition, they are responsible for the development of most inflammatory airway diseases, including COPD. It is known that macrophages can be divided into different subsets depending on the different pathways that are required for their activation, namely M1 and M2a, M2b and M2c [61]. According to this, many studies have investigated if a certain subset of macrophages is involved in the development of COPD. An alternative pathway is thought to be the main pathway that activates this special subset, called M2 macrophages and this is driven by IL-4 and IL-13 secretion[62].

The number of macrophages are rapidly increased in the lungs of COPD patients and they circulate to the sites of alveolar destruction. It is believed that the pathophysiological features of COPD are related to the secretion of inflammatory proteins, which are released by alveolar macrophages (AMs)[63]. In the inflammatory response to lung injury AMs are known to be important and play a critical role in host defense, not only through phagocytosis, but also by secreting a

variety of active molecules, including cytokines, TNF, IL-1B, MCP-1 and MIP-1B.

For the first step of recruiting white blood cells to the sites of inflammation many adhesion molecules such as ICAM-1, CD54 and VCAM-1, play a crucial role, for example, by the adherence of ICAM-1/VCAM-1 to respiratory endothelium. Indeed, these molecules have also been shown to help the adherence of AM to the respiratory endothelium[64].

1.2.1.5 NK and NKT cells

Natural killer cells are classified as innate immune cells which are heterogeneous, and one of the main classes of human killer cells. There are two main subsets of NK cells CD56^{dim} and CD56^{bright} that are classified according to the expression of CD56 molecules. 90 % of the NK cells in the body are CD56^{dim}, whereas only 10 % are CD56^{bright}. Indeed, CD56^{dim} cells have a stronger cytotoxic role than the second subset. With regard to NKT cells, they are defined as innate-like lymphocytes which share features with both innate and adaptive immune cells[65]. Both cells NK and NKT cells have an important role in the pathogenesis of COPD. NK cells can cause damage in pulmonary tissues using different approaches, for instance, apoptosis that is induced by FASL or by a direct cytotoxic activity of the lung tissue by releasing perforin and granzymes which form pores in the cell membrane of the target cell, inducing either apoptosis or osmotic cell lysis. In addition, the secretion of molecules such as cytokines and chemokines from these cells could recruit other inflammatory cells, which can also cause the damage to lung tissues[66, 67]. Within the sputum of COPD patients studies have shown there are increased levels of NK and NKT

cells, and there is evidence to suggest these cells produce higher levels of cytotoxicity in this group compared to healthy smokers and non-smokers[68].

1.2.1.6 Dendritic cells

Dendritic cells (DCs) are powerful cells that play an important role in immune response; they are known as professional antigen presenting cells (APCs) and they are responsible for the proliferation of T cells[69]. There is evidence to show that there is a significant increase in the quantity of DCs in smokers and COPD patients compared to healthy controls. There is evidence from many studies that some components of cigarette smoke have immunomodulatory effects on lung DCs, and can induce DCs to release chemokines which can play a role in COPD pathogenesis[70, 71]. Some studies have suggested that the increase in the number of Langerhans-type DCs present in COPD patients correlates with disease severity[72].

1.2.2 Adaptive immune response in COPD

1.2.2.1 CD8⁺ T lymphocytes

CD8⁺ T cells are thought to contribute to progression of COPD, and the mechanisms in which these cells play a role may be directly by cytolysis or indirectly via the production of IFN- γ [73]. This mechanism has been supported by work conducted with inducible transgenic murine systems, that have shown high levels of the expression of IFN- γ caused lung inflammation[74]. Another suggested mechanism is that CD8⁺ T cells have a cytotoxic effect in which they directly kill lung parenchymal cells. It has been demonstrated that T lymphocytes, in particular CD8⁺ T cells, are significantly increased in the patients with COPD and many studies have shown these cells produce several cytokines, such as IP-10

and IFN- γ , which are increased rapidly in emphysema cases and are also known to be stimulators for the production of MMP-12 in AMs[75]. Studies have also demonstrated that there are increased numbers of CD8⁺ T cells in both the lower respiratory tract and peripheral airway of COPD patients, which suggests there is some trafficking of these lymphocytes between the inflammatory sites, and this may influence disease progression[76] [77].

1.2.2.2 CD4⁺ T cells

Although CD8⁺ T cells are considered to have an important role in COPD, CD4⁺ T cells also have been implicated in disease progression. In emphysematous lungs, the numbers of CD4⁺ T cells are increased significantly and this occurs mainly in proximity to the bronchus associated lymphoid tissue (BALT). CD4⁺ T cells release a range of activated cytokines that are important and implicated in inflammatory responses[78]. These cytokines can be either Th1 cytokines (e.g., IL2-INF- γ) or Th2 (IL4, IL5 and IL-10)[78]. CD4⁺ T cells have a major role in promoting CD8⁺ T cell responses and their survival. The significant increase in the number of AMs in the lungs of smokers may suggest the involvement of CD4⁺ T cells in this inflammatory response[79].

As mentioned previously, lymphocytes are one of the key components of the adaptive immune response and can cause an inflammation in COPD. Th17 cells are one of the CD4⁺ T cell subsets and they produce IL-17A, IL-17F and IL-22, which are thought to be involved in the pathogenesis of many inflammatory disorders and autoimmune diseases. Many inflammatory cells, including neutrophils and lymphocytes, depend on IL-17 cytokines for their recruitment into inflamed tissues. Additionally, most parenchymal cells express IL-17 receptors, such as macrophages

and DCs, and many recent studies have reported a significant role of Th17 in the lung pathology of COPD[80]. IL-17 cytokines can also stimulate airway epithelial cells to secrete mucus and MMP-9, and the over expression of such cytokines leads to mucus over production[81]. Another cytokine produced by Th17 cells is IL-21, which has a major role in differentiation of Th17 cells; but despite its positive role it also inhibits FOXP3 expression and the development of regulatory-T cells (Tregs cells)[82]. IL-22 is also produced by these cells and is thought to be important in IL-10 production and acute phase proteins. Nevertheless, further investigation is needed into the role and regulation of Th17 cells in COPD especially for designing future therapies[83].

Tregs cells are one of the subpopulations of CD4⁺ T cells that have an important role in preventing autoimmunity[84]. As COPD shares features with some autoimmune diseases, this has led to an interest in a potential role for Tregs cells in the pathogenesis of COPD[85].

Recent studies have shown that there are three distinct populations of human Tregs cells: the suppressive CD25⁺⁺⁺ CD45RA⁻ activated Tregs (aTregs), CD25⁺⁺ CD45RA⁺ resting Tregs (rTregs), and the pro-inflammatory CD25⁺⁺ CD45RA⁻ cytokine-secreting (Fr III) cells. These cells may have an important role in the progression of COPD as there is evidence to suggest that an imbalance occurs between the subsets in patients with COPD; studies show that in smokers there was an increase in aTregs, rTregs and Fr III cells (compared to never-smokers), whereas COPD patients had a significantly increased Fr III cells with decreased aTregs and rTregs, when compared to smokers[86].

Further evidence for the suppressive effect of Tregs comes from studies that show

there was a significant increase in the number of myeloid-derived suppressor cells in COPD patients, which can lead to suppression of the immune system by upregulation of immunosuppressive cytokines or Tregs[87].

1.2.2.3 B lymphocytes

Another important cell in the adaptive immune responses is the B-cell; these cells are derived from bone marrow and their development occurs in both bone marrow and the peripheral lymphoid organs. B lymphocytes play an important role because they are responsible for the production of antibodies, and they are also thought to be responsible for some allergic and inflammatory airway pathologies[88]. There are three subsets of human B-cells; B-1a cells which are fetal progenitors and their development occurs in adult life, B-1b cells which are formed in adult bone marrow, and both of these cell types are responsible for production of natural antibodies. The final subset are B-2 cells, these cells produce antibodies that are induced by exposure to antigens and are responsible for isotypes switching[89].

There are five isotypes of antibody, which are divided according to the structural differences in the constant region of the heavy chains; IgG, IgM, IgA, IgE and IgD[90]. Recent evidence has shown that smokers with COPD produced more IgG than healthy smokers who produced more IgA[91]. In terms of the structure all types of antibodies have two identical heavy and two light polypeptide chains bound together through disulfide bonds, which consist of constant and variable regions with a different molecular weight for each chain. In IgG the molecular weight for the heavy chain is around 150 kDa and the light chain of approximately 25 kDa. IgG itself is composed of four subclasses: IgG1, IgG2, IgG3 and IgG4, and each one has a distinct function in protecting the body against infections[92].

Many studies have shown that smoking tobacco is the main risk factor that effects the concentrations of antibodies in the blood. In smokers the levels of IgG in serum are shown to be lower than non-smokers, which can result in changes to the immune response, and this issue has been supported by many studies in this field[93].

There is evidence from surgical biopsies of lungs that the numbers of B cells were increased in the small airways in COPD patients. In addition, the numbers of B cells were increased in patients with COPD more than smokers without COPD, and the numbers of cells were much higher in severe cases of COPD[94].

1.3 Autoimmunity in COPD

Many studies have shown a prevalence of IgG autoantibodies in patients with COPD, which strongly supports the influence of an autoimmune component in disease progression. However, the nature of the antigens that bind to these autoantibodies in COPD subjects is not clearly understood[95]. There have been many investigations that have showed an adaptive immune response can play a role in the progression of COPD; T cells can cause tissue damage via pro-inflammatory mediators, and also by the activation and recruitment of other effector cells, such as B cells, which produce antibodies (and autoantibodies). The activation of CD4⁺ T cells in particular leads to antibody-isotype switching for example, from IgM to IgG[96]. Therefore, the role of the adaptive immune response in COPD patients has guided many researchers to investigate the presence and role of autoantibodies in COPD.

Autoimmunity is a chronic inflammatory disorder characterized by the body being attacked by its own immune system, which can lead to several autoimmune diseases, such as rheumatoid arthritis (RA)[97]. With regard to the association between COPD

and autoimmune diseases, they both share many clinical and pathophysiological features, which leads to the hypothesis that COPD should be considered as an autoimmune disease. There are many similarities between RA and COPD, for example smoking is a risk factor for both RA and COPD, and the inflammatory cells (neutrophils, macrophages and T lymphocytes) and cytokines (IL-6, IL-8 and TNF) are the same for both diseases[98]. Furthermore, after smoking cessation the pulmonary inflammation in COPD is still progressive and this supports the possibility that autoimmunity has a role in disease progression[99]. Several population-based cohort studies have assessed the association between RA and Systemic lupus erythematosus (SLE) with increased risk of COPD. They found patients with RA and SLE had a significantly higher risk of developing COPD than that the control population of non-RA and SLE participants, which suggests RA or SLE may be a determining factor for COPD incidence and/or they may facilitate the shortening of the time course for developing COPD. However, further investigation is needed to support and corroborate this hypothesis[100, 101].

Recent studies in RA have suggested that citrullinated antigens and anti-citrullinated protein antibodies may play an important role in disease progression; other studies have suggested that the presence of these antigens is not limited to RA, and therefore could be the result of an inflammatory process. Citrullination of proteins can be defined as the post-translational conversion of arginine residues to citrulline residues by peptidylarginine deiminase enzymes (PADs; EC 3.5.3.15)[102]. Many studies have investigated the relationship between anti-citrullinated antibodies (ACPA) and lung diseases; one such study assessed the levels of ACPA in the serum of non-RA heavy smokers with COPD, heavy smokers without COPD, and compared them with healthy never-smokers and patients with RA[103]. The study showed that the levels

of ACPA in the serum of heavy smokers with COPD were significantly higher compared to those without COPD; the prevalence of ACPA in heavy smokers without RA were also low[103].

Other studies have shown that there are citrullinated proteins in the lung of patients with RA, which may occur due to smoking damage, and in the serum of patients with RA there were also antibodies against these citrullinated proteins detected. These results were also supported by evidence of an immune response to citrullinated proteins in RA patients[104].

Recent studies have suggested that there are distinct sub-sets of RA, and the molecular basis of these can be further understood by investigating how environmental and genetic predisposing factors interact with specific immunity, including potential pathogenic immune reactions that may occur at sites other than the joints, for example in the lungs. The discovery of local immunity towards citrullinated proteins and the associated inflammation in early disease development in the lungs, suggests there is potential for future development of therapies that could target this disease-inducing immunity in the very early stages of the disease, before joint destruction and inflammation has taken hold[105].

Recent studies of autoantibodies in RA have focused on citrullinated proteins, as these have a strong association with genetic and environmental risk factors in RA-susceptible individuals, and can mean that the arginine residues of some native proteins (including collagen types I, II, III, IV, and V) become modified within the joints, which can influence disease progression. The underlying pathophysiology of the citrullination process for these proteins is not fully understood; there are some studies that have shown that these proteins become exposed during apoptosis, and

dysfunction in clearing dying cells, which would allow the citrullination process to occur in genetically susceptible RA patients. Further investigation has highlighted a group of citrullinated auto-antigens in the synovial joints of RA patients, including α -enolase, vimentin, collagen type II, fibrinogen, keratin, fibronectin, and vitronectin, all of which could affect the progression of the disease[106].

Further evidence for an autoimmune response involvement in COPD comes from studies of circulating anti-nuclear antibodies (ANA) prevalence, that showed high levels in COPD patients, and the relationship between ANA and lung function supports a role for autoimmunity in the pathogenesis of COPD[107]. Studies on the presence of autoantibodies in patients with COPD suggest that moderate to severe COPD cases may have an auto-immunity problem due to a significant number of patients with significant levels of autoantibodies in their serum[108]. Recently, IgG antibodies that bind to lung tissue components were also investigated; in a study that investigated the presence of autoantibodies in the serum of some COPD smokers subjects, the results showed high levels of IgG autoantibodies specific to cytokeratin-18 and collagen-5 (and also to cytokeratin-8 and collagen-4), compared to non-smoking sera, which supports the role of autoimmunity in COPD[109].

Collagen is recognized as a self-antigen in many autoimmune conditions and it has been studied intensively. The studies have shown that in the serum of patients with lung cancer, high levels of antibodies to collagen (in particular type V and V) were detected, which suggests they may play a role in disease progression[110]. Precursors of type I and III collagen proteins have also been shown to be increased in fibrotic pulmonary disease. This has been confirmed by other studies which aimed to determine whether these proteins were also increased in the small and large

airways of COPD patients. The results showed that the levels of precursor proteins for collagen I and III were increased significantly in both the small and large airways for patients with various stages of COPD[111].

Within the body there are different classes of collagens involved in tissue elasticity, shape and organisation; each have different specific roles and can be involved to a different extent in autoimmune diseases. Fibrillar collagens are found in the tissues, for example I and III are found in the skin and bone; type II is found in the joint cartilage, type V is found in synovial membranes, and collagen type IV forms into sheets that are a key constituent of basement membranes[112, 113]. Studies that have investigated collagen autoantibodies in the synovial fluid of active RA patients found antibodies for native collagens I, II, III, IV, and V; whereas these were found less frequently in patients with degenerative joint disease[114, 115]. The underlying pathophysiological mechanisms of how collagens induce autoimmunity and can trigger arthritis are not yet fully understood. There is some evidence from a study conducted with a denatured form of collagen type II, that the collagen may be exposed to antibody formation during the process of cartilage degradation, which would suggest the antibody formation is due to the arthritis and not a trigger. Another possible mechanism for the formation of collagen antibodies is the exposure of similar epitopes during the inflammatory response within the joint[116].

In some studies autoantibodies specific to elastin were detected in the serum of patients with COPD, and the number of these anti-elastin antibodies was also increased significantly in the lungs of these patients, however, other researchers did not detect this increase in autoantibodies[117]. A study by Catherine *et al.* investigated the levels of anti-elastin antibodies in patients with chronic

inflammatory lung disease and compared the results with healthy controls. They found that there were no significant differences between the patient groups, which suggests the presence of anti-elastin antibodies in COPD needs further investigation to elucidate if there is an effect[118, 119].

1.3.1 Autoantibodies

The effect of autoantibodies in COPD has been questioned by a study that found that there was no significant difference between the levels of these antibodies in patients with clinically stable COPD and the healthy non-smoking control group. Another study found there was no statistical difference in autoantibody levels between the population variables within the COPD population, such as BMI, 6MWD, age, spirometric and arterial blood gas parameters; which agreed with a study by Cottin *et al.* [118], that found within patients with emphysema and pulmonary fibrosis, there was no evidence of anti-elastin antibodies. Overall, these results suggest this area needs further investigation to fully elucidate the role of autoantibodies in the progression of COPD.

A wide range of autoantigens that are associated with many autoimmune diseases, such as RA, SLE and Sjögren's Syndrome (SS), have been examined in this study in order to investigate the autoantibody response to these antigens in COPD and if any of them associate with COPD.

Anti-neutrophil cytoplasmic antibodies (ANCA) are developed against the proteins in the cytoplasmic of neutrophils. The response of autoantibodies to these type of antigens were detected first in Wegener's granulomatosis (WG) one of the systemic autoimmune diseases[120]. There are two different types of ANCA antigens that have been found in patients with WG; the first type is cytoplasmic ANCA or (c-

ANCA) and the second type is perinuclear staining pattern or (P-ANCA). Each type of ANCA recognizes two different constituents of the azurophilic granules of neutrophils (PMN), and the lysozymes of monocytes; proteinase 3 (PR3) is recognized by c-ANCA and myeloperoxidase (MPO) is recognized by p-ANCA[121, 122]. The initial self-tolerance of ANCA antigens may be broken by the stimulus of ANCA antigens displayed within neutrophilic apoptotic bodies, and the ANCA autoimmune response may be augmented by ANCA related opsonization of apoptotic neutrophils, once the immune response has started[123].

Autoimmune syndromes are often accompanied by deregulated neutrophil cell clearance and/or cell death, which has been suggested to play a role in disease pathogenesis, as the cytotoxic and proteolytic molecules released in this process can cause organ damage[124]. Products produced by neutrophils can be mediators and targets of autoimmunity, for example ANCA auto-antibodies respond to antigens in the neutrophil cytoplasm, and they can also bind PR3 and MPO on active neutrophils, which leads to the release of chemo-attractants, ROS and degranulation, which causes tissue damage and inflammation in a vicious cycle. Studies have suggested that after the initiation of inflammation, ROS-dependent apoptosis is up regulated by ANCA in the neutrophils, which results in a feed-forward cycle ending in organ damage[125].

Recent studies have challenged the long standing belief that proteinases produced by neutrophils, and the neutrophils themselves, are the main cause of lung tissue breakdown COPD, by suggesting that the critical mediators are actually the MMPs released by macrophages. Evidence suggests that neutrophils still play a key role as they act as initiating cells, and they produce epitopes and attractants which are

involved continuing the process of inflammation[126].

Another group of antigens examined in this study are the nuclear antigens (ANA). These antigens can be found in the nucleus and cytoplasm of the cell and include small nuclear ribonucleoproteins (snRNPs), alanyl-tRNA synthetase (PL-12) and threnoyl-tRNA synthetase (PL-7). There are other components of nucleic acids antigens that have also been tested such as histone, nucleosome and ribosome. Extractable nuclear antigens (ENA) are subtypes of ANAs and include sm antigen, RO/SSA, RO52, La/SSB and SCL-70. Studies have shown that antibodies bind to ANA and ENA in organ-specific autoimmune diseases systemically such as SLE and RA, so they may have a role in COPD[127].

1.3.2 Autoantigens in COPD

Another group of proteins thought to have a role in the pathogenesis of COPD and therefore have been studied in this thesis include serum amyloid A (SAA), cytochrome c, aggrecan and decorin. SAA is an acute phase protein induced by inflammatory mediators such as IL-6 and TNF- α . In humans SAA consists of four types (SAA 1, SAA2, SAA3 and SAA4), and during tissue injury, SAA1 and SAA2 in particular are released in the sites of inflammation. It has been demonstrated that SAA could be used as a systemic biomarker for acute exacerbations of COPD (AECOPD) and may have utility in the clinical identification of AECOPD, or provide new suggestions into the pathogenic mechanisms involved[128]. The further involvement of SAA in COPD has been demonstrated by the fact it promotes neutrophilic inflammation and interaction with lung mucosal ALX/FPR2 receptors[129].

It has been demonstrated that decorin production is present in high levels in the lung

fibroblasts of patients with severe emphysema. In addition, another study observed that high levels of anti-decorin IgG antibodies were not significantly different between COPD patients and healthy controls, however, there were significantly higher levels in the COPD ex-smokers group than COPD smokers[117, 130].

Cytochrome c (cyt-c) belongs to the cytochrome protein family which are found in the membrane of the mitochondria. It is thought to be associated with COPD as many studies have shown a high levels of cyt-c present in patients with COPD. A study in this field observed an abnormal cyt-c release from skeletal and respiratory muscles of COPD patients in the moderate stage of the disease[131].

Aggrecan is also one of the tested auto-antigens in this thesis as it is thought to be associated with COPD as indicated in some studies. Aggrecan is a large proteoglycan and it is also known as cartilage proteoglycan[132]. A study observed that COPD was associated with the production of autoantibodies to self-antigens, including Aggrecan and many other autoantigens, which shed light on the possibility of using these autoantibody-specific antigens to determine COPD risk, or could be used to monitor therapeutic interventions[133].

1.4 Enzyme-linked immunosorbent assay (ELISA)

Several laboratory methods have been used in order to detect autoantibodies in the serum of COPD subjects, including Enzyme-Linked Immuno-Sorbent Assay (ELISA), and indirect immunofluorescence microscopy. In the 1970s ELISA was introduced to measure levels of antibodies in serum samples[134]. There are different types of ELISA assay including sandwich ELISA, indirect and direct ELISA. Sandwich ELISA is the most sensitive type as it contains two layers of antibodies, capture and detection, and its widely used especially in the measurement

of antigens in specific samples as it provides accurate detection of the antigen of interest[135]. All ELISA type results are highly quantitative and generally reproducible, which makes them suitable for use in biomedical laboratories[136]. These methods have many disadvantages, for example they are time consuming and also they require high sample volumes[137]. Detection of individual protein levels are commonly carried out using a traditional ELISA or Western blot, but these need a high sample volume therefore other techniques are more suitable for high throughput screening[138].

1.5 Microarray Technology

In recent years, the use of microarray technology has increased rapidly for many applications, and has been used to identify therapeutic markers, molecular classification and diagnosis of multiple diseases[139]. This technology was originally used in genetics research, and has been developed into different applications including antibody microarray, peptides and proteins microarray, tissue microarray and others.

Antibody microarrays have been shown to be a powerful tool for analysis of protein expression and protein-protein interactions, which has led to this method being considered as a diagnostic tool in many diseases. Evaluation of the effect of various factors, such as the glass surface, pH of the spotting buffer, antibody concentration and blocking reagents, are important in the production of an antibody microarray[140]. There are many examples of how this technique can be used to identify multiple antigens associated with diseases. Tumours elicit an immune response in the host organism, and this has been investigated in many studies using traditional methods, such as sandwich ELISA, in order to identify tumour-

associated antigens. However, using a microarray technique has become more efficient, and it has been shown that these antigens can be used as targets for immunotherapy as well as biomarkers for cancer[141]. These types of arrays, including antigen microarrays (Figure 1.5), can help to detect autoantibodies in diseases such as COPD, which are thought to be involved in the pathogenesis of the disease. Multiple sclerosis (MS) is a chronic inflammatory disease and an autoimmune response can play an important role in the pathogenesis of the disease, which has been detected in many studies. It has been shown that different patterns of MS pathology were associated with unique antibody patterns, as seen by using antigen microarray technology. This was done by identifying antibodies that were reactive to lactosylceramide and L- α -lysophosphatidylserine, which are involved with pattern II of MS; whereas an increase in the level of IgG antibodies to HSP60, OSP and PLP peptide epitopes were detected in pattern I MS [142]. Another study similar to this was conducted in rheumatoid disease; it detected autoantibodies in patients with rheumatoid diseases using 15 autoantigens to create profiles to distinguish the autoantibodies specific to different disorders, including RA, SLE, SS, polymyositis (PM), and systemic sclerosis (SSc). The difficulties in the recognition of these diseases, particularly in the early stage, makes microarray a more efficient technique for diagnosis than other laboratory methods[137].

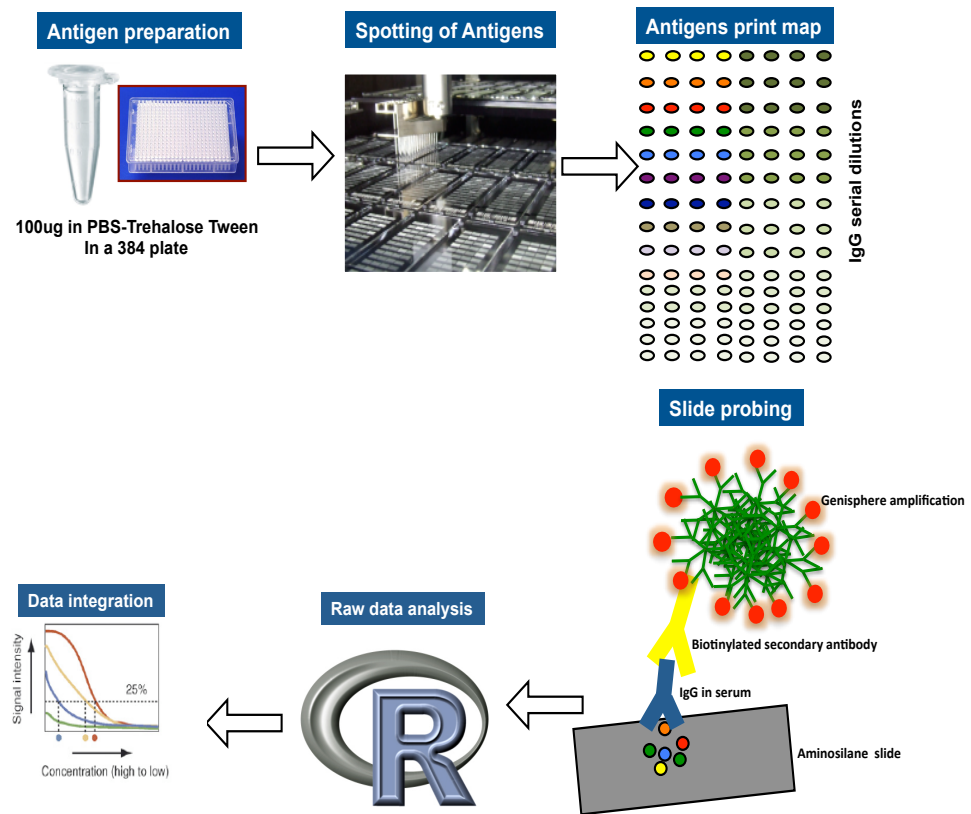


Figure 1. 5: Principle of antigen microarray

Antigens of interest diluted in printing buffer and coated a 384 wells plate. Antigens were spotted on the slides using microarray machine, then the slides were processed manually by adding the serum that contained the antibodies. A secondary antibody, which tagged with biotin, was added as a detection antibody and amplification was performed.

Finally, despite the fact that DNA microarrays have shown to be successful in

discovering gene expression patterns associated with specific diseases, nowadays, protein microarrays have become a successful tool for profiling and identification of biomarkers specific to certain diseases[143]. Different types of protein microarrays, particularly the antigen microarray, have been used in the measurement and profiling autoantibodies in chronic inflammatory diseases such as COPD[144], and also in the development of novel diagnostic methods as well as new options for therapy in COPD[145, 146].

Multiplex microarrays have many advantages compared with traditional ELISA:

- 1) High throughput multiplex analysis: a fast high-throughput approach is required for population-based epidemiological studies due to the high sample size. Currently studies of FBHs use antibody and molecular detection carried out by immunoassays, however these techniques have limitations, for example they need to run separate tests to investigate different parasitic infections in each sample. The use of bio-chip technology has some advantages over the currently used methods: there are miniaturized, versatile, convenient, and can be easily adapted, which means they can be used in high-throughput diagnostics. Within the bio-chip field, protein microarrays are becoming more popular; they can be used to investigate the activity and interactions of proteins, which can help to determine their individual and large scale function. The arrays use a support surface to capture the proteins under investigation, and these can be nitrocellulose membranes, glass slides, micro-titre plates, or beads, which gives the assay extra versatility.
- 2) Less sample volume needed: ELISA needs 50–100 μl of a sample per protein investigated, and requires 500 ng of capture antibody, which means

investigating 10 different proteins, without replicates, could consume the entire clinical sample; whereas a microarray would only need 10 μ l of the sample to measure dozens of protein targets, and would only need 0.2 ng of each capture antibody[147].

- 3) Efficiency in terms of time and cost: less time for one assay with multiple targets instead of separate assays for each target.
- 4) Ability to evaluate the levels of one given inflammatory molecule in the context of multiple others.
- 5) Ability to perform repeated measures of the same antigen panels in the same subjects under the same experimental assay conditions.
- 6) Ability to reliably detect different proteins across a broad dynamic range of concentrations[136].

1.5.1 Microarray slide surfaces and immobilization

Microarray slides are glass slides, like a microscope slides, but they are modified before use to be a suitable substrate for microarray. The glass slides are coated with chemical functional groups (eg. amino group) and this allows the attachment between the slide surfaces and the target molecules. Moreover, the coating must be non-fluorescent and suitable for the hard physical conditions which might affect the slides[148].

The most common method to modified the slides surfaces and provide organic functional groups is silanized glass slides, this nowadays has become commercially available so they can be ordered from several companies (Figure 1.6). Silanized slides means the slides are placed into a solution containing silane proteins, and the silanes can contain different functional groups such as; epoxy groups, amino groups or aldehyde groups[149]. Amino-silane, epoxy-silane,

hydrogel and aldehyde coatings are the most commonly used for slide surface modifications, and each provide different properties[148].

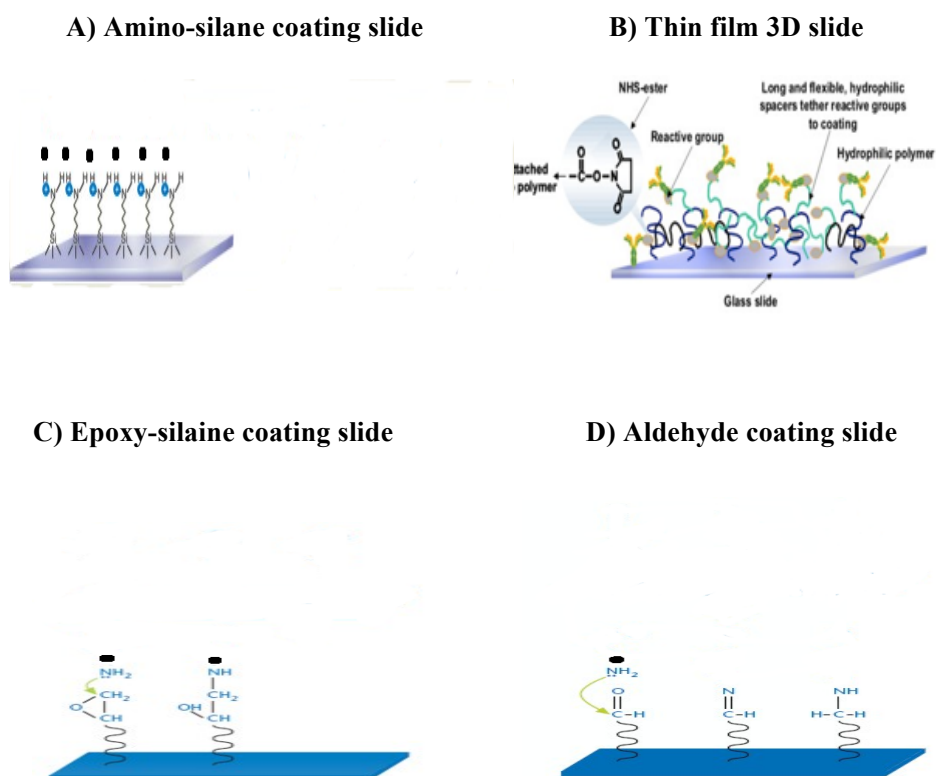


Figure 1. 6: Diagrams show a schematic representation of four different types of the commercial NEXTERION slides.

- A) Amino-silane coated slide has a high concentration of primary amino groups available at the surface. Biomolecules spotted onto the slide surface have amino linkers (NH_2), which covalently linked to the slide surface by either heating, or an exposure to ultraviolet (UV) light. B) Thin film 3D polymer coated slide, SCHOTT NEXTERION[®] Slide H consists of a cross-linked, multi-component polymer layer activated with N-Hydroxysuccinimide (NHS) esters to provide covalent immobilization of amine groups. C) Epoxy-silane coated slide, the slide is coated with a multi-purpose epoxy-silane layer that will covalently bond to most types of biomolecules via their amino and hydroxyl groups. D) Aldehyde-silane coated slide, the uniform surface features aldehyde groups that readily react with primary amino linkers (NH_2) on the spotted biomolecules to form covalent bonds. Adapted from [139].

1.5.2 Spot size and morphology

Once the antigen has been printed on the slide surface, it appears as a circular spot on the slide. The size and the morphology of this spot is affected by the slide surface chemistry and printing buffers used[150]. Poor spot morphology can have an effect on the slide performance, due to a decreased antigen activity and can cause difficulties in signal quantification. Evaluation of the spot morphology can be achieved visually based on variations of signal intensity within individual spots[151]. The current commercial microarrays use spots that have been calculated to provide the optimal probe/analyte capture efficiency (50- to 200 μm diameter), but any further reduction of the spot size to the nm scale may not result in a better efficiency, due to kinetic-limiting behavior. The use of nm-to- μm surface capture features can provide other useful characteristics besides assay sensitivity, such as higher reporting content, higher feature density, and easier integration with active transport for use in microanalytics; but this scale will produce other technical challenges, for example reliable detection and fabrication. Microarrays can be further enhanced before running experiments by using numerical models to predict sensitivity, fractal occupancy and hybridization/incubation times, which can save time and resources[152].

1.5.3 Signal detection and generation

One of the most commonly used methods for signal generation is fluorescence, which is generated when a substance absorbs electromagnetic radiation or light of a long wavelength (high energy), and then emits light of a shorter wavelength (lower energy). The excitation wavelength can be in the wavelengths visible to human eyes, or the UV region of the spectrum, and some fluorophores, for

example Cy5, are excited by wavelengths around 625 nm and emit light in the red spectrum (532 – 670 nm)[153, 154].

Currently signal detection in microarray depends on two different strategies: a label-free strategy such as surface Plasmon resonance (SPR), or labeled-probes which can be used directly, indirectly or in a sandwich assay[155]. The direct method uses labeled antibody bound directly to the target molecule of interest, whereas the indirect method works by immobilizing the target antigens first by using a primary antibody, then a second labeled antibody is used for detection. A sandwich assay needs two distinct antibodies; the capture antibody and the detection labeled antibody used to detect the target molecule between the two of them (Figure 1.7)[156]. The most commonly used method in an antigen-antibody microarray is the fluorescence detection method, which includes using Alexa fluor, Oyster or fluorescent dyes such as Cyanine[157, 158].

In this study, UltraAmp reagent amplification was used which is a 3-dimensional structure made entirely out of DNA. This reagent is labeled with hundreds of signal producing molecules such as fluorescent, biotin or enzymes. The amplifier improves the sensitivity of immunoassays including antigen microarrays, and the sensitivity of the assay can increase up to 100 fold compared to other amplification systems.

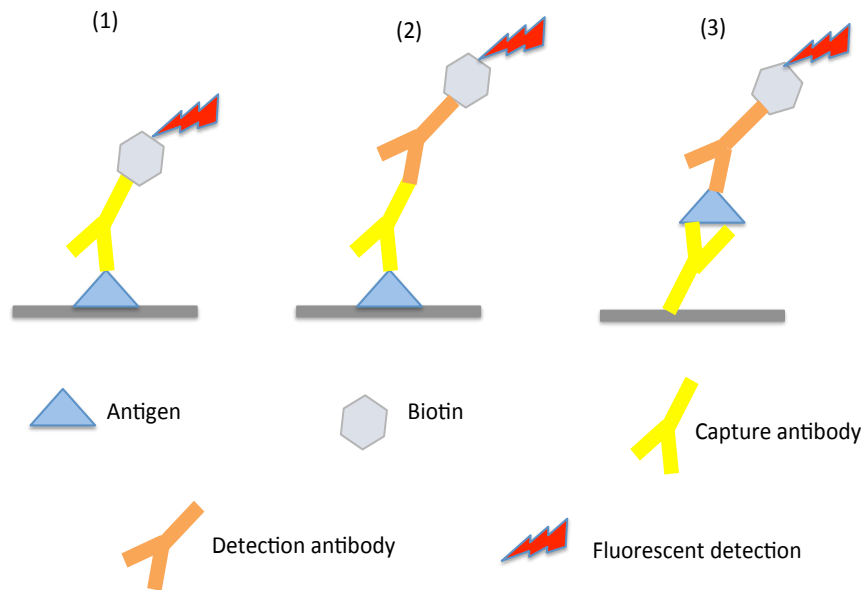


Figure 1. 7: Methods of detection and signal generation in microarray

- (1) represents the direct way to detect the antigen of interest by labeling the capture antibody. (2) represents the indirect method that requires the labeling of the detection antibody, or the labeling of tertiary antibody (3).

1.6 Assay validation

Assay validation is an important step to evaluate the experimental method and to determine how well it fits for a specific use. Most importantly the use of validation enables one to understand the limitations of the method, and where it might be improved. There is little the guidance on method validation for the submission of bioanalytical methods to journals, which results in a variable quality of such manuscripts, as the work conducted depends on the analyst's experience and judgement[159, 160].

Assay validation can be defined as 'the documenting of the performance characteristics of the method in question by specific laboratory investigations to ensure it is reliable and suitable for the analytical application'. How well the analytical data is accepted depends directly on the criteria used to validate the method. All analytical laboratory methods should be analyzed and verified to ensure they are appropriate and reproducible, with production of the correct documentation (standard operating procedure, method development and quality control) to allow the method to be followed, and audited if necessary[161]. A good starting point for the production and validation of an analytical method are the industrial guidelines produced by the U. S. Food and Drug Administration, and the American Association of Pharmaceutical Scientists, which can be modified and adjusted depending on the requirements of the analytical method being used[162].

In the recent literature there have been reports by major manufacturing companies, for example BIO-RAD and ThermoFisher, as well as in house microarray systems, about a variety of validation protocols for different microarray techniques, which can be used in the general laboratory.

Multiple parameters can be investigated in the validation process for antigen microarray platform. In this study, four parameters have been tested; limit of

detection, precision, cross-reactivity and correlation of results between ELISA and the microarray assay (Chapter 5).

1.7 Hypothesis of study

The hypothesis of this research is that, due to lung tissue being destroyed during the progression of the disease, the prevalence of autoantibodies against lung tissue in COPD patients may be increased. This would suggest that autoimmunity plays a role in the pathogenesis of the disease. The investigation of these autoantibodies in the serum of patients with COPD can be carried out by measuring the level of autoantigen-specific antibodies using microarray technology. Ultimately, these autoantibodies may have the potential be used as biomarkers in the diagnosis of COPD at an early stage of the disease.

1.8 Aims and objectives

1.8.1 Aims

The aim of this study is to develop an antigen microarray in order to apply this technique to test the autoantibody responses in patients with COPD compared to healthy controls (smokers and non-smokers).

1.8.2 Objectives

- To optimize the procedure of antigen microarray using quality control experiments.
- To perform a series of validity tests to prove the assay is accurate and reproducible.
- To apply the optimized technology to the sera of 62 patients with COPD, which will be compared with 30 sera samples of healthy subjects, both smokers and non-smokers, to investigate whether there are any significant differences between the groups in relation to the clinical information, such as sex, age and FEV-1.

2. Materials and Methods

2.1 Materials:

2.1.1 Printing buffer

PBS-Trehalose-Tween-20 buffer: x1 PBS (Sigma), 50 mM Trehalose, 0.01 % Tween-20 (Sigma) (v/v) was used to dilute all antigens including the positive controls and candidate antigens for the printing process. Tween is used as a blocking agent for membrane based immunoassays usually at a concentration of 0.05 %.

2.1.2 Coating buffer for ELISA

Carbonate-bicarbonate buffer capsules (SIGMA). For use in coating ELISA plates, dissolve contents of one capsule in 100 ml distilled water.

2.1.3 Blocking buffers

Three blocking buffers were tested in this study, namely I-Block, PVA and I Block plus PVA (Table 2.1).

Table 2. 1: A selection of blocking buffers investigated to identify the ideal buffer for printing antigen microarrays.

Name	Ingredients	Purchased from
I Block (is a highly purified casein protein-based blocking reagent)	0.05g I Block in 25mL PBS-Tween-20 (0.05%) (Sigma)	Tropix (Bedford, MA)
PVA (Polyvinyl alcohol, is a water based-synthetic polymer)	Diluting 2g in 50mL in distilled water and heated until dissolved	Sigma, UK
I Block + PVA	A mixture of both buffers	

2.1.4 Wash buffer (PBS-Tween 0.05 %)

PBS (x10) tablets were diluted in distilled water (100 ml per tablet) with 0.05 % Tween-20 to form PBS-Tween (PBST).

2.1.5 Serum diluent

Serum samples were diluted 1:1000 in antibody diluent solution purchased from (Dako, UK Ltd).

2.1.6 Streptavidin CY5

Streptavidin conjugated cyanine 5 fluorescent dye (eBioscience, Ltd, UK) were diluted 1:5000 in washing buffer (PBS-Tween 0.05 %) to detect the binding of biotinylated antibody for microarray and ELISA experiments.

2.1.7 Streptavidin infrared dye

800CW Streptavidin dye (LI-COR) was diluted 1:5000 in wash buffer (PBS-Tween 0.05 %).

2.1.8 Streptavidin –HRP conjugated for ELISA

Horseshoe peroxidase enzyme (HRP) (R&D, UK) was diluted 1:5000 in washing buffer (PBS-Tween 0.05 %).

2.1.9 Substrate solution for ELISA

This is a ready-to-use solution of tetramethylbenzidine (TMB) used for colorimetric HRP-based ELISA detection (Sigma-Aldrich, UK).

2.1.10 Sephadex G-25

One gram of Sephadex G25 powder (1000–5000 MW cut off) was added to 4–6 ml of PBS-trehalose Tween (PBSTrehTw) and allowed to rehydrate for about 3 h at room temperature (RT).

2.1.11 Amplification reagents (Ultrapamp™ 40-Oyster-650)

A 3DNA labeled with fluorescent dye molecules. It is called also Genisphere's core nanotechnology. Purchased from Genisphere^R company (USA) (Chapter 1).

2.1.12 Slide surfaces for microarray

A range of surface modified glass slides were optimised for microarray printing. All were purchased from Schott (Germany); Amino-silane, epoxy-silane, aldehyde and 3d hydrogel slides surfaces. Diagrams of each slide type shown the mechanism of attachment in chapter 1 (Figure 1.5).

2.1.13 Candidate antigens

2.1.13.1 Antigens for optimisation and validation tests

Four control antigens, chosen due to the common occurrence of autoantibodies to them in human sera. These were *E. coli* lysate, Tetanus toxoid, *Haemophilus influenza B* (*H. influenza*) and *Candida Albicans* (Candida). The Tetanus toxoid was a purified protein preparation, while *H. influenza* and Candida preparations were extracted mixtures of bacterial or fungal antigens. To prepare the *E. coli* lysate *E. coli* was grown in (LB) Luria broth and Luria agar (1.5 % w/v, sigma) for one day then lysis buffer (10 mM Tris, 1 mM MgCl, 0.1 mM CaCl, 1 mg/ml Lysosome, 10 µl protease inhibitor and 5 µl of 1000 U/ml penzonase) was added into bacteria tube. Vortex mix and incubated for 4 h at 4 °C. It was centrifuged for 30 minutes at top speed (16,000) and stored in the freezer (-20 °C) for future. To measure the concentration of the protein in the lysate, Nanodrop was performed.

2.1.13.2 Antigens for application

The antigens chosen for this study (Table 2.2) were selected on the basis of their involvement in other autoimmune diseases.

Table 2. 2: A list of all autoantigens used for running patient samples.

* List of control antigens

Antigen name	Source
Haemophilus influenza B	National institute for Biological standards and control(NIBSC)
Tetanus toxoid	
Candida	

* List of autoantigens

Antigen name	Source
Azurocidin	AROTEC Diagnostics Ltd
CENP-B	
PL-12	DIRECT AG, Freiburg, Germany
PL-7	
GBM	AROTEC Diagnostics Ltd
histone	
HNRP D	
La ssb	
Nucleosome	
proteinase (cANCA)	
p ANCA	
Ribosomal p	
RNP/sm	
RNP 68k (sm free)	
RNP/sm free	
Ro-ssa	
Ro-52	
SCL-70	
sm antigen	
cit-collagen II	Citrullinated in-house
cit-collagen III	
cit-collagen IV	
cit-collagen V	
cit-fibronectin	
cit-keratin	

Antigen name	Source
native collagen II	Merck Millipore, Billerica, MA, USA
native collagen III	Sigma-Aldrich
native collagen IV	
native collagen V	
Keratin 18	
Keratin 8	
Decorin	
Aggrecan	
Serum amyloid 2(SAA2)	
Cytochrome c	

2.2 Methods:

2.2.1 Study population for microarray

The study population for the microarray study included 62 COPD participants, 15 healthy smokers and 15 never smokers. Of the COPD group 27 were males and 33 females with a mean FEV-1 % of 48 %. Unfortunately, pack years and current treatment details are not available for this patient cohort. The healthy smokers were defined by spirometry as an FEV1/FVC of above 70 % (with a median FEV1/FVC 77.16). The control non-smokers were questioned on smoking history and they were all never smokers. The study was approved by the local research ethics committee (Leicestershire, Northamptonshire, Rutland (LNR), REC 10/H0406/65). Samples were collected and stored at -70 °C until use on the microarray to prevent repeated freeze-thaw cycles.

Table 2. 3: Demographic data of the study participants.

Values are expressed as mean and (range). FEV-1 % (Percentage of Expected Forced percentage of Expiratory Volume in one second).

	Age Mean (Range)	Gender Male/female	FEV-1% Mean (Range)
COPD (n= 62)	66 (54-80)	27/33	48 % (29-73)
Healthy Smokers (n=15)	65 (51-81)	7/14	107 % (83-140)
Control Non- Smokers (n=15)	32 (25-40)	11/4	--

2.2.2 Study population for ELISA

The same eight healthy serum samples used for validation experiments were selected to run ELISA in order to do a comparison between both methods microarray and ELISA.

2.2.3 Buffer exchange

Four antigens were buffer-exchanged (Decorin, cytochrome c, amyloid A and aggrecan), as they were bought in new for this study. The rest of the autoantigens were already buffer-exchanged in a prior study. Briefly, 1 ml of Sephadex beads (Section 2.1.9) was added in PBSTrehTw buffer. For separation a 1 ml column tube (Thermo Fisher Scientific) that contains 35- μ m pore size filter (MoBiTec GmbH, Göttingen, Germany) was used. The separation column was centrifuged at 1200 rpm for 5 min to remove excess buffer. The column was rehydrated by adding 50–100 μ l of PBSTrehTw buffer and excess buffer removed by centrifugation as before. A new collection tube was placed under each separation column. The volume of each antigen required for buffer exchange (20 μ l) was added to the separation column and centrifuged as described above. The eluate from this step contains the buffer exchanged antigen preparation in PBSTrehTw buffer.

2.2.4 Biotinylation method

Before coating the antigens, investigation of the binding of new autoantigens was also required (Decorin, Aggrecan, Cytochrome c and Amyloid). The binding of the remaining 36 autoantigens were investigated in prior study through the binding between the patient sample and these antigens (Figure 5.1).

Briefly, 10 μ l of NHS-Biotin reagent was diluted into water (1 ml) and 10 μ l of

the required antigens were added into new tubes. Diluted NHS-Biotin was then added to each 10 μ l of each antigen. All the tubes were placed on ice and incubated for 2 hours. Next, 100 μ l of printing buffer was added into each antigen. A spin column containing 1 μ l of Sephadex G10 was centrifuged for 1 min, then 400 μ l of printing buffer was added into the column and it was then centrifuged for 1 min, this was repeated 5 times. Finally, 100 μ l of each antigen was added into each column in the middle of the packed beads and centrifuge for 2 min. The eluted samples were placed in new tubes and were now ready to be added to a microarray plate for printing.

2.2.5 The investigation of the binding of patient autoantibodies to candidate antigens

In a prior study, the binding of the rest of the autoantigens examined in this study were demonstrated through the binding that occurred between the patient sample and these autoantigens (Table 2.2). In brief, all antigens were printed onto an amino-silane slide and probed with a mixed serum sample, then probed with an anti-IgG to show reactivity.

2.2.6 Protocol for printing antigens on the slide surface

Diluted antigens (Figure 2.1) were loaded onto a 384 well plate (Genetix), and arrayed onto the different slides using a Biorobotics Microgrid II arrayer (Microgrid) and silicon contact pins (Parallel Synthesis Technologies, USA). The array chamber was set at 60 % humidity and run at room temperature during printing. The distance between spots was set to 315 microns, the dwell time was to 0.400 mm and target height printed was 0.04 mm. The average spot diameter varied between 50-150 microns.

2.2.6.1 Process of printed slides

After printing, slides were stored under vacuum until use. Printed slides were blocked for 1 hour in PVA, I Block or mix of both buffers (I-block and PVA) on a shaker. After blocking, slides were washed three times with PBST (containing 0.05 % Tween-20) and then incubated with the diluted serum samples that contained the capture antibodies. The incubation was followed by washing steps and incubated with the detection antibody conjugated with biotin for 1 hour. The signal of the binding between the antigen specific-antibody and immobilized antigen was detected by fluorescence; slides were washed with PBST (as described above), rinsed briefly in ultrapure water, dried by spinning at 1200 for 5 min using a slide rack and then scanned using a 4200 AL microarray scanner (Axon 635 nm GenePix®).

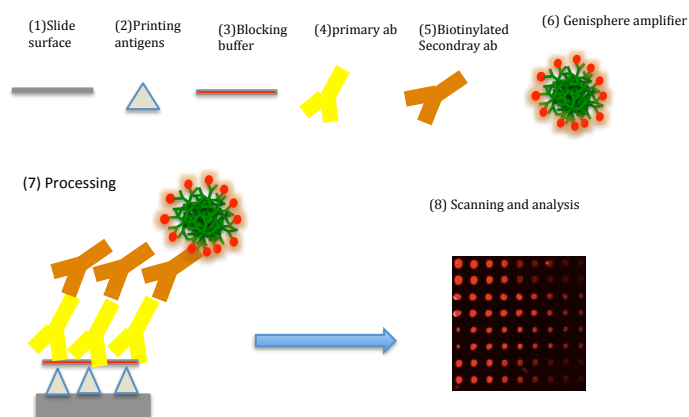


Figure 2. 1: Illustration of the procedure of printing antigens on a slide surface

Antigens were diluted in printing buffer then printed on slide surface (1,2). The slide was blocked with blocking buffer (3), probed by primary and secondary biotinylated antibodies (4,5). Amplifier labeled with fluorescent dye (Ultraamp 40-Oyster-650) was added to detect the signals (6). After scanning the slide (8), then analysis was done using Genepix and Prism software.

2.2.7 Data Analysis

16 pads are used to print identical arrays of candidate antigens including a standard, this allows 15 arrays to be used for samples and one to be used as a negative control pad (no serum). A standard curve of IgG each target specially separated in a regular array to allow them to be distinguished. The final pad (number 16) is used as a no-serum control well. The pads are processed with the sample of interest, and each pad on the microarray slide is equivalent to a well on an ELISA plate.

For the analysis undertaken in this thesis, the median values of the spots pixels were considered, which was defined as the “intensity value that splits the distribution of the signal pixels in half”. For each spot, the number of pixels above the median must be the same as the number below. One of the key advantages of using the median value is that takes into account any outliers of within the spot, which are not covered by the mean value[163].

Scanned images of the slides were analysed using image analysis software called Genepix pro. The scanned image was saved as a TIF file and imported into the image analysis software. The median pixel intensity of all the spots on each array was calculated, after subtracting for the local background, then saved as a GPR file. The GPR file (Figure 2.2) contained the localization and identification variables of the antigen targets on the array, and also the median fluorescence intensity and the local background that represented the autoantibody binding signal values of each spot.

BackgroundSubtraction=LocalFeature								
ImageOrigin=0, 0								
JpegOrigin=4420, 930								
Creator=GenePix Pro 6.1.0.4								
Scanner=GenePix 4200A 01 Autoloader [94353]								
FocusPosition=20								
Temperature=22.94								
LinesAveraged=1								
Comment=								
PMTGain=420								
ScanPower=100								
LaserPower=2.69								
Filters=Standard Red								
ScanRegion=0,0,2185,6900								
Supplier=BioRobotics								
ArrayerSoftwareName=TAS Application Suite (MicroGrid II)								
ArrayerSoftwareVersion=2.7.1.18								
Block	Column	Row	F635 Medi	F635 Mear	F635 SD	Log Ratio (F635 Medi	F635 Mean - B635
1	1	1	172	177	61	Error	4	9
1	2	1	154	162	65	Error	-3	5
1	3	1	162	167	64	Error	5	10
1	4	1	154	156	60	Error	-1	1
1	5	1	159	158	64	Error	15	14
1	6	1	148	155	63	Error	5	12
1	7	1	142	149	60	Error	-8	-1
1	8	1	157	175	147	Error	-2	16
1	9	1	168	172	62	Error	0	4

Figure 2. 2: Example of GPR file produced.

These delimited text files contain the localization and an identification variable of the samples on the array. The values used for subsequent data analysis are highlighted in pale blue in column AS.

2.2.8 ELISA Protocol

The 96 well micro-titer plates (Figure 2.3) were coated with 100 µl of candidate antigens at 10 mg/ml diluted in bio-carbonate buffer. HIgG was coated as semi log dilutions (1:5) in duplicate for standard curve and the plate incubated overnight at room temperature. The next day, the plate was washed three times using wash buffer (PBS-0.05 % Tween-20) and then blocked with 300 µl of 0.2 % I Block buffer and incubated for 1 h. After that, the plate was washed three times using the same wash buffer. Serum samples were diluted 1:100 in protein diluent and 100 µl of the sample was added to the plate (in duplicate). For the secondary antibody control (the control wells), blocking buffer instead of diluted serum was used in these wells. The plate was incubated for 2 h at room temperature. After the 2 h incubation, the plate was washed three times with washing buffer and then the secondary antibody was added to all wells (Biosource anti human Ig-G –Biotin), covered and incubated for 2 h at room temperature. Enzyme linked Streptavidin- HRP was then diluted 1:200 and 100 µl was added per well, the plate was covered and incubated for 20 minutes at room temperature. The plate was washed three times with wash buffer. Finally, the Substrate Development solutions (Sigma, UK) were added (100 µl per well). The plate was then incubated for 10 minutes to allow for colour development, and 50 µl of stop reaction (H₂SO₄) was added to each well before the colour change was detected (OD) 450 nm on a Fluorostar optima plate reader software. The concentrations of control antigens were determined from a IgG standard curve on each array. Finally, the level of correlation between the ELISA and microarray methods was investigated by comparing the results.

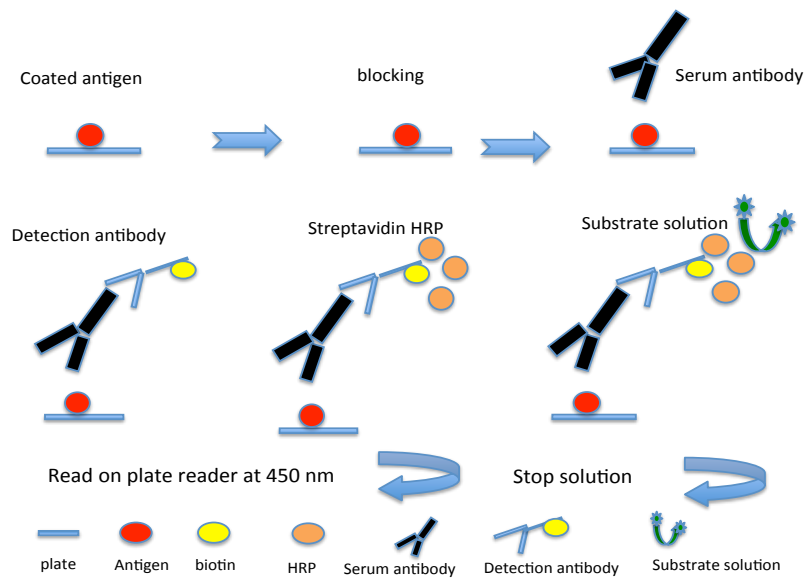


Figure 2. 3: Illustrated ELISA method.

Briefly, ELISA plates are coated with candidate antigens overnight. The plate is washed and blocked. The plate is washed and serum samples are added. The plate is washed again and detection antibodies are added for another 2 h. The plate is washed and streptavidin HRP is added for 20 min and the plate is kept in the dark. The plate is washed three times and substrate was added for 20 min and finally stopped with sulfuric acid (H_2SO_4). The absorbance is read on a plate reader and graphs are plotted with the appropriate standard curve and samples.

2.2.9 Generating microarray standard curves

Briefly, human IgG was diluted using semi log (1:5) dilution and IgM and IgA were diluted as 2-fold dilution (1:2) in the microarray plate, then printed on the slides in triplicate. Different serum samples were added into each block of the slide incubated then probed with the detection antibody (Section 2.2.5) and the florescent signal from binding was detected. Replicates of each dilution spot of Immunoglobulin (Ig) were plotted using Graphpad prism to generate standard curves for each serum sample. Signal intensities of each candidate antigen spot were determined from the standard curves to calculate the concentration of each antigen-specific antibody.

2.2.10 Microarray validation

For protein microarray assays there are limited guidelines in the literature, therefore the accuracy and reproducibility of the methodology used here was established based on the guidelines outlined by the Food and Drug Administration (FDA) for pharmacokinetic assay validation, which suggests multiple validation experiments should be performed, including intra- and inter assays, limit of detection and cross-reactivity assays[161]. Additionally, correlation of the results of microarray and ELISA experiments were performed to investigate the comparison between both techniques.

2.2.11 Statistical analysis

Flourostar optima plate reader software was used to read ELISA plates at 450 nm to detect HRP. After that, the ELISA results were analyzed using Microsoft Excel according to this equation:

(Coat with serum- Coat without serum)-(No coat/no serum- No coat with serum), The results then plotted as mean values \pm S.D using Graph Pad

Prism5. Statistical test; Mann-Whitney was also run between the candidate antigens by using the Prism software.

The results for the signal intensity, minus the local background, for each antigen with the serum specimens from the microarray data were obtained from the GPR file of each block. Signal intensities and the background for each antigen were plotted and compared using Graph Pad Prism5.

To compare the level of auto-antibodies in COPD patients and healthy controls (smokers/non-smokers), a Mann-Whitney test was carried out in GraphPad Prism5, and P values were considered to be significant if they were less than 0.05.

For the comparison between ELISA and microarray techniques, correlation between both methods was performed by GraphPad prism5.

For the correlation studies between the concentrations of autoantibodies and FEV-1 for COPD and smokers Spearman's r coefficient was performed (Chapter 5). Age and gender significances between groups were performed using Fisher's exact test. All heat maps and hierarchical clustering was performed using MultiExperimentViewer (MEV) version 4.7.4.

3. Optimisation of an Antigen Microarray Platform

3.1 Introduction:

Antigen microarray is a format of protein microarray that can be used to study the interaction between antigen-antibody in a high throughput. The procedure of antigen microarray is dependent on the printing of autoantigens on microarray glass slides; these autoantigens are then reacted with test sera, and the binding between antibodies and autoantigens are identified by fluorescently labeled secondary antibodies[164]. There are several properties that need to be considered for the production of a microarrays such as: surface chemistry, coating procedure and blocking buffers, as these play a major role in reducing the non-specific binding of proteins. The surface substrate that is mostly used is glass, this usually activated by silanes and coated with different materials such as poly-vinylidene difluoride (PVDF), acrylonitrile butadiene styrene (ABS), polystyrene, and nitrocellulose[165, 166].

There are some other factors that influence the success of microarray production, such as the spot morphology for each printed antigen, the spot size, the printing buffer and blocking buffer used. The spot morphology includes its size, and is often dependent on the slide type (chemistry surface) and the printing buffer used, therefore it is important to select the optimal slide surface that provides good spot morphology and higher signal intensity[167] [150].

Prior work in our laboratory optimised parameters such as; blocking buffer, printing buffer and serum dilution that are most efficient for antigen microarray[168] [169]. Therefore, we further optimized multiple parameters, such as different blocking buffers (namely I Block, PVA, and a mixture of both

blockers) on four different slide surfaces to investigate the impact on intensity and spot morphology. These are important measures to build a successful antigen microarray platform. In addition, here we tested eight different concentrations of UltraAmp in order to increase the sensitivity of the assay.

3.2 Materials and methods:

Briefly for the optimisation stage, different slides surfaces (epoxy-silane, aldehyde, amino-silane and hydrogel slides) were purchased from Schott Company (UK). The same blocking buffers and amplification method, with the three positive control antigens (*E. coli* lysate, Tetanus and *H. Influenza* antigens) were used. The antigens were diluted in printing buffer (PBS Trehalose -Tween 20), in order to make 10 µl of antigen at 0.1 µg/µl concentrations. 10 µl of each antigen mixture was transferred into 384 well microtitre plates. In addition, a two-fold serial dilution of human IgG was prepared to be a positive control for the anti-IgG secondary antibody, and this was placed on the same microtitre plate in 10 dilutions. The plate was covered with foil and centrifuged. All control antigens were printed onto 4 different types of glass slides: Amino-silane-slide, Epoxy-slide, Hydrogel slide and Aldehyde slide. The human IgG serial dilution was printed in duplicate, the three control antigens (*E. coli*, Tetanus and *H. Influenza*) were printed in triplicate, and 16 identical grids were printed onto each slide using a silicon pin in the Arrayer.

3.3 Results:

Each slide type was blocked with three different blocking buffers, namely I Block, polyvinyl alcohol (PVA) and a mixture buffer of both I Block and PVA, in order to test which blocking buffer gave lowest backgrounds with each slide surface tested. The microarray was probed with a healthy serum sample at 1:1000 dilution; antigen-antibody complexes were then incubated with secondary antibody (biotinylated anti-human IgG) and detected by incubating the arrays with Streptavidin CY5 dye. The median signal intensities of the spots for the antigen-antibody complexes were calculated and the optimal blocking buffer was selected according to the highest signal intensities and lowest background.

3.3.1 Amino-silane slides

Amino-silane slides have a high concentration of primary amino groups available at the surface. Biomolecules spotted onto the slide surface have amino linkers (NH_2), which covalently linked to the slide surface (Figure 1.5).

The scanned images of amino-silane slides (Figure 3.1) show good spot morphology in terms of the brightness, circularity and size. The shape of the spots were doughnut-round and fairly consistent with all of the blocking buffers. However, the data analysis of spots printed on amino-silane slide using Genipix software programme (Figure 3.2 C + D) showed that I Block buffer gave the lowest background and highest signal intensities for all the autoantibodies to each positive control, with the highest reading for Tetanus and followed by *E. coli* and finally *H. influenza*. *H. influenza* signals were low and no spots visible may due to low concentration of antigens or because one serum sample is used in this chapter so may this individual does not has antibodies against H.I. The

high antibodies levels to Tetanus antigens might be due to the examined subject having received a vaccine against Tetanus. In addition, when comparing the three-dilution curve of hIgG for each blocker (Figure 3.2), the highest signal and best dilution curve fit was with I Block buffer (Figure 3.2 A), and the highest background was observed with mix buffer (I Block+ PVA), which was the same for the three positive control antigens (Figure 3.2 B).

Overall the analysis of the results for the amino-silane slide demonstrated that highest signal intensities of positive antigens and lowest background was shown with I Block buffer, compared to the incubation with PVA only or the mix of both.

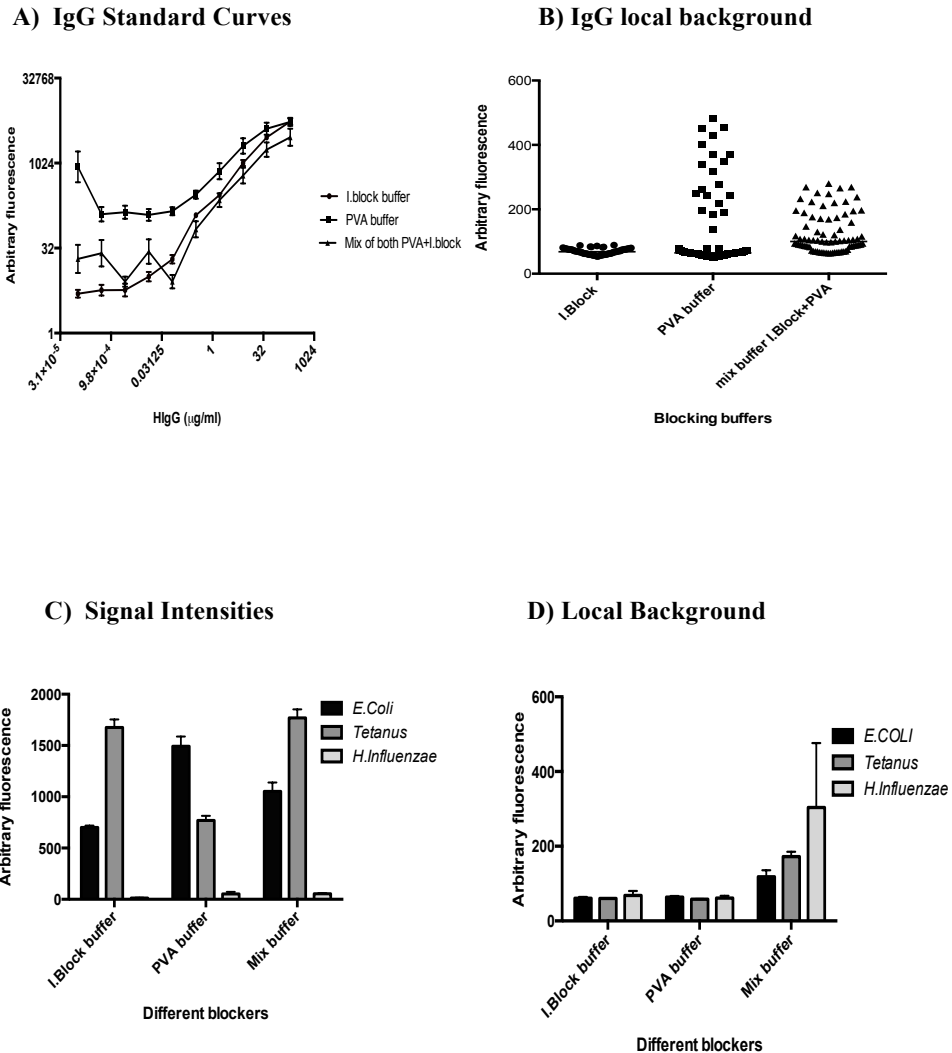


Figure 3. 2: Analysis results of amino-silaine slide:

A) Human-IgG dilution curves that were blocked with different blocking buffers (I Block, PVA and mix of both buffers). B) Background signal of Human-IgG with the three different blocking buffers. C) Signal intensities of IgG antibody responses to *E. coli*, Tetanus and *H. influenzae* antigens from one “healthy” serum sample tested with different blocking buffers (I Block, PVA and mix of both buffers). Results were detected by microarray and are presented as mean (\pm SD) by Prism software. D) Local background for the antigens detected using the three different blocking buffers.

3.3.2 Epoxy-silane slides

Epoxy-silane slides provide an epoxy ring that reacts with the amine group on antibodies and proteins that are spotted. The scanned image of the epoxy-silane slide (Figure 3.3) showed 16 arrays and each set of 4 arrays was blocked by a different blocking buffer. Poor spot morphology and signal intensity were found when the arrays were blocked with PVA (Figure 3.3), with the merging of the spots of hIgG that occurred due to blocking process. The results of data analysis of this image showed the highest signal for the dilution curve of hIgG occurred when the slide was blocked with the mix buffer, compared to other blockers (Figure 3.4 A). The three positive control antigens (Figure 3.4 C) also gave high signals with PVA buffer and the mix of both blocking buffers, but the background readings was the lowest with PVA buffer only for h-IgG (Figure 3.4 B) and positive control antigens (Figure 3.4 D), and the lowest signal intensities were observed when the slide blocked with I Block buffer. Overall this experiment shows that the epoxy slides surfaces are not ideal for antigen microarray.

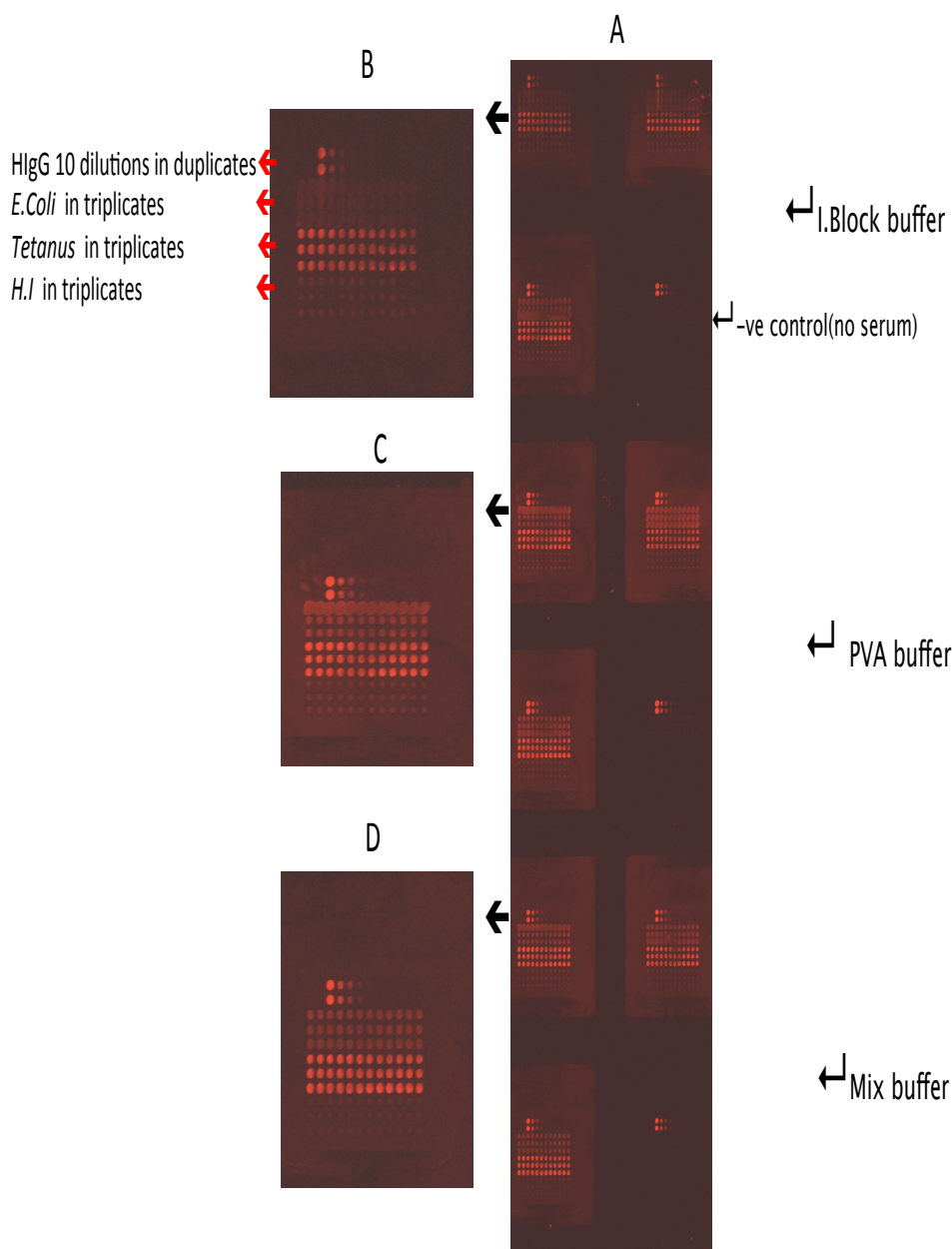


Figure 3. 3: Scanned image of epoxy-silane slide surface with different blocking buffers:

A) The arrays contain 10 dilutions (in duplicate) of the positive control for the secondary antibody HlgG antigen, and the 3 positive control antigens for the serum sample in triplicate printed on epoxy-silane slide, which were blocked with B) I Block, C) PVA and D) a mix of both buffers. The slides were probed with one serum sample at 1:1000 dilutions, and the secondary antibody (anti-IgG) at 1:5000 dilution. The binding between antigen specific-autoantibodies was detected by fluorescence of the CY5 dye. Each of the 4 arrays on the slide was blocked by different blocking buffer.

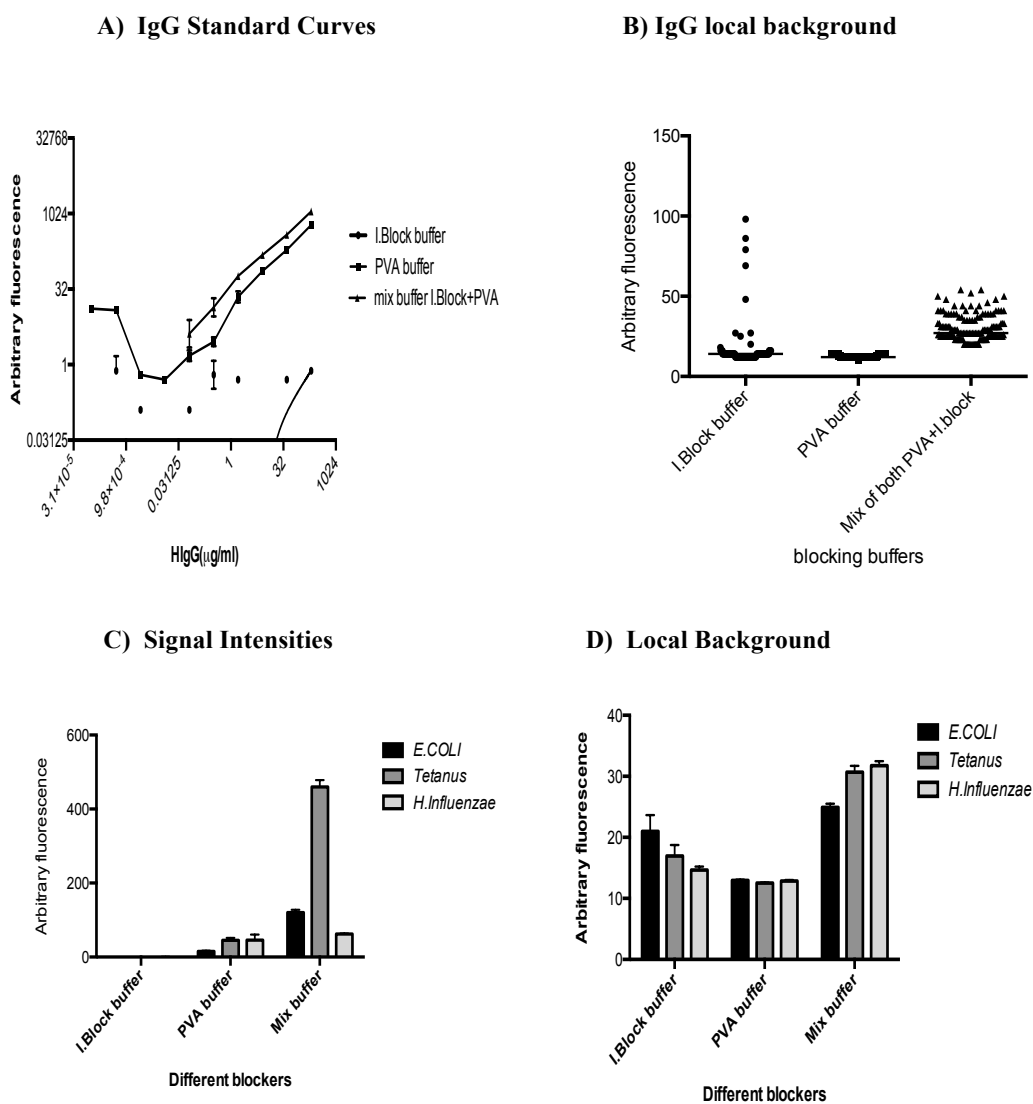


Figure 3. 4: analysis results of epoxy-silane slide surface:

Graphs of data analysis from scanned image of epoxy-silane slide show A) signal intensities of the dilution curves of hIgG with three different blockers (I Block, PVA and mix of both buffers), B) signal of background of Human-IgG with each blocking buffer, C) signal intensities of positive control antigens *E. coli*, Tetanus and *H. Influenzae* and D) Their background with three blockers (I Block, PVA and mix buffer).

3.3.3 Thin film 3D polymer slides (Hydrogel):

The 3D thin film slide consists of a cross-linked, multi-component polymer layer activated with N-Hydroxysuccinimide (NHS) esters to provide covalent immobilization of amine groups.

A scanned image of the slide (Figure 3.5) shows good spot morphology (brightness and circularity) for *E. coli* and Tetanus antigens. After the test serum was added to the slide with all blocking buffers, analysis of the scanned image has shown very low sensitivity and poor uniformity of the standard curves for Human-IgG in all blocking buffers (Figure 3.6 A). There were very high signal intensities observed for the positive control antigens (*E. coli*, Tetanus and even *H. influenza*, Figure 3.6 C). Data analysis for the background of all antigens in all of the blocking buffers were also high, with the best results coming from the mix of both buffers which gave lowest background readings and the highest signal in terms of all positive control antigens (Figure 3.6 C + D). Overall these results show that the thin film 3D polymer coated slide worked for this one time and gave the best results when incubated with a mix of both block buffers, however, intensive efforts were carried out to repeat this experiment but failed, suggesting this is not ideal for future use in antigen microarray.

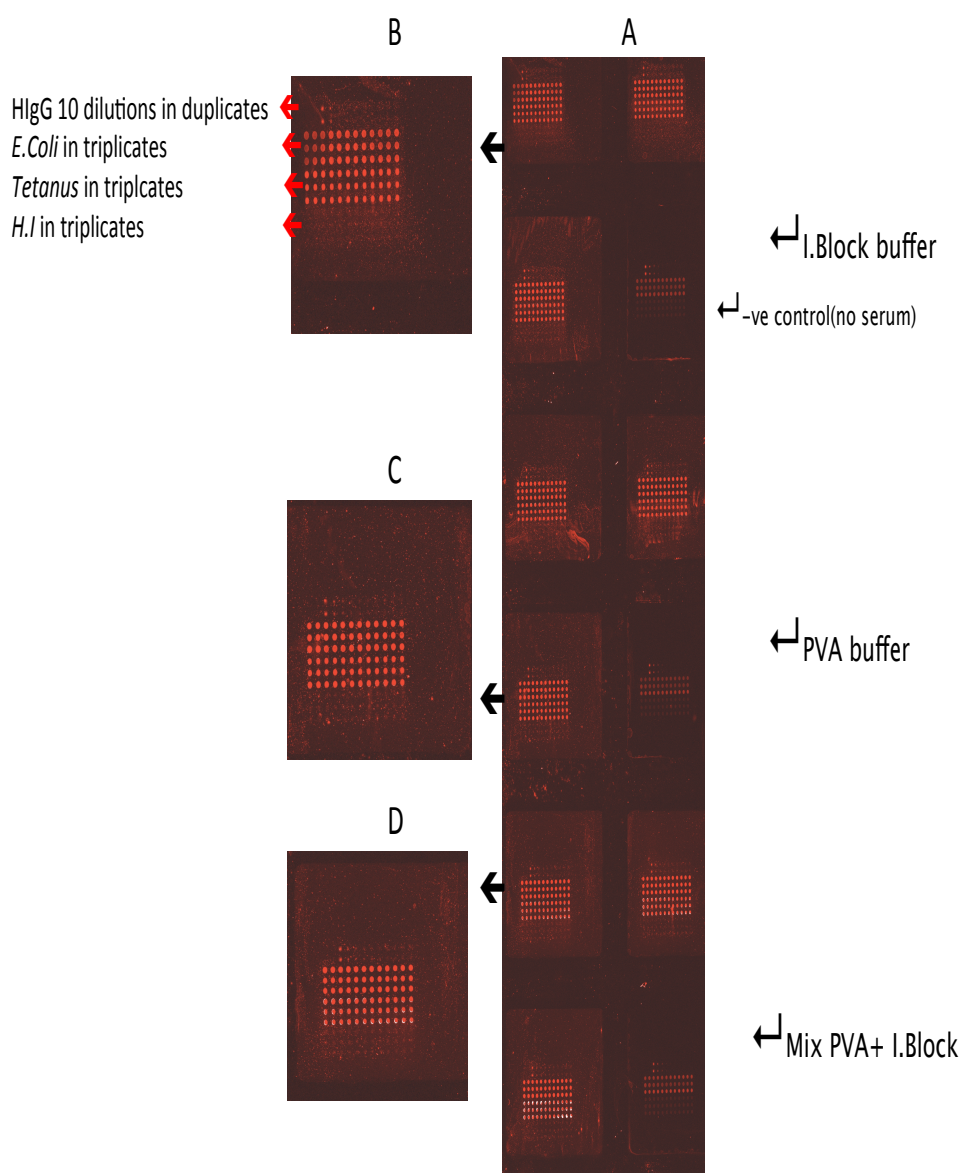


Figure 3. 5: A scanned image of hydrogel slide surface with different blocking buffers:

A) Scanned image of 3D slide contains 10 dilutions (in duplicate) of the positive control for the secondary antibody hIgG antigen, and 3 antigens in triplicates (as positive controls for the serum sample) printed on 3D slide and incubated with B) I Block, C) PVA and D) a mix of both buffers. The slide was probed with one healthy serum sample at 1:1000 dilution and secondary antibody (anti-IgG) at 1:5000 dilution. The three blocks of the slide as indicates in the image are identical and the 4th block is the negative control without the serum sample. Spot morphology as shown from the image are clear and indicate high signal of positive control antigens except *H. influenza* antigens with all blockers.

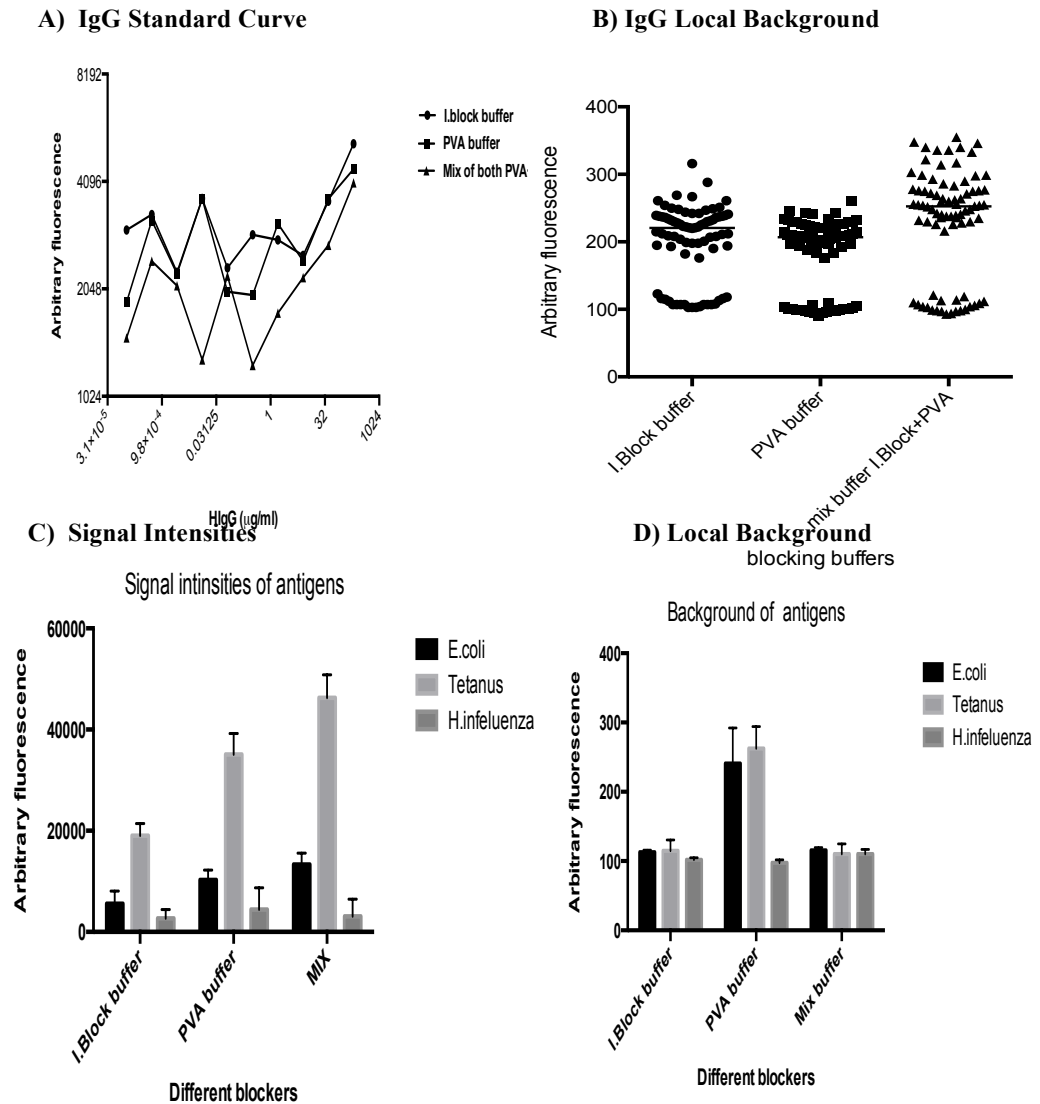


Figure 3. 6: Data analysis of thin film 3D slide surface

Graphs of data analysis from scanned image of the slide (Figure 3.5) show, A) signal intensities of dilution curve of hlgG at three different blockers (I Block, PVA and mix of both buffers). B) Signal of Background of Human-IgG with each blocking buffer. Results are presented as mean (\pm SD). C) Signal intensities of positive control antigens and D) their background and results present as mean (\pm SD). Best signals of all positive antigens are with mix of both blocking buffers which also gave the lowest background.

3.3.4 Aldehyde slides

The capture mechanism of this slide involves the uniform surface features aldehyde groups that readily react with primary amino linkers (NH₂) on the spotted biomolecules to form covalent bonds.

The scanned slide image (Figure 3.7) shows excellent spot morphology of the Tetanus antigens in particular, which had a very high signal with all the blocking buffers. The spots of human hIgG dilutions were spotted in order according to the dilution from the highest to lowest one, and these also showed good spot morphology. Upon data analysis of the results for the hIgG and control antigens by Genepix software, the lowest background signal for hIgG was with I Block buffer (Figure 3.8 B) and for control antigens were with both I Block and PVA buffer (Figure 3.8 D). The highest signal intensities for control antigens were observed with I-Block buffer (Figure 3.8 C), however the dilution curves of hIgG had low sensitivity (Figure 3.8 A). Overall these results showed similar performance as to the amino-silane slide with same blocking buffer.

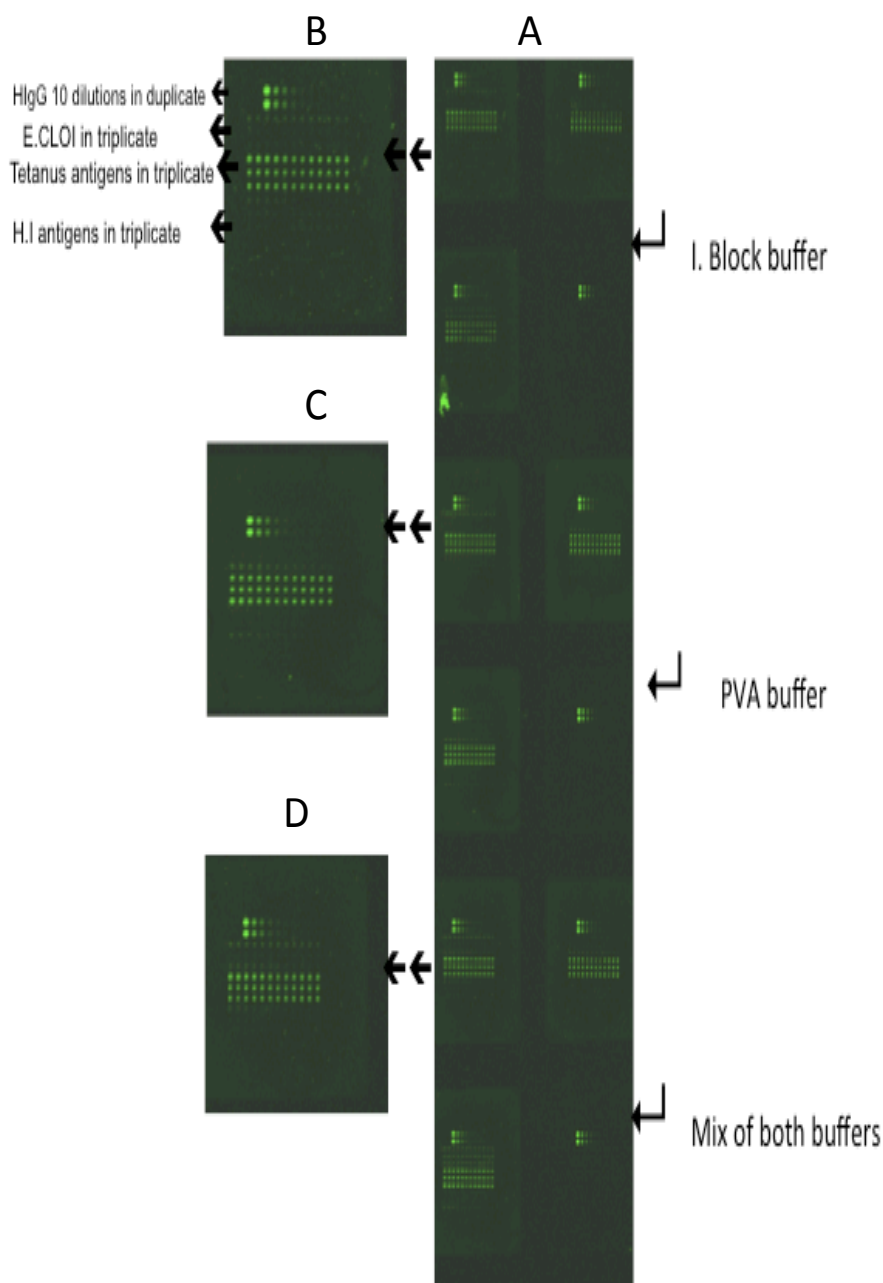
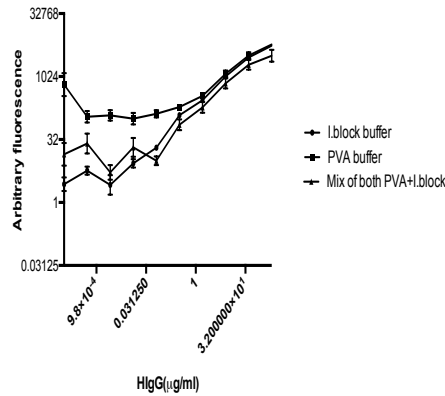


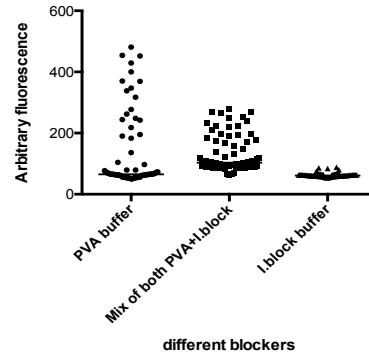
Figure 3. 7: Spots morphology of aldehyde- slides with different blocking buffers:

A) Scanned image of Aldehyde slide includes 10 dilutions of human-IgG and 3 different positive control antigens (*E. coli*, Tetanus and *H. influenza*) printed on an aldehyde slide and incubated with 3 different blocking buffers B) I Block, C) PVA buffer and D) a mix of both I Block and PVA. The slide was probed with one healthy serum sample followed by anti-IgG secondary antibody; signals then were detected by fluorescence CY3 dye using a Genepix scanner. As shown from the image each 4 arrays were incubated with different blocker, I block buffer gave the best spot morphology with lowest background.

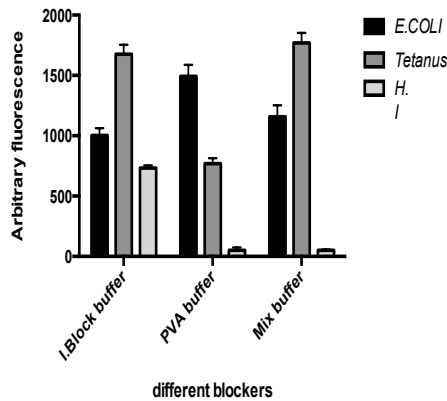
A) IgG Standard curve



B) IgG Local Background



C) Signal Intensities



D) Local Background

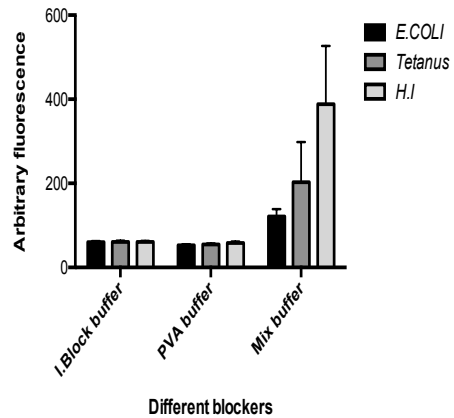


Figure 3. 8: Data analysis of aldehyde slides surface.

Graphs show A) signal intensities of hIgG dilution curves with three different blocking buffers I Block, PVA and mix of both buffers I Block, PVA and mix of both buffers. As shown from the graph, the curves had low sensitivity but compared together I Block buffer was the best. B) Background readings for hIgG at same blocking buffers, showing that I Block gave lowest background. C) Signal intensities for three positive control antigens (*E. coli*, Tetanus and *H. influenza*) with different blocking buffers, D) their background with the same blocking buffers. As shown from graph (C) the highest signal intensities of the three antigens were observed with I Block buffer and the background of these antigens was also low with this buffer.

3.3.5 Summary of optimisation using the different slide types

The amino-silane and aldehyde slides perform equally well with the I Block blocking buffer, as this gave the highest signal intensities and lowest background for both the standard curves and positive controls. Overall the results were slightly better with the amino-silane slide, so this was selected for future experiments. However, the sensitivity of the assay was still considered to be insufficient so further tests were carried out to test different methods to amplify the signal.

3.3.6 Amplification

3.3.7 Testing different concentrations of 3DNA amplyfier

Amplification was used to improve the sensitivity for the lowest concentrations of the standard curves to enable relative quantification of the low abundant antibodies. Signals were amplified using the 3DNA nanotechnology, which is commercially named Genisphere (more details in the material and methods chapter).

Eight concentrations of Genisphere were tested with an amino-silane slide to find out which was the optimum concentration of Genisphere suitable for amplifying the signals. 10 dilutions of hIgG in eight replicates, a 1:10 dilution of Tetanus, *E. coli* and *H. influenza* antigens (in 12 replicates) were printed on the surface of amino-silane slide in the first day and incubated in a desiccator. The next day, the slide was blocked with I Block buffer for one hour then probed with one “healthy” serum sample followed by anti-IgG as the secondary

antibody. The binding between IgG antibody and control antigens was detected by fluorescence. The experiment was repeated different times to confirm the results.

An exemplar image of the scanned slide showed the spot morphology were fairly consistent and did not vary between dilutions (Figure 3.9). IgG dilutions curves were generated at eight different dilutions of amplifier (Genisphere), the mean results of the all experiments showed reproducible signals intensities and background in all the eight dilutions (Figure 3.10 + 3.11) with slightly lower background at 1:200 dilution of Genisphere (Figure 3.10). Furthermore, as expected, a reduction in signal intensity was observed with increasing dilution of Genisphere. Overall, this amplification method using Genisphere worked well at any dilutions as observed from the experiments however, evaluating concentrations of each control antigen in the serum sample was also required at these eight dilutions of Genisphere.

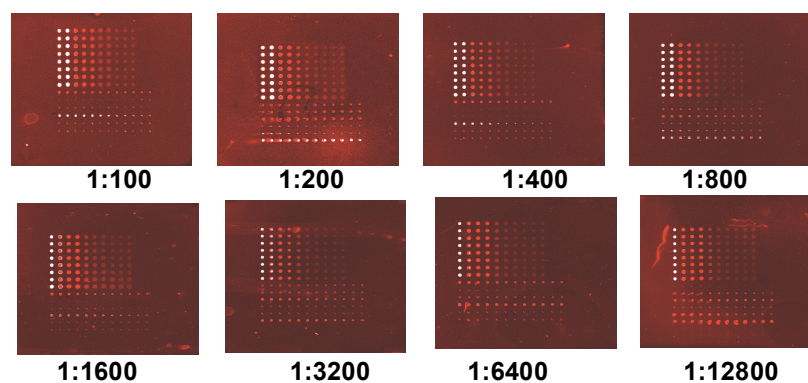
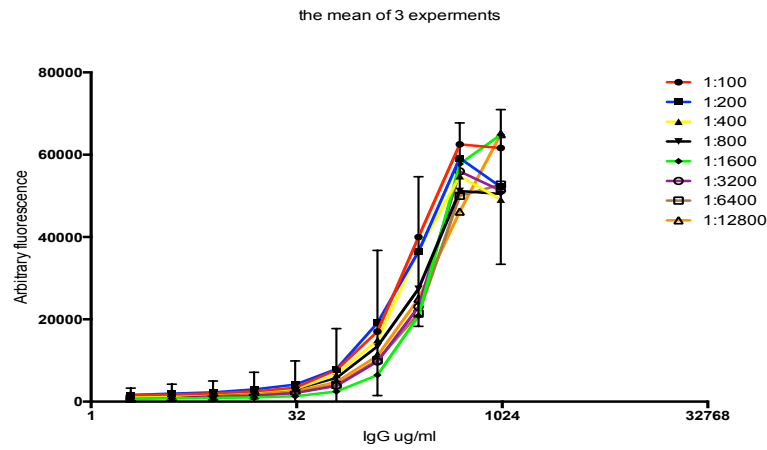


Figure 3. 9: Spots morphology of testing different concentrations of Genisphere amplifier with amino-silane slide:

Scanned images of eight arrays of amino-silane slide, which include 10 dilutions of HIgG in 8 replicates and positive controls (*E. coli*, Tetanus and *H. influenza*) in triplicates. Each array was amplified with a different concentration of Genisphere amplifier.

A)



B)

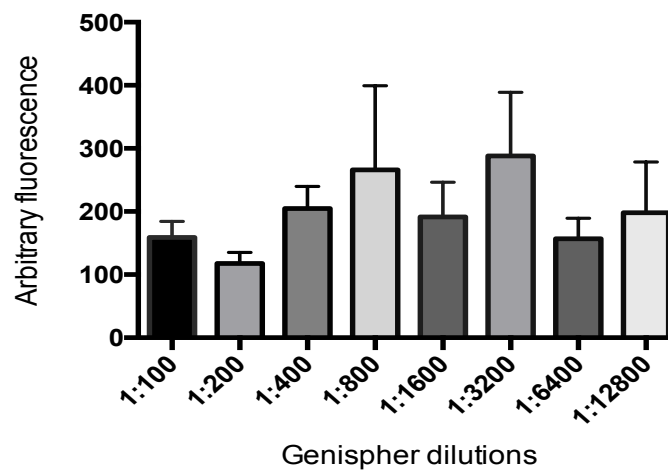


Figure 3. 10: Data analysis of scanned arrays of aminosilane slide for IgG dilution curve at eight dilutions of Genispher amplifier.

A) represents the mean with SD of human-IgG dilutions curves obtained from different experments (n = 3) at different dilutions of Genisphere amplifier. the highest signals intinsities of dilutions curves observed with 1:100 dilution of Genisphere. B) represents of background signals for the eight curves per dilution. 1:100 and 1:200 dilutions show low backgrounds reading with compare to otherdilutions.

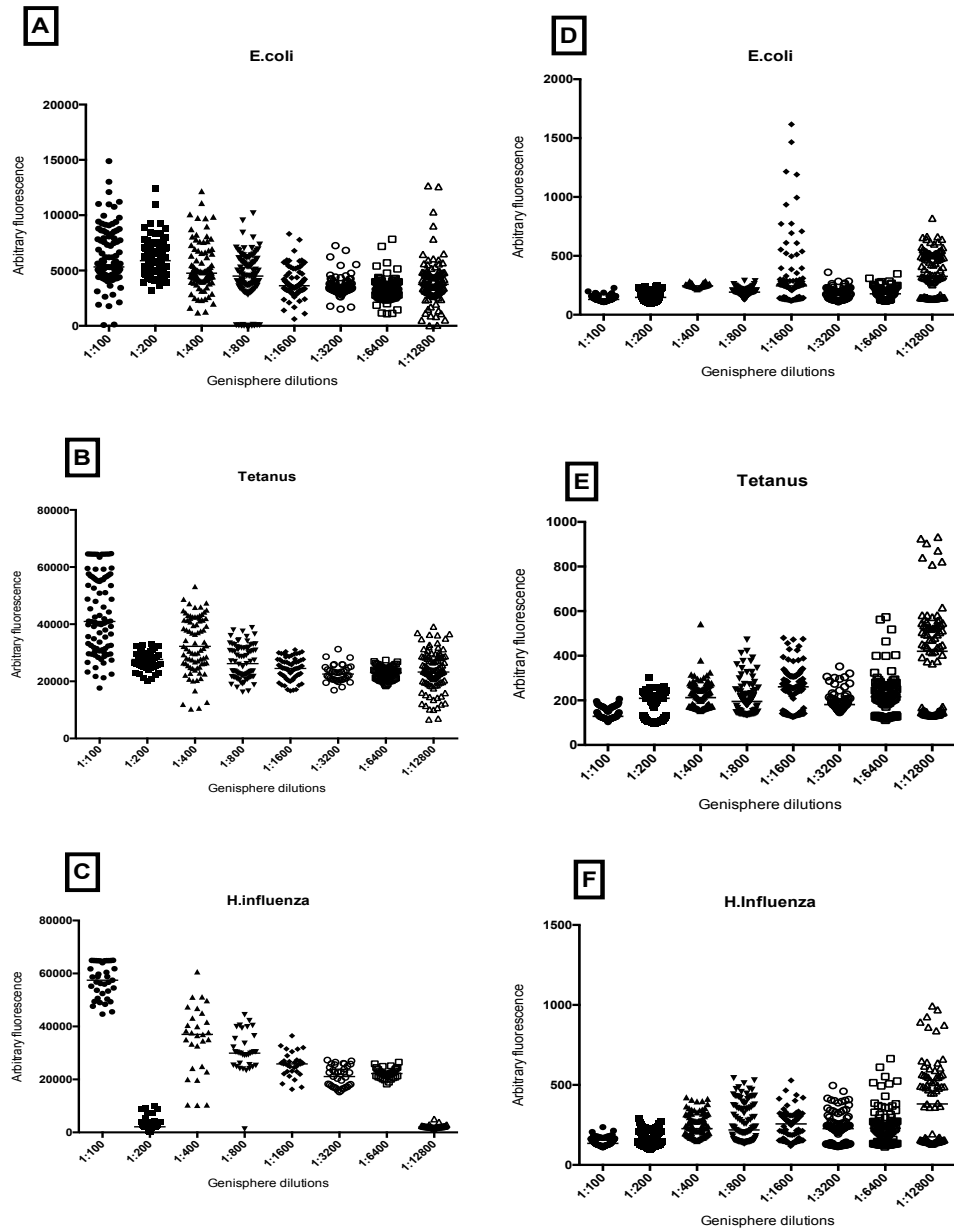


Figure 3. 11: Data analysis of scanned arrays of amino-silane slide for control antigens at different dilutions of Genisphere.

Graphs (A, B and C) represent the mean of signals intensities of autoantibodies against each control antigen; *E. coli*, Tetanus and *H. influenzae* printed on amino-silane slide for one serum sample, at eight different dilutions of amplifier (Genisphere) obtained from different experiments ($n = 3$). The highest signals were observed with (1:100) dilution of amplifier for all control antigens. Graphs (D, E and F) represent the background readings for these control antigens respectively which show also lowest given background was at 1:100 dilution of Genisphere.

3.3.8 Measuring the concentration of control antigens at different dilutions of Genisphere amplifier

Optimising the dilutions of Genisphere needed to amplify the signal is necessary to find out the optimal dilution of the amplifier that increases the sensitivity of the assay for the lowest concentrations of low abundant antibodies. After testing the signal intensities for the dilution curves and control antigens at the eight different dilutions of the amplifier it was found that 1:100 dilution seems to be suitable to use. Testing the concentrations of control antigens after interpolating them on standard curves at the eight dilutions of Genisphere also was required to evaluate the best dilution as well that gave the most reproducible concentrations. Values of control antigens were interpolated on the IgG standard curve of one serum sample at eight different dilutions of Genisphere (Figure 3.12). Then the interpolated values (mean) were presented as concentrations of each antigen (Figure 3.13). The highest concentrations for IgG antibodies against *H. influenza* and Tetanus antigens were observed with 1:100 dilution in contrast to other tested dilutions. Interestingly, *E. coli* always gives low signals, whatever the concentration of Genisphere, and that may be due to low concentration of protein in *E. coli* lysate or because the antibodies in this serum sample has no response against *E. coli*.

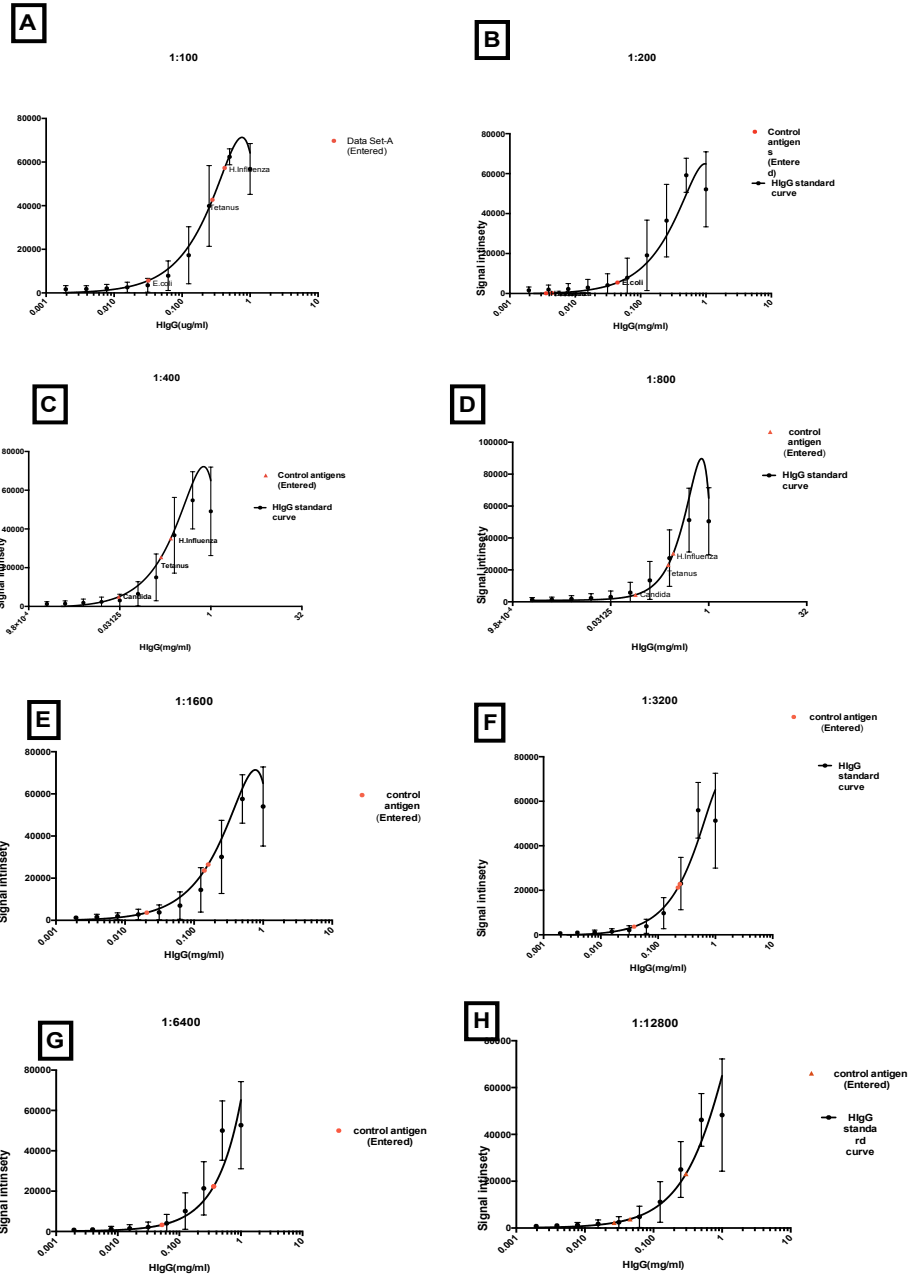


Figure 3. 12: illustrated the interpolation of control antigens on HIgG standard curve at eight dilutions of Genisphere.

Graphs above represent IgG standard curve in one serum sample and interpolated mean values of control antigens on a standard curve at eight different dilutions of Genisphere from (A) 1:100, (B) 1:200, (C) 1:400, (D) 1:800, (E) 1:1600, (F) 1:3200, (G) 1:6400 and (H) 1:12800, respectively. Red spots represent the interpolated antigens and statistical analysis was done by prism6 software.

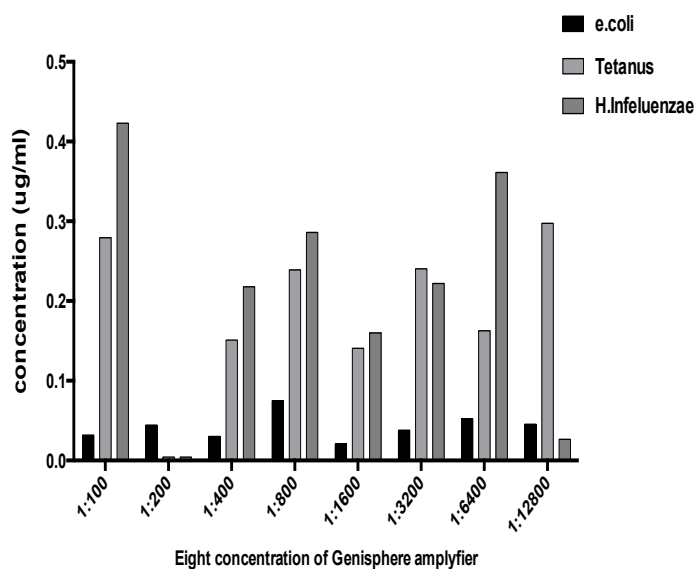


Figure 3. 13: concentration of autoantibodies -specific control antigen at eight different dilutions of Genisphere.

The graph shows the concentration of each of the autoantibodies in a healthy serum sample against three positive control antigens (*E. coli*, Tetanus and *H. influenzae*) in eight different concentrations of Genisphere amplifier. Autoantibodies specific *H. influenzae* shown the highest concentration with 1:100 dilution however, in the dilution 1:6400 the concentration of both antigens (*H. influenzae* and tetanus) were high and very low at 1:200 irrespective of *E. coli* concentration which was mainly reproducible with all dilutions of Genisphere.

3.4 Discussion:

A microarray that achieves a consistently good performance can be obtained by evaluating and optimizing all essential aspects that could affect sensitivity and reproducibility. Within this study the aspects that were examined and optimized were the slide surface chemistry, detection method and blocking buffer. The correct choice of surface chemistry has a direct influence on the critical step of immobilization in the assay. Spot morphology can determine the quality of the performance of a test slide, for example the amino-silane slides gave a high performance, and the epoxy-silane slides had a poorer performance, which agrees with previous studies[151] [170]. Although Hydrogel slides worked well in other studies[171] [172], in this study antigens cannot bind onto the slide surface and even the once that this slide worked, it was difficult to analyse the slides and generate good standard curves. Aldehyde slide surface also has been tested in previous studies for antigen microarray application but was tested with different conditions like; printing buffers and blocking buffers for instance[173], in this study aldehyde slides also and amino-silane slides perform equally well, but for future experiments amino-silane slides with I Block blocking buffer were selected as these conditions were good for both standard curves and positive controls.

Another important factor affecting the development of antigen microarray is non-specific protein binding by affecting the background and spot signals. Therefore, optimizing blocking buffers (I-Block buffer, polyvinyl alcohol (PVA) and the mix of both buffers) in this study was required in order to reduce any non-specific binding.

The signal intensities for *H. influenza* were always low and this might be because when not using amplification the signal intensities were very low, or it

may be due to the serum sample of this specific subject, which has been used in all experiments in this chapter.

In general, the signal intensities were very low in all experiments, which was not as expected, as the detection of the binding of autoantibodies to candidate autoantigens is the main purpose of this study during microarray optimisation and thus, in order to improve the signal intensities amplification was required.

The sensitivity of any diagnostic assay can be affected by the level of amplification that occurs within the assay. This means it is important to determine the most suitable method of amplification which will increase the dynamic range of detection and sensitivity. Fluorescent detection methods commonly employ conjugated fluorescent dyes which have a good dynamic range, but can produce lower sensitivity[174]. There have been many advances that have led to improvements in detection methods, for example amplification by a fragment of DNA conjugated to streptavidin and fluorescent dye molecules (referred to as Genisphere). Different concentrations of signal amplifier (Genisphere) were incubated with three different antigens and a human IgG dilution curve to find the optimum conditions for the highest signal to background ratio. After testing Genisphere from several experiments, the results showed that high concentrations of control antigens were detected at a dilution of 1:100 of Genisphere and so, this dilution of the amplifier was chosen to be used to amplify the signals intensities of examined antigens over experiments. Another study has shown the successful use of this 3DNA method (Genisphere) in processing DNA microarray which provide a high arbitrary signal and acceptable backgrounds[175].

3.5 Conclusions:

The findings of this chapter show that a combination of amino-silane surface and I Block buffer gave the highest quality performance when compared to other tested slides surfaces and blocking buffers. The results show that a signal amplifier was required to improve the sensitivities of the assay and the optimal dilution of the Genisphere amplifier observed at 1:100.

4. Validation of an Antigen Microarray Platform

4.1 Introduction:

The key aspect of any bio-analytical method is the measurements of proteins or analytes in a biological sample like serum. However, for an assay to be considered suitable, a series of validity tests should be performed to prove it can be both accurate and reproducible. In the case of an antigen microarray, the following validity tests were investigated:

- A) Limit of detection
- B) Reproducibility
- C) Precision (intra and inter assay)
- D) Cross-reactivity
- E) Comparison between microarray and ELISA technique

These five tests serve to provide a firm investigation into the nature of the antigen microarray technique, and will allow decisions to be made as to whether the antigen microarray is a reliable method to ultimately measure multiple proteins in the serum samples of COPD[176].

For microarrays, assay precision is defined as the coefficient of variation (CV %) between measurements within same slide (intra-assay), or across a few days and different slides (inter-assay). To calculate the CV % the standard deviation of multiple measurement repeats is divided by the mean of the same repeats. At each concentration level the precision should not exceed 15 % of the CV[177].

The smallest concentrations that can be measured reliably by an analytical technique are referred to as the limit of detection (LOD), the limit of quantification (LOQ), and the

limit of blank (LOB). There are various approaches to determine LOD due to a lack of agreement of how to describe a LOD. For the traditional method used in this thesis, LOB measures the highest *apparent* concentration of analyte determined by repeat measures of a sample containing no analyte (blank)[178]. The LOD measures the lowest concentration of analyte that can be detected and distinguished reliably from the LOB, meaning the LOD has to be higher than the LOB. The standard method for determining the LOD involves measuring replicates ($n = 20$ usually) of a blank or zero calibrator, then calculating the mean and standard deviation (SD), and the LOD is calculated as the mean plus 2 SD[179] [180] [181].

The LOQ measures both the highest (ULOQ) and the lowest (LLOQ) points (expressed as concentration) that can be quantified and detected in an assay with an acceptable level of precision and accuracy. The LLOQ is usually higher than or equal to the LOD, but it should not be lower. The LOD, LLOQ and ULOQ can all be measured using standard curves to determine the concentration[182] [183].

Cross-reactivity tests for any given assay are important, and in this chapter investigations were carried out to ensure that no-cross reactivity occurs in this microarray platform. Ideally, the microarray platform should be specific for the target analytes, and show no cross-reactivity with other analytes printed on the slide in the same experiment. The number of proteins that can be used on a multiplexing platform is usually affected by cross reactivity that occurs between the detection antibodies and the capture antibodies. A non-specific analyte also can cause cross reactivity. However, it is thought that the other reagents in which antibodies are diluted could produce cross reactivity in the assay; for example, a large background signal and low sensitivity of the assay can result from non-specific binding during the assay. In addition, there is also evidence to show that some reagents can irreversibly affect the protein structure in the array due to their pH,

hydrophobicity or ionic strength, which can lead to a reduction of efficiency of the array through cross reactivity[184] [185].

Within this thesis another important factor in assay development was a comparison between ELISA and microarray techniques, as this tested the level of correlation between existing methods and the newly developed assays, especially as the antigen microarray was developed from ELISA for protein detection.

4.2 Materials and methods:

For validation, amino-silane slides were used to measure the concentration of antibodies against control antigens in healthy patient serum samples; briefly human IgG antibody was printed in 10 dilutions on the slides to generate standard curves. *Candida*, Tetanus and *H. influenza* antigens also were printed as positive control antigens and the slides were processed the next day. They were blocked with I Block buffer for one hour, washed, and then 100 μ l of eight healthy patient serum samples were added, after dilution of 1:1000 in antibody diluent solution, into corresponding wells on the slides, and incubated for one hour. After washing, 100 μ l of the appropriately diluted biotinylated detection antibody was added and incubated for one hour. Finally, 50 μ l of Genisphere amplification reagent was added for 10 minutes in the dark. Slides were washed after each step using PBS tween washing buffer. The last wash was carried out three times with PBS tween washing buffer and once with ultrapure water, then centrifuged dry and scanned with the 4200 AL microarray scanner at 635nm (Axon GenePix®). Fluorescence was quantified using the GenePix Pro Software (Axon GenePix®), and the median fluorescence of each spot was measured (minus background).

To investigate the level of correlation between ELISA and antigen microarray assays, an

ELISA experiment was performed using the same positive control antigens and eight healthy patient serum samples. The 96 well microtiter plate was coated with 10 dilutions of human IgG for the standard curve. In addition, 100 μ l of the same positive control antigens were added at 10 μ g/ml and incubated overnight at room temperature. The plate was washed three times using wash buffer (PBS-0.05 % Tween-20) and then blocked with 300 μ l of 0.2 % I Block buffer, and incubated for 1 h. The plate was then washed three times using the same wash buffer. Eight serum samples were diluted 1:100 in protein diluent buffer and 100 μ l sample was added to the plate. Positive control wells for each serum (NO coat), and negative control wells (no serum) were left with blocking buffer only. The plate was then incubated for 2 h at room temperature, then washed three times, secondary antibody was added to all the wells (Biosource anti human Ig-G – Biotin), covered, and incubated for 2 h at room temperature.

The enzyme linker (Streptavidin- HRP) was then diluted 1:200 and 100 μ l added per well, which was covered and incubated for 20 minutes at room temperature. The plate was washed again three times. Finally, equal volumes of substrate development solution (solution A and solution B) were mixed to give a total volume sufficient for 100 μ l per well. The plate was incubated for 5-30 minutes to allow for colour development, and after incubation the plate was not washed, instead 50 μ l of stop reaction (H_2SO_4) was added to each well then the color change was detected (OD) on Flourostar optima plate reader software. The concentrations of control antigens were interpolated from the standard curve for each serum sample. Finally, the level of correlation was investigated between the ELISA and microarray methods.

For the microarray platform, concentrations of the three positive controls were interpolated from the IgG standard curves which were generated from the eight healthy patient serum samples. The LOD was determined as the mean of blank plus 2 SD. The

blank was the empty spots in the negative control pad of the slide that did not contain serum.

To determine the precision (CV %) of the microarray, intra- and inter variability assays were performed. Intra-assays were performed repeatedly over the same slide on the same day, and inter-assays were performed between different days.

Different experiments were conducted to test for cross-reactivity in the antigen microarray platform. In addition, human IgG, IgA and IgM were printed on amino-silane slides in replicates, blocked with I Block buffer, followed by the addition of the biotinylated detection antibody (anti-IgG, anti-IgA and anti-IgM) to identify any cross reactivity between the detection antibodies.

4.3 Results:

4.3.1 Limits of detection

The LOD is defined as the lowest detectable value of a sample that can be distinguished from a blank, lacking the protein of interest. It can be calculated as the mean of blank plus 2 SD of the blank. The results for eight serum samples (Figure 4.1) show that for

these samples the *H. Influenza* antibody response was below the LoD, but IgG autoantibodies responses to Tetanus and Candida were detected at different levels for each patient.

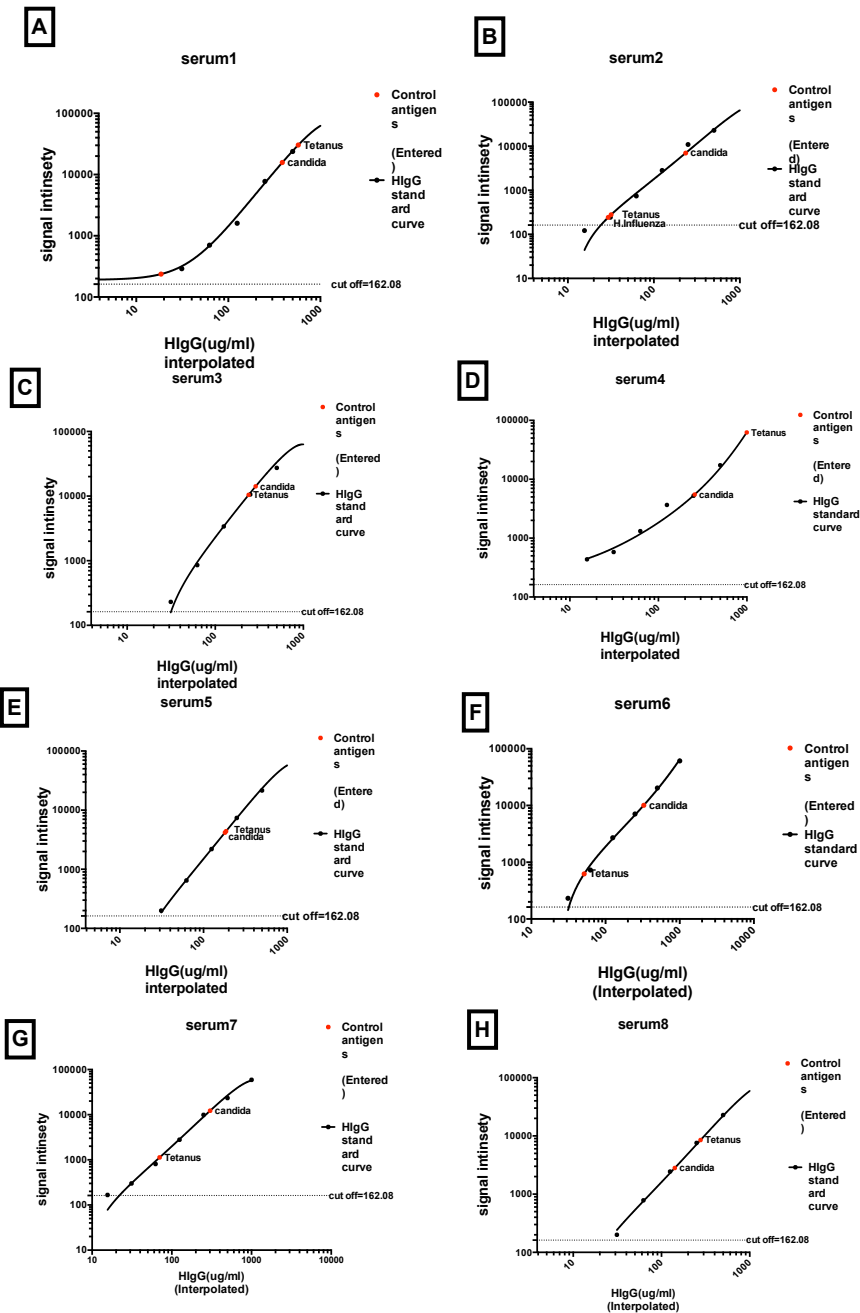


Figure 4. 1: Assay limit of detection.

The x-axis represents the semi-log dilution of IgG standard curve, and the y-axis represents the fluorescence signal. The dashed line represents the limit of detection (LOD = 162.08). Red spots represent the control antigens (Candida and Tetanus) interpolated on IgG curves per each serum sample (A to H) (n = 8).

4.3.2 Reproducibility

Over three different days the signal detection was investigated to determine how reproducible the assay was in terms of signals intensities and background. To do this the IgG dilution curves and eight serum samples were tested on the three consecutive days (figure 4.2 A, B + C), and the results showed a good level of reproducibility. The signals of antibody responses to control antigens were also investigated on the same three days (Figure 4.2 D, E + F), and showed good reproducibility with the highest signals for Tetanus antibodies was detected with serum sample 4, which may be due to an immunization against Tetanus that this individual may have had.

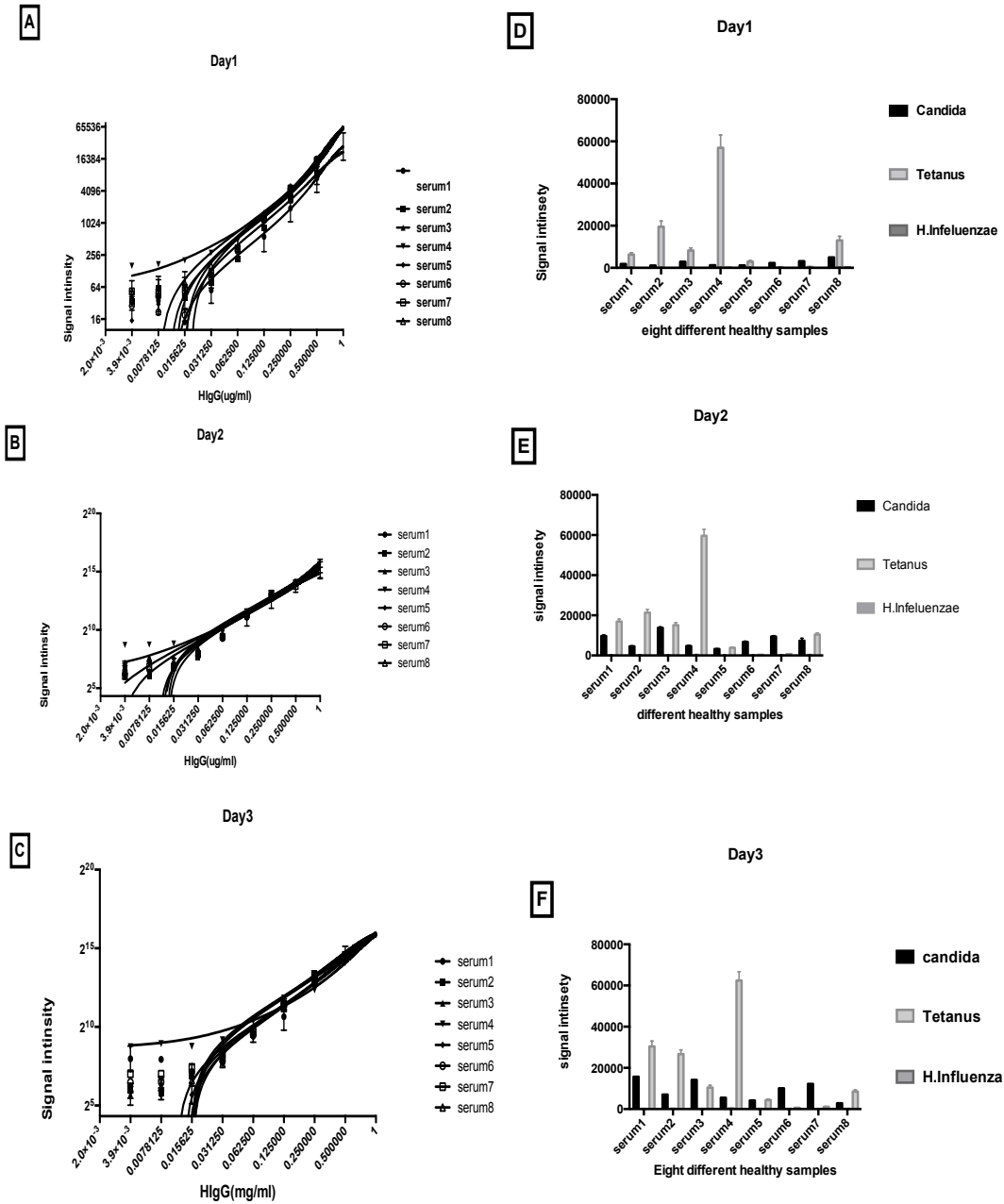


Figure 4. 2: Reproducibility of signal detection for antigen microarray

A, B, and C graphs represent the signals of IgG dilutions curves generated from 8 healthy serum samples on different days (n = 3). D, E, and F graphs represent the signals of the control antigens (Candida, Tetanus and *H. influenzae*) on the same three days. Tetanus antigens shows highest signal intensities compared to the other control antigens in serum 4 for all three days. In general, the signal over the different days showed reproducibility for the dilution curves and control antigens for all eight serum samples.

4.3.3 Assay precision

The measurements of antibodies to antigens on the same slide surfaces, and on different days, were assessed to measure the reproducibility by measuring intra- and inter-assay precision (CV %). The intra-assay precision was assessed on one day after printing and inter assay on three different days (different slides). In the intra-assay test (Figure 4.3 A). It was found that the antibody responses to *Candida* and Tetanus antigens produced a CV % of less than 10 %, which is within the acceptable limit of this assay. However, the CV % of the antibodies to *H. Influenza* antigen was variable (figure 4.3 a), possibly due to very low IgG levels detected, only two of the eight serum samples tested had detectable levels. In terms of inter-assay (Figure 4.3 B), antibody responses to all antigens investigated produced an acceptable inter-assay range of CV =15 %.

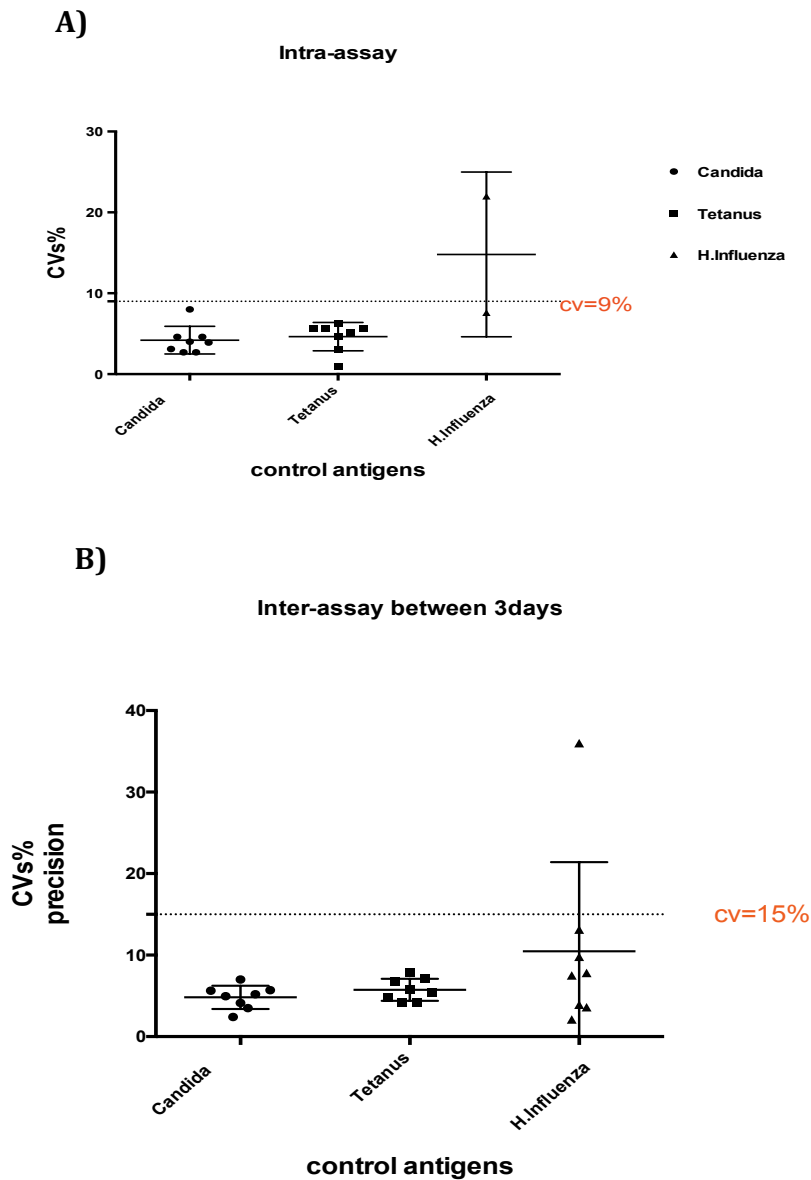


Figure 4. 3: precision of three positive control antigens

A) Intra -assay coefficient of variation (CV %) for the antibody responses to three positive control antigens (Candida, Tetanus and *H. Influenza*) within same slide. Each represents 24 replicates of the eight serum samples. The x-axis represents each antigen and Y-axis represents the CV % measurements. The dashed line represents the acceptable limit of precision (CV % \leq 10).

B) Inter -assay coefficient of variation (CV %) for the antibody responses to three positive control antigens (Candida, Tetanus and *H. Influenza*) between different slides on different days. Each represents 24 replicates of the eight serum samples. The x-axis represents each antigen and Y-axis represents the CV % measurements. The dashed line represents the acceptable limit of precision (CV % \leq 15).

4.3.4 Cross-reactivity

Cross-reactivity is an important validity test in antigen binding based assays. A series of experiments were conducted to determine if cross reactivity occurs in this microarray platform. The first experiment was performed to check the anti-IgG cross-reactivity with IgM and IgA by spotting different concentrations of each antibody and probing with only anti-IgG, (Figure 4.4) and this showed a high cross-reactivity with IgA and IgM antibodies.

As a high cross-reactivity was observed in the first experiment, a second experiment was performed to investigate the IgG detection antibody at different dilutions in order to find which dilution of anti-IgG gave no cross-reactivity with IgA and IgM. The results (Figure 4.5) showed that an anti-IgG dilution of 1: 20,000 gave the best results, with low cross reactivity for IgM and IgA, and high signal intensities. Anti-IgA and anti-IgM were optimized in prior study in our lab and the optimum dilution was at (1:20,000) thus, this dilution was tested. This dilution, though acceptable, produced a small percent of cross reactivity which affected slide analysis. To determine if the amplification used caused the cross-reactivity, a series of experiments were carried out using an avidin biotin blocking step before the slides were processed with detection antibodies, and only half the slides were treated with amplification to allow comparisons to be made. The results (Figure 4.6) showed that after stopping the amplification there was no cross-reactivity observed for all antibodies; this may be due to their being low concentrations of biotin in the antibody preparations which get left on the surface of the slide after printing.

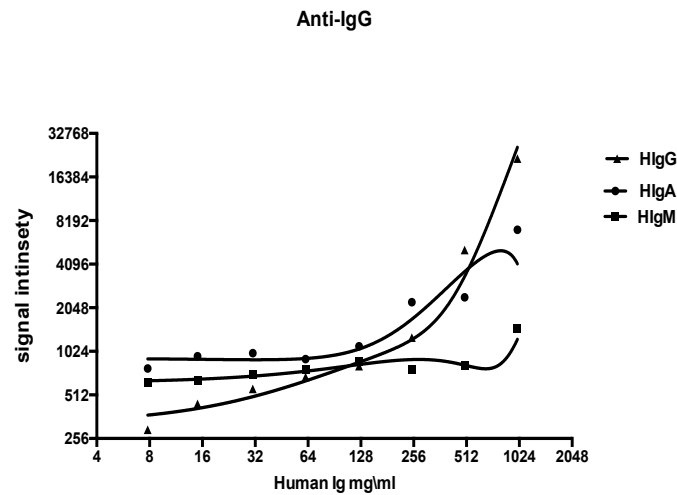
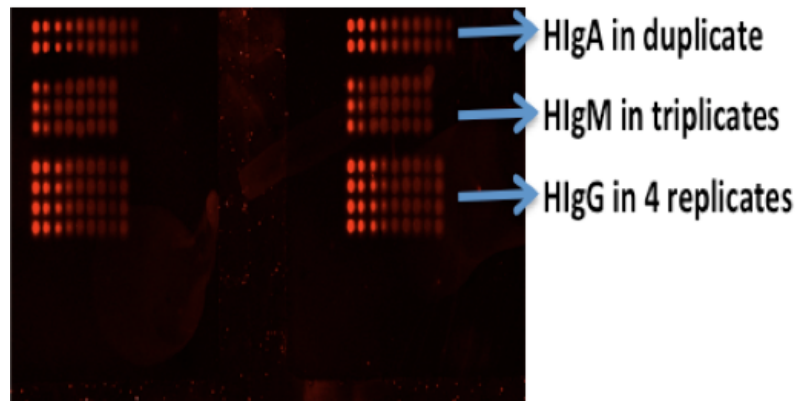


Figure 4. 4: Investigation of cross-reactivity for anti-IgG detection antibody (test 1)

Top) A scanned array showing human IgG, IgA and IgM were printed as ten semi log dilutions (1:5) in different rows to distinguish between them. A high cross reactivity was observed when the anti-IgG detection antibody was added. The image should only show the last four rows for the IgG printed spots, however, the anti-IgG bound with all of the capture antibody isotype spots. Bottom) Data analysis for this test shown a graphical representation of the IgG, IgM and IgA standard curves generated from a microarray panel printed with different capture antibodies and probed by Anti-IgG detection only. IgA and IgM appear to be detected, as shown by an increase in signal intensity of the standard curves, which indicates cross-reactivity occurred in this experiment.

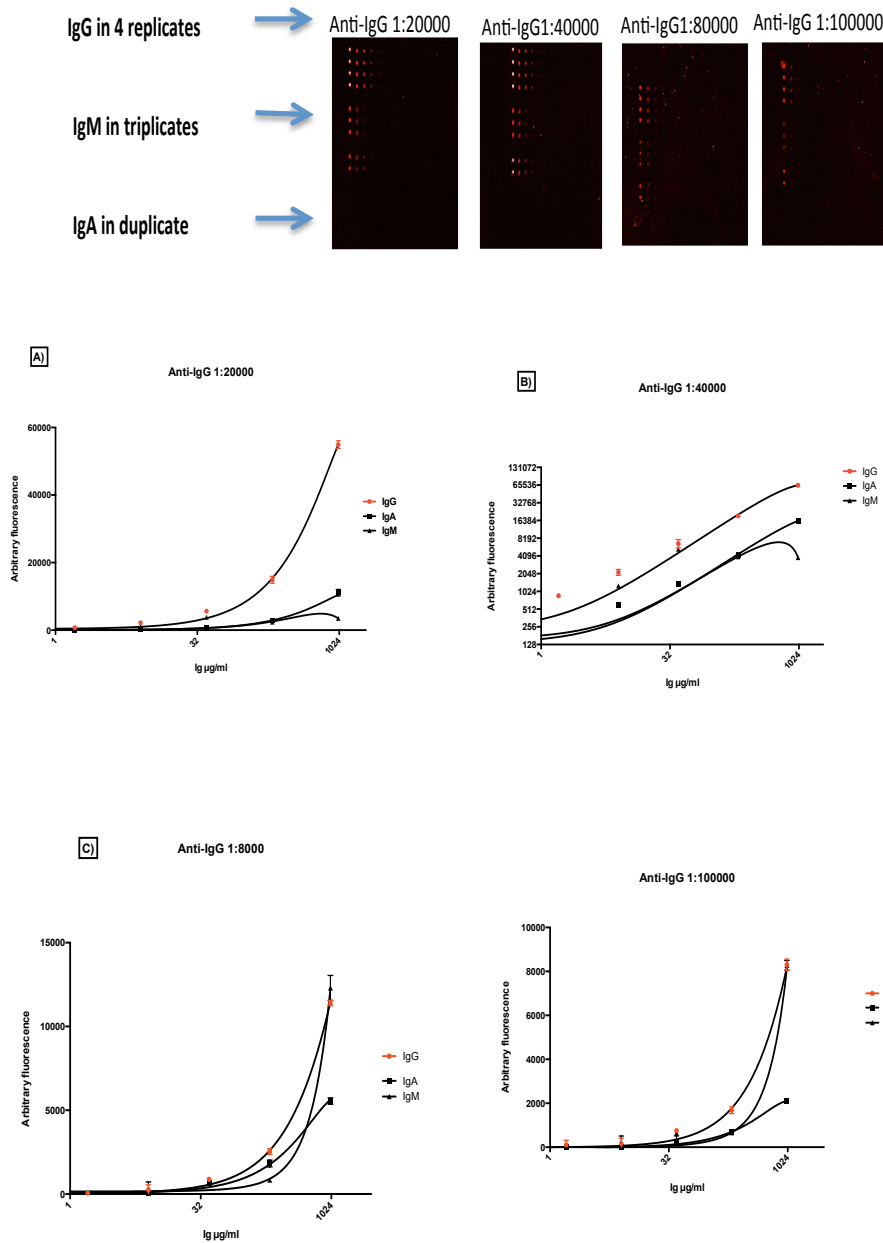


Figure 4. 5: cross-reactivity test with anti-IgG at different dilutions

Top) A scanned array showing human IgG, IgA and IgM were printed in ten dilutions in different rows. Each array was probed with a different dilution of IgG biotinylated detection antibody. As seen from the spots, a small percentage of cross-reactivity was shown in all arrays, and this was confirmed in the data analysis Bottom) Data analysis shown as a graphical representation of the microarray panel printed with a variety of capture antibodies IgG, IgM and IgA. A) Shown anti-IgG at 1:20000 dilution B) anti-IgG at 1:40000 dilution, C) anti-IgG at 1:80000 dilution and D) anti-IgG at 1:100000 dilution. As seen from graph (A) the dilution of 1:20000 of anti-IgG was the optimal dilution as it shows low cross reactivity with IgM and IgA and gave high signal intensities.

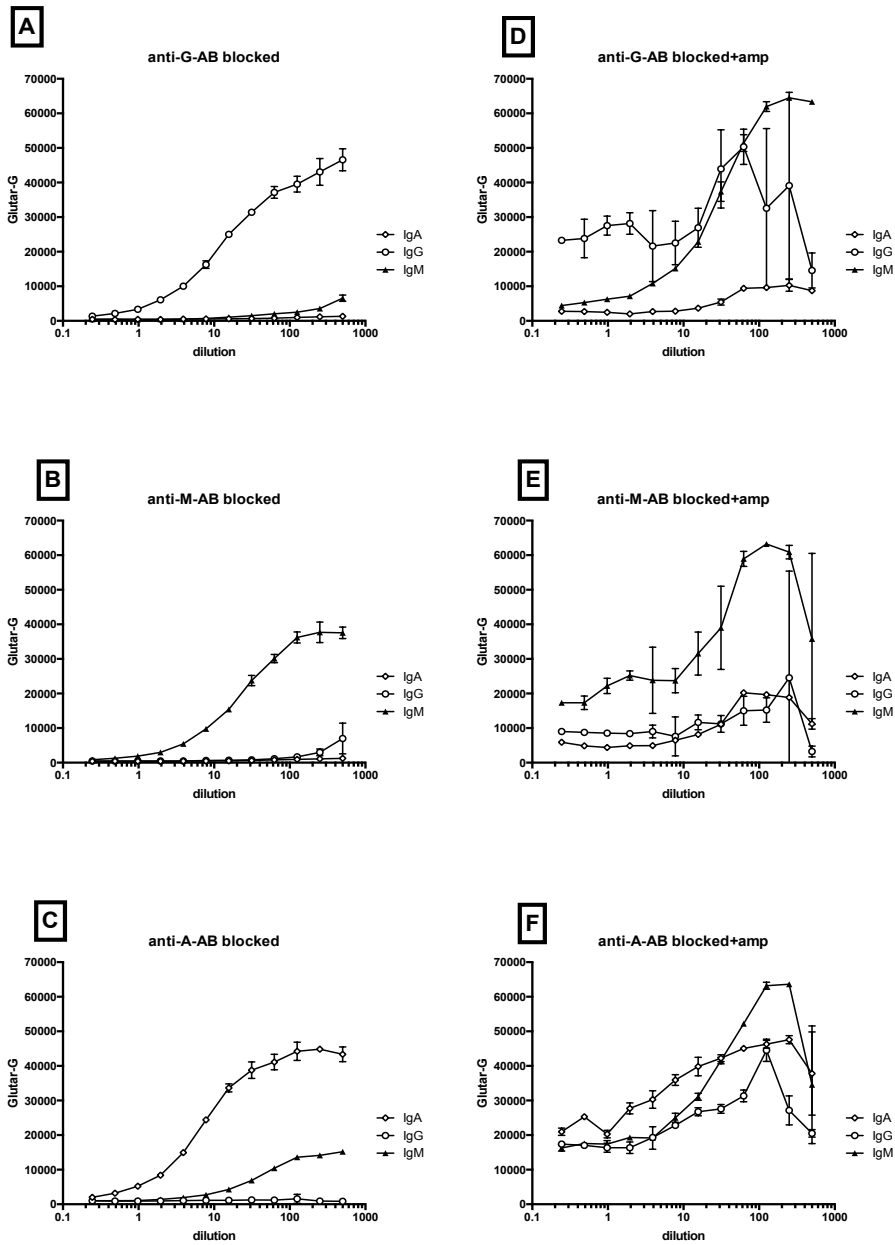


Figure 4. 6: cross-reactivity test of the detection antibodies with and without amplification

Microarrays were printed with dilutions of IgG, IgM and IgA human-antibodies in duplicates. Biotinylated detection antibodies were added: A) anti-IgG, b) anti-IgM and C) anti-IgA. Avidin biotin blocker was added and the in the left panels (A, B, and C) so the graphs represent the results without adding the amplifier (Genisphere), whereas the right panels (D, E, and F) the graphs represent the results with amplification. Without amplification there was no cross-reactivity observed compared to using amplification.

4.3.5 Comparison of microarray technology with ELISA

The next stage of validation was to compare the ELISA and microarray methods in order to investigate if there was a correlation between both sets of results. The concentration of the control antigens (*Candida*, Tetanus and *H. Influenza*) in the eight healthy serum samples was measured by both ELISA and microarray protocols (section 2.2.2 to 2.2.7). The results (Figure 4.7) showed a correlation between both methods, ($p = 0.0002$ for *Candida*, 0.0007 for Tetanus and 0.053 for *H. Influenza*). The lack of a significant correlation for *H. Influenza* is probably due to the low signal produced in the samples tested.

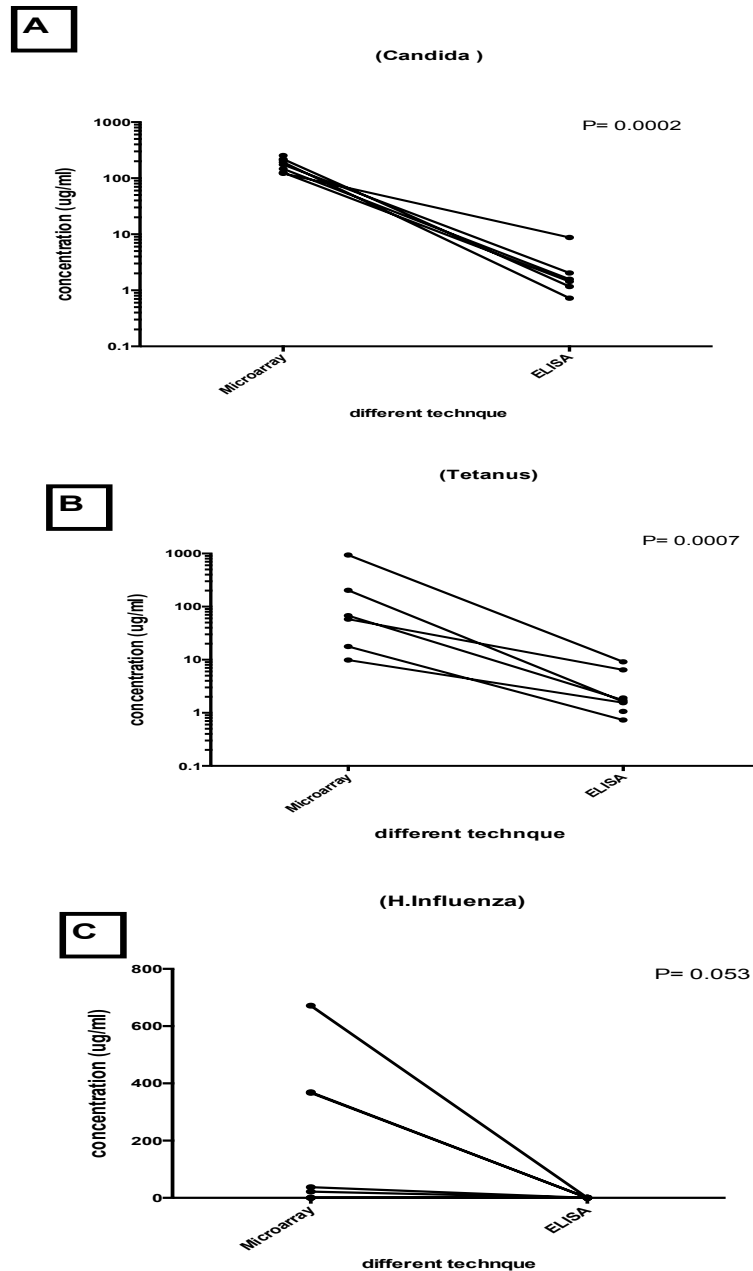


Figure 4. 7: correlation between ELISA and microarray methods

A, B and C) graphs show the correlation between the results for the ELISA and microarray methods for each control antigen (*Candida*, *Tetanus* and *H. influenza*) respectively, to investigate the correlation. Sera were obtained from eight healthy individuals and quantified for all control antigens using both microarray and ELISA. There was a strong degree of correlation between both methods for *Candida* and *Tetanus* antigens, which show a statistically significant difference $p = 0.0002$ for *Candida* and $p = 0.0007$ for *Tetanus*. The results for the *H. influenza* antigen showed no correlation ($p = 0.05$). The Mann-Whitney test was performed to assess statistical significance and $p < 0.05$ were considered as significant.

4.3.6 Biotinylation of proteins results

Before printing the full selection of antigens, investigation of the binding properties of some new autoantigens selected for this study was required (decorin, aggrecan, cytochrome and serum amyloid 2). The autoantigens were printed on an amino-silane slide, and the results (Figure 4.8) showed clearly that biotinylated autoantigens were printed on the slide as spots could be detected for all antigens.

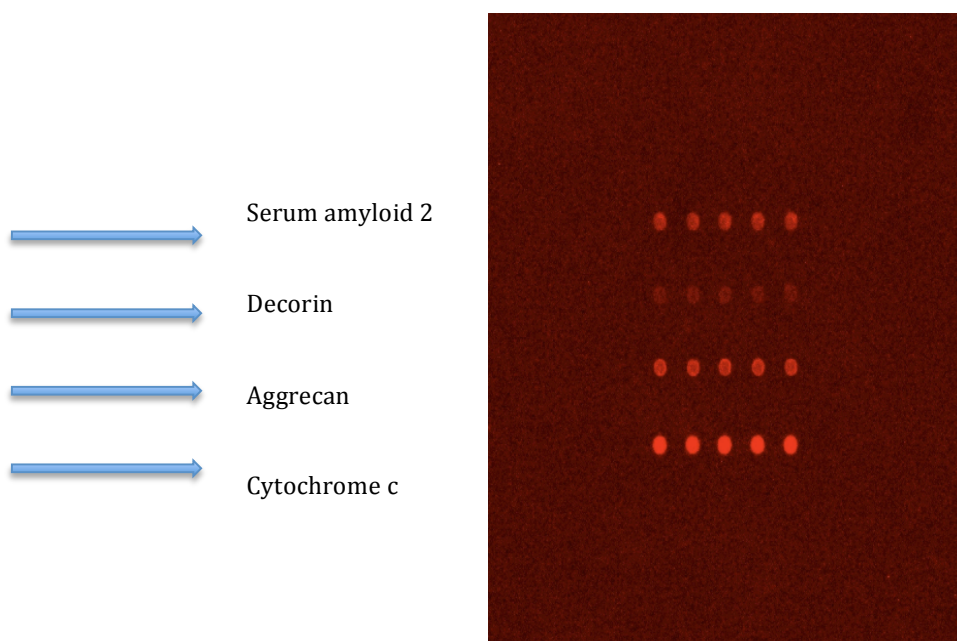


Figure 4. 8: Image of an array printed on an amino-silane slide with biotinylated autoantigens.

Each row represents one antigen printed in 5 replicates of autoantigens on amino-silane slide surface. Autoantigens were detected by blocking with streptavidin-CY5, washing and scanning using 635nm laser excitation. The red spots of each antigen on the array show clearly there is binding.

4.3.7 Investigation of the binding of patient autoantibodies to the candidate antigens

In a prior study, the ability to bind to the slide of the rest of the autoantigens selected for this study was investigated, and the results (Figure 4.9) demonstrated there was binding between the patient sample and the autoantigens suggesting they are all suitable for use in this study.

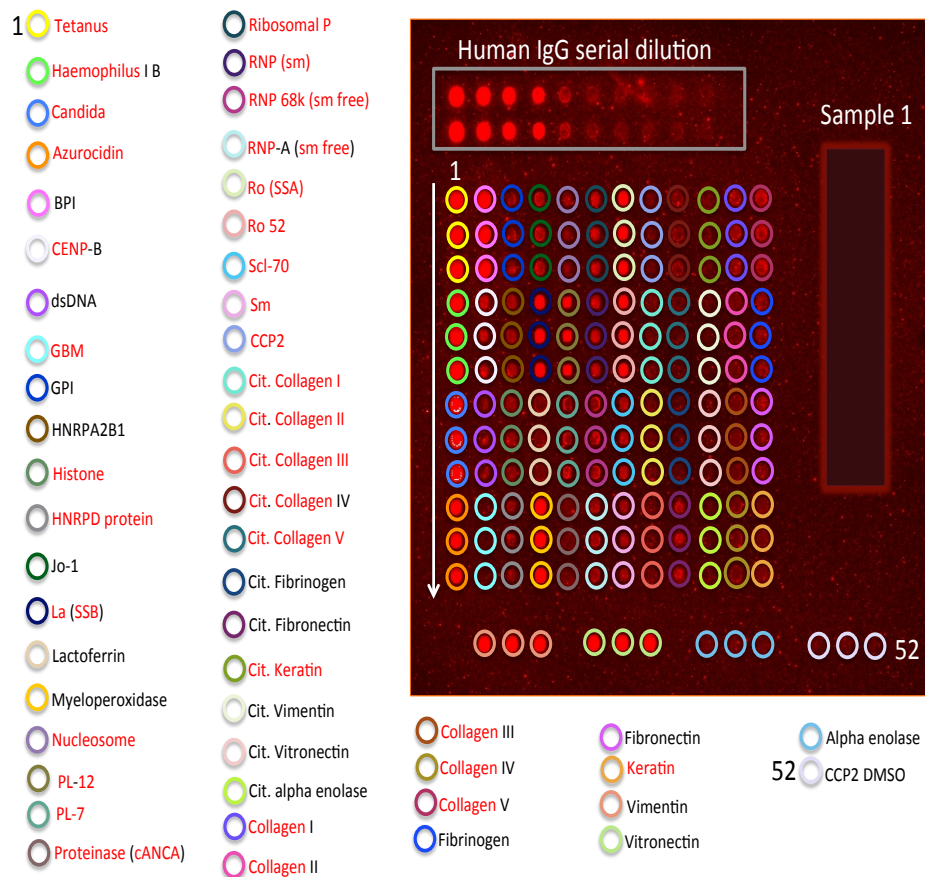


Figure 4. 9: Diagram representing the interaction between patient sample and autoantigens on amino-silane slide

Each colour circle represents a different antigen. All antigens in red as shown above represent the examined antigens used in this study. Red spots on the array above show the binding between the serum sample and these antigens, which show that serum autoantibodies bind to these antigens on the slide surface. **Picture from Amna Al-mahari thesis.**

4.4 Discussion:

Microarray technology is becoming more widely used, but currently there are no validation guidelines that comprehensively cover the use of protein biomarkers in microarray studies[186, 187], therefore it would be beneficial to establish criteria that could standardize research across different institutions. By using the FDA guidelines for pharmacokinetic immunoassays, this chapter established a method to validate antigen microarrays[188].

Within the development of a diagnostic assay, after optimization, validation is the next most important step, and this usually involves measuring different parameters including LoD, assay precision, and comparison to an established method. For a high throughput technology such as microarray, the validation method needs to be examined to ensure that the sensitivity and reproducibility of the assay are of a high enough standard, as this will allow any measurements made to be precise, accurate and reliable[188].

Within this thesis LoD was defined as the lowest concentration of autoantibodies that could be measured in biological samples[189]. The LoD shown in this chapter was very low, therefore it was not chosen as the limit to measure antigens in serum samples for this microarray platform. In a study that was similar to this study, the LoD was also not selected as a limit of detection on the antibody microarray as it was also too low[169].

Precision was also examined in this chapter by assessing the intra- and inter-assay coefficients of variation (CV %). The results showed that the intra-assay variation (within the slide) for most antibodies to antigen controls was below 9 %, which is at an acceptable limit, but the intra-assay variability was unacceptably high for the antibody responses to the *H. Influenza* antigen, which was above 10 % (Figure 4.3 A). Explanations for the variability in the antibodies to *H. Influenza* antigen could be due to

irregular spotting on slides, or due to differences in the response to the *H. Influenza* antigen between individuals used in this study, especially as the response was generally low in the patient samples investigated[177]. However, all the control antigens had an acceptable inter-assay variability (CV % = 15) (Figure 4.3 B).

Intensive cross reactivity experiments were performed in this chapter to identify any cross-reactivity of the detection antibodies. The optimal dilution of the detection antibodies (IgG) was found at 1:20,000 (Figure 4.5 A), however, the results still show a small level of cross reactivity with IgM and IgA and therefore, other experiments were performed in order to eliminate any cross reactivity in our antigen microarray platform. The experiments investigated the effect of using the amplification and interestingly, the results showed no cross reactivity occurred when the amplification was stopped. This is most likely due to low levels of biotin in the antibodies printed onto the slide surface, giving a false positive result.

The optimization of anti-IgM and anti-IgA were not included in this study as they were optimized in previous studies in our lab.

The results of the evaluation of these assay validation techniques showed that the FDA validation criteria were met for the test antigens. The next step before using the microarray to investigate the proteins of interest and clinical samples, was to compare the analytical performance of this technique with an ELISA, which is well established and routinely used to analyse biomarkers in serum samples[190] [136, 190]. The results of this comparison showed a correlation between both methods with a statistically significant increase in sensitivity for the microarray, with $p = 0.0002$, 0.0007 and $R = -0.8144$ and 0.4791 for *Candida* and *Tetanus*, respectively. However, for some low abundance antibodies like, *H. influenza*, there was no correlation observed ($p = 0.053$)

and ($R = -0.6389$), which may be due to the sensitivity of the ELISA assay being lower than the microarray, and the low signal produced for these antibodies in both methods for the patient samples investigated. ELISA uses optical density (OD), whereas microarrays measure antigens by fluorescence intensity, which gives the microarray a large advantage as it can measure over 10,000s of absorbance units (AU) instead of the 0-3 scale of OD, allowing a greater scope for biomarker detection.

4.5 Conclusions:

The use of microarray technology is currently expanding, as too is the number of commercial kits available for protein microarrays, but the cost of these is prohibitive for many research groups. This chapter details the establishment of a protocol for the optimization and validation of a microarray that can detect multiple biomarkers at low concentrations and at a comparatively low cost. This protocol established the use of 39 biomarkers, but this could be expanded to include more markers as required.

Overall the results of this chapter demonstrate that the developed microarray can identify multiple biomarkers relatively easily, with a smaller sample volume than the equivalent standard ELISA assay, and with greater dynamic range of detection.

5. Application of an antigen microarray as a diagnostic platform for COPD

5.1 Introduction:

COPD is a chronic abnormal inflammatory response of the lungs that encompasses two different diseases, chronic bronchitis and emphysema. Both diseases are characterised by airflow limitation that is not fully reversible[1].

The diagnosis of COPD is difficult as this disease has no single gold standard diagnostic test available. Several symptoms can aid in the diagnosis of the disease, such as wheezing, chronic cough, sputum production and breathlessness. Other physical attributes have also been implicated in the diagnosis of COPD, such as increased paradoxical abdominal movement, use of accessory muscles during exhalation and weight loss, which could be used as predictors of disease development [191, 192].

There are many different strategies in order to diagnose patients with COPD; spirometry tests are a very common measurements of the physical symptoms of COPD that should be used in all people who have one of the common symptoms of the disease, for example the presence of cough with increased sputum production [34]. Currently, spirometric airflow tests usually measure FEV-1 and FVC; FEV-1 measures the volume of air expired in one second by the patient after a full intake of breath, whereas FVC is the measure of the maximum exhaled air volume after a full intake of breath[193, 194]. A patient is defined as having COPD if they have an FEV-1 < 80 % and a ratio of FEV-1/FVC below 0.7; however, the results of the spirometry test are not the only criteria for diagnosing COPD, radiography of the chest may also help confirm the diagnosis[195].

It would therefore be beneficial to have a diagnostic platform that would allow the different stages of the disease to be determined by physicians, as this could help the treatment be tailored to the patients' needs and speed up detection, but such a method is currently is unavailable.

This thesis has previously described (Chapter 3 and 4) the development, optimisation and validation of a microarray platform to detect the concentrations of the autoantibodies of IgM and IgG for 39 auto-antigens that could be relevant to COPD progression. This chapter has used the validated microarray to investigate the differences in these markers between healthy non-smokers, smokers without COPD symptoms, and patients with COPD. This investigation was used to highlight any differences that could improve the understanding of disease progression, and which could also be used as biomarkers for the early detection of COPD in at risk patients, such as in healthy smokers.

5.2 Materials and methods:

The final optimised and validated antigen microarray protocol used in this study was as follows:

- A) **Antigen preparation;** due to the spreading and washed out spots, antigens were buffer exchanged from the manufacturer's buffer to PBSTrehTw buffer (Section 2.2.3).
- B) **Plate preparation and slide printing;** a 384-well polypropylene plate was prepared containing a serial dilution of human IgG and human IgM. Candidate autoantigens (Table 5.1) were diluted to a concentration of 100 µg/ml and 20 µl was loaded into each well of the same 384 well plate. The plate and slide were placed in the MicroGrid II BioRobot arrayer and printed under 60 % humidity.
- C) **Slide probing;** the printed slides were blocked with I Block for 1 h and washed with 1X PBS-Tween-20 three times (5 min each). Avidin/biotin blocking buffers (Invitrogen Life Technologies Ltd, UK) were added for 10 min each, which was followed by three washes (5 min each) with 1X PBS-Tween-20. Primary antibody (patient sera) was diluted in Dako antibody diluent (1:1000), and 100 µl of each serum sample was added to each pad. After washing the slides three times with

1X PBS- Tween-20, 100 µl of biotinylated anti-human IgG (secondary antibody) was diluted to 1:20,000 using the washing buffer and was added to each pad. The same was done for the IgM (secondary antibody) experiments. The slides were washed three times with 1X PBS-Tween-20, following which a 1:5000 dilution of streptavidin Cy5 was added to each pad, and the pads were incubated in the dark for 15 min. Slides were washed three times (5 min each) with 1X PBS-Tween-20 and rinsed with ultra-pure water. Slides were dried by centrifugation and scanned with a GenePix 4200 AL scanner at 635 nm.

D) After scanning the images, data were analysed using GenePix Pro Software (section 2.2.6).

Table 5. 1: A panel of control antigens and autoantigens examined in this study and source obtained from.

Control Antigens	Source
<i>Haemophilus influenza B</i>	National institute for biological standards and control(NIBSC)
Tetanus toxoid	
Candida	

Autoantigens	Source
<i>Haemophilus influenza B</i>	National Institute for Biological Standards and Control (NIBSC)
Tetanus toxoid	
Candida	
Azurocidin	AROTEC Diagnostics Ltd
CENP-B	DIRECT AG, Freiburg, Germany
PL-12	
PL-7	
GBM	AROTEC Diagnostics Ltd
Histone	

HNRP D		
La ssb		
Nucleosome		
Proteinase (cANCA)		
p ANCA		
Ribosomal p		
RNP/sm		
RNP 68k (sm free)		
RNP/sm free		
Ro-ssa		
Ro-52		
SCL-70		
sm antigen		
cit-collagen II		Citrullinated in-house
cit-collagen III		
cit-collagen IV		
cit-collagen V		
cit-fibronectin		
cit-keratin		
native collagen II	Merck Millipore, Billerica, MA, USA	
native collagen	Sigma-Aldrich	
Inactive collagen III		
Native collagen IV		
Native collagen V		
Keratin 18		
Keratin 8		
Decorin	Abnova, UK	
Aggrecan		
Serum amyloid 2(SAA2)		
Cytochrome c		

5.3 Results:

5.3.1 Age and gender differences between study groups

The effect of age was investigated statistically between the study groups using Mann-Whitney test as the data was non-normally distributed. Between COPD patients and healthy smokers, there were no statistically significant differences in the mean age of the two groups (data not shown). However, there were significant differences observed between COPD patients and the non-smokers ($p = 0.0001^{**}$). Regarding gender, Fisher's exact test was performed between the three groups and showed there was no significant differences in gender between the groups.

5.3.2 Antigen microarray quality control

The concentration of antibodies in the sera of the different study groups was investigated for three control antigens, Tetanus, Candida, and *H. influenza*. The results (Figure 5.1) showed there were no significant differences observed between the groups in terms of the reactivity of their IgG antibodies to Tetanus and *H. Influenza* antigens, however, between COPD patients and the healthy non-smoking (HNS) group there was a significant difference; with increased IgG antibodies to Candida in the COPD group ($p = 0.0286$) (Figure 5.1 C). There was also a significant difference of an increased level of antibodies to Candida in the healthy smoker group (HS) compared to the HNS group ($p = 0.0056$). These results suggest that smoking may be associated with a higher incidence of Candida infection, and COPD makes the patients more vulnerable to this type of infection.

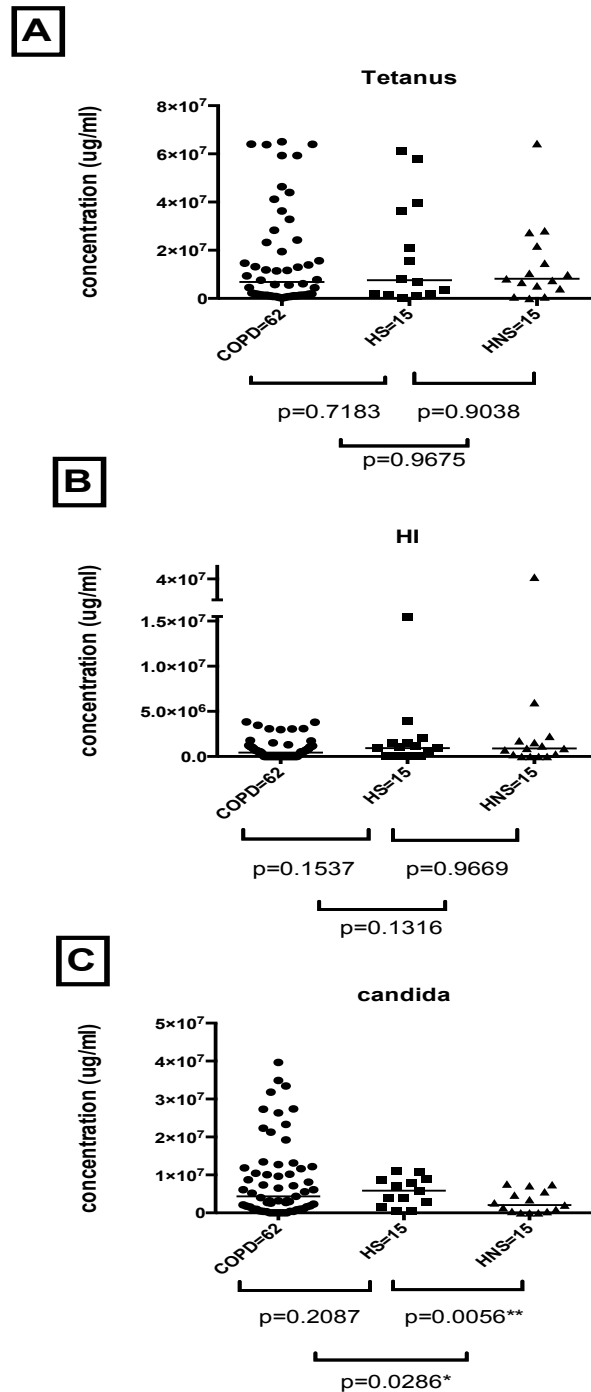


Figure 5. 1: Total IgG levels in sera against three control antigens.

Sera from healthy smoking (HS), healthy non-smoking (HNS) and COPD individuals were analysed by the antigen microarray for determination of the concentrations of antibodies to control antigens; A) Tetanus, B) *H. influenza* and C) Candida. Each point represents an individual serum sample. Statistical comparisons between groups were performed using the Mann-Whitney test. P values < 0.05 were considered as significant.

5.3.3 Levels of IgG-autoantibodies in sera of COPD individuals, non-smoking controls and smoking controls

Sera from HNS controls, HS controls and COPD individuals were analysed on the microarray platform for IgG autoantibodies to all the different autoantigens to be investigated (Table 5.1). Significant differences between groups were measured using a Mann-Whitney test. In addition, for all autoantibody results a line representing the 95 th percentile of the healthy non-smoking control group was drawn to allow detection of significantly higher results within the data sets. Furthermore, to ensure a more stringent cut-off, the 95 th percentile of the healthy smoker group was also used to determine those patients with higher autoantibody responses to autoantigens.

Autoantibodies that could be associated with a variety of autoimmune diseases, namely Aggrecan, azurocidin, c ANCA, CENP-B, cytochrome c and decorin were measured (Figure 5.2). Interestingly, autoantibodies to cANCA showed a significantly higher in HS compared to HNS ($p = 0.0042^{**}$) and to HS ($p = 0.0012^{**}$). No significant differences were observed for the autoantibodies to aggrecan, azurocidin, CENP-B and cytochrome c. Interestingly, 12 out of 62 COPD patients had levels of autoantibodies to Decorin higher than 95 th percentile of control group, and non-of 62 had levels higher than that of the healthy smokers group.

With regard to the autoantibodies against citrullinated antigens (Figure 5.3), overall very low levels were detected. Significant differences were detected for cit-collagen5, cit-fibronectin and cit-keratin between COPD and the controls, but this mainly due to one or two outliers rather than the full set of data.

The key findings of the autoantibody responses to the collagens (Figure 5.4) showed a significant increase in autoantibody responses to collagen V in COPD compared to HNS, and in the group of COPD patients, 25 out of 62 had autoantibody levels higher than 95

th percentile of the healthy control group for both collagen I and collagen V (Figure 5.4). In addition, using the more stringent cut-off and 31 out of 62 had levels higher than that of the healthy smokers group.

For the nuclear proteins, 11 out of 62 COPD patients had an autoantibody response to nucleosome higher than 95 th percentile of the control group (Figure 5.3 D). In addition, using the more stringent cut-off and 8 out of 62 had levels higher than that of the healthy smokers group. However, no significant differences were found for GBM, keratin8, la ssb, pl-12 and pANCA between the groups (Figure 5.5).

There were significant increases for RNP/sm autoantibodies in the COPD group compared to controls ($p = 0.0071^{**}$ HS and $p = 0.0003^{**}$ NHS, Figure 5.8D), while autoantibodies against ro-52 were significantly lower in the COPD group compared to controls ($p = 0.0090^{**}$ HS and 0.0007^{***} NHS, Figure 5.6 F). In addition, 15 out of 62 COPD patients had autoantibody responses to PL-7 higher than 95 th percentile, and 9 out of 62 patients had autoantibody responses to ribosome p higher than 95 th percentile (Figure 5.6 A + B). In addition, using the more stringent cut-off and 6 out of 62 had levels higher than that of the healthy smokers group.

In the last group of examined antigens (Figure 5.9), SCL-70 and histone autoantibodies showed a significant increase in the COPD group compared to HS ($p = 0.0200^{**}$) ($p = 0.0012^{*8}$), whereas with ro-ssa, SAA2, sm and HNRD antigens there were no significant differences observed between groups.

The significant differences between groups measured using a Mann-Whitney test (Table 5.2) showed 7 out of 39 autoantibodies were significantly increased in COPD patients compared to the controls. Interestingly, in the HS group cANCA, citrullinated fibronectin, collagen 1 and CENP-B were also significantly higher than the HNS group, which suggests that those patients may have susceptibility to developing a disease (COPD) in the future.

However, for other antigens investigated (Table 5.1), there were no significant differences between any of the three groups.

To summarise these statistical differences between the COPD and HS groups, there were significant differences (higher for COPD) observed for serum concentrations of IgG autoantibodies for RNP/sm (Figure 5.6; $p \leq 0.0071^{**}$, $p \leq 0.0090^{**}$, respectively) SCL-70, and histone (Figure 5.7; $p \leq 0.0200^*$, $p \leq 0.0012^{**}$, respectively). In terms of COPD and the HNS groups, significant differences (higher for COPD) were found for IgG autoantibodies-specific to CENP-B, collagen5, La-ssb and RNP/sm (Figures 5.2; $p \leq 0.0041^{**}$, Figure 5.4; $p \leq 0.0348^*$, figure 5.5; $p \leq 0.0120^*$, and Figure 5.6; $p \leq 0.0003^{**}$, respectively). Between the two control groups (HS and HNS) there were significant differences with autoantibodies to the RNP/sm autoantigen $p = 0.0071^*$, $p = 0.0003^{**}$ which was higher in COPD than in both control groups, and this suggests this antigen could be a marker to help monitor COPD development.

We also examined the increase of autoantibody response per COPD patient to determine if all COPD patients had an autoantibody response above 95 th percentile of the control group. The results (Table 5.3) showed that only 7 out of 62 COPD patients had no detectable autoantibody response above the 95 th percentile of those that did have responses.

In addition, the number of autoantibody responses above the 95 th percentile of the healthy smokers group was measured, and this showed that only 9 out of 62 COPD patients had no detectable autoantibody response above the 95 th percentile of those that did have responses.

We also examined the autoantibody response per healthy smoker (Table 5.4) and again, most had at least one response above the 95 th percentile (13 out of 15).

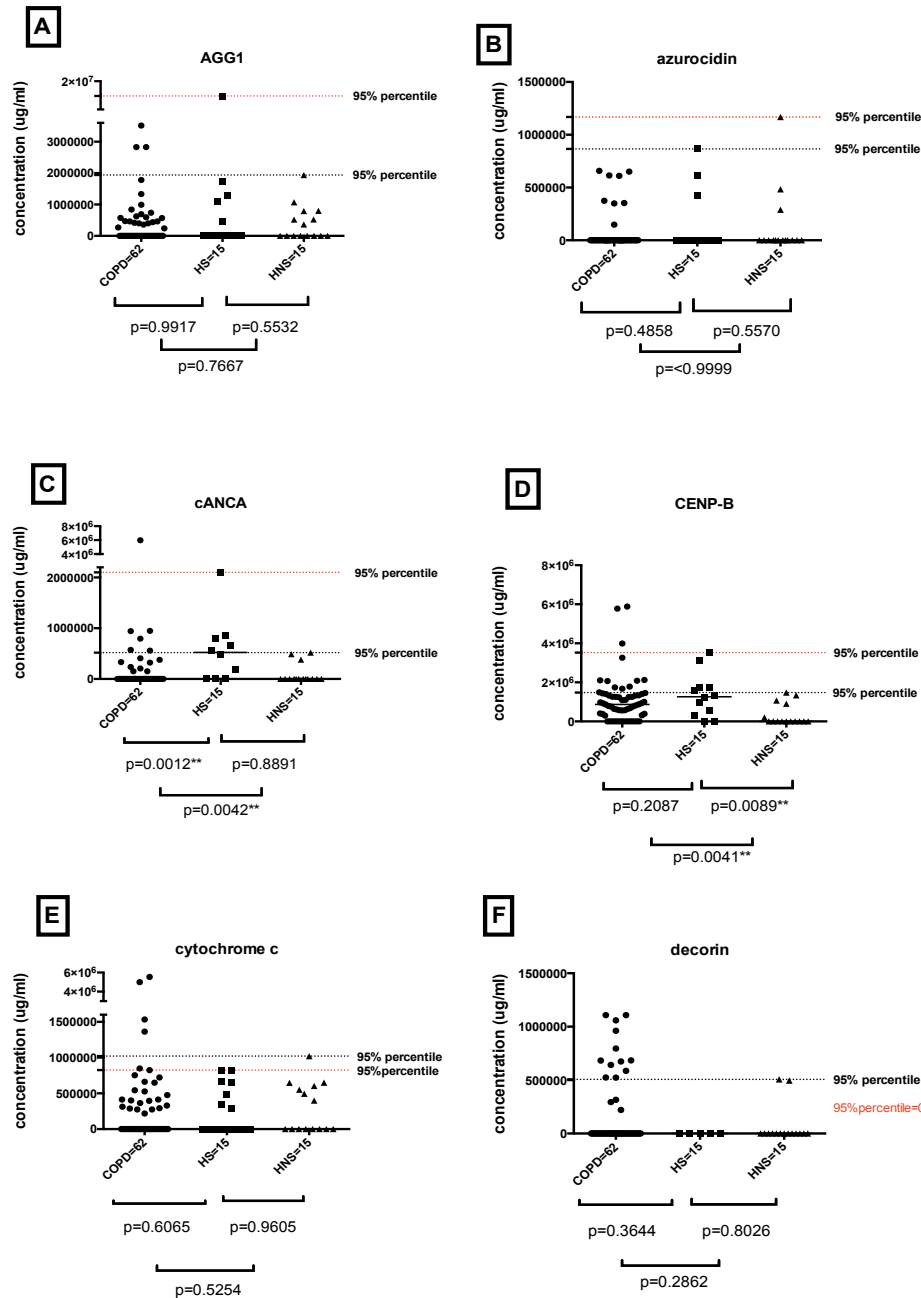


Figure 5. 2: The reactivity of IgG-autoantibodies against different antigens between patients with COPD, healthy non-smokers and healthy smoker controls.

Serum samples from COPD patients (n = 62) and healthy individuals (HS = 15 and HNS = 15) were analysed using antigen microarray for detection of IgG autoantibodies to the autoantigens: A) AGG1, B) azurocidin, C) cANCA, D) CENP-B, E) cytochrome c and F) decorin. Each point represents an individual serum sample, and the lines between the points are the median IgG concentrations of the groups. Black dashed lines are the 95 % percentiles of the healthy non-smokers and red dashed lines are the 95 % percentile of the healthy smokers' Statistical comparison between groups were performed using the Mann-Whitney U-test and P values < 0.05 were considered as significant.

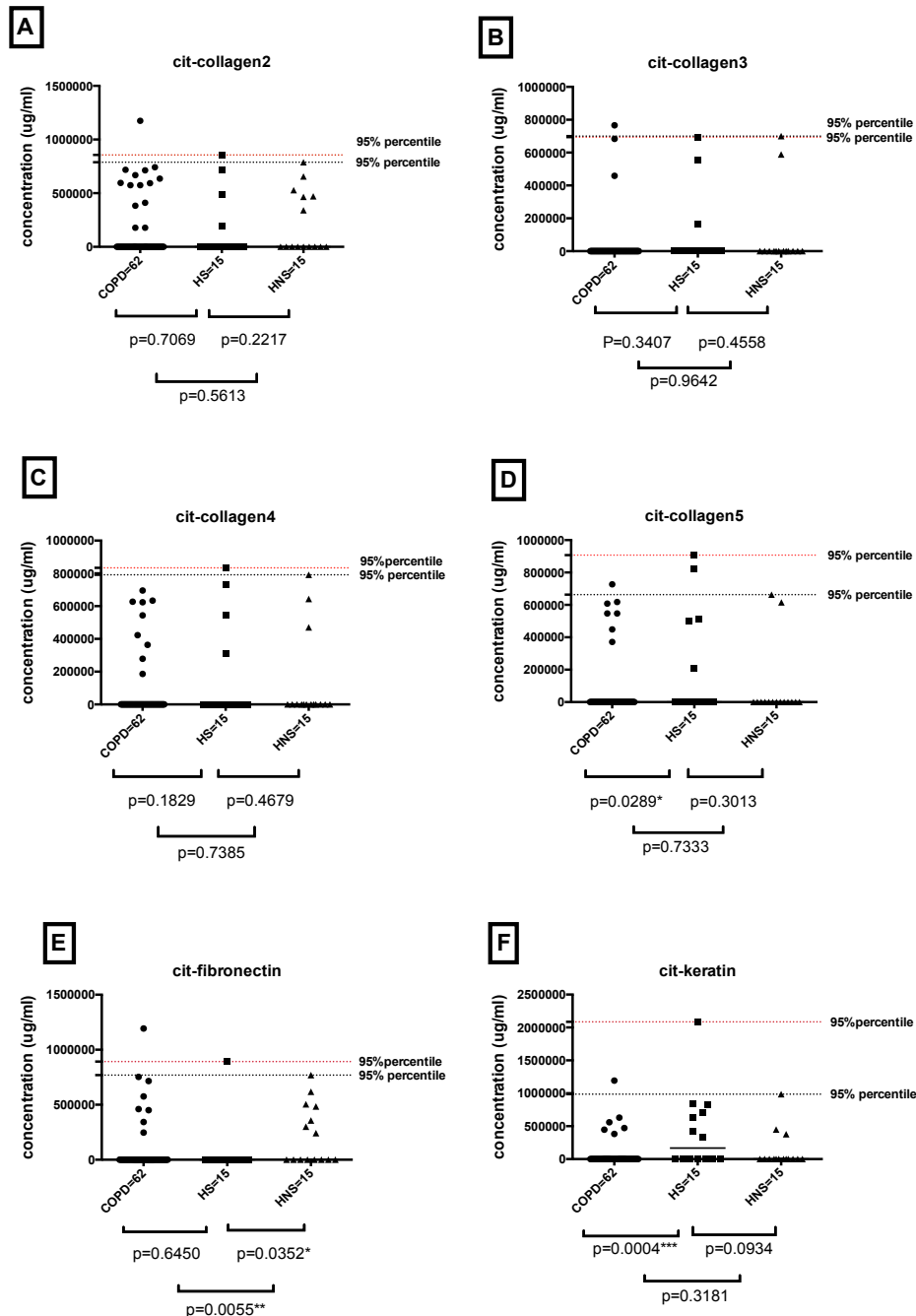


Figure 5. 3: The reactivity of IgG-autoantibodies against different antigens between patients with COPD, healthy non-smokers and healthy smoker controls.

Serum samples from COPD patients (n = 62) and healthy individuals (HS = 15 and HNS = 15) were analysed using antigen microarray for detection of IgG autoantibodies to the citrullinated antigens (collagen2-keratin; A-F respectively). Each point represents an individual serum sample, and the lines between the points are the median IgG concentrations of the groups. Black dashed lines are the 95 % percentiles of the healthy non-smokers and red dashed lines are the 95%percentile of the healthy smokers. Statistical comparison between groups were performed using the Mann-Whitney U-test and P values < 0.05 were considered as significant.

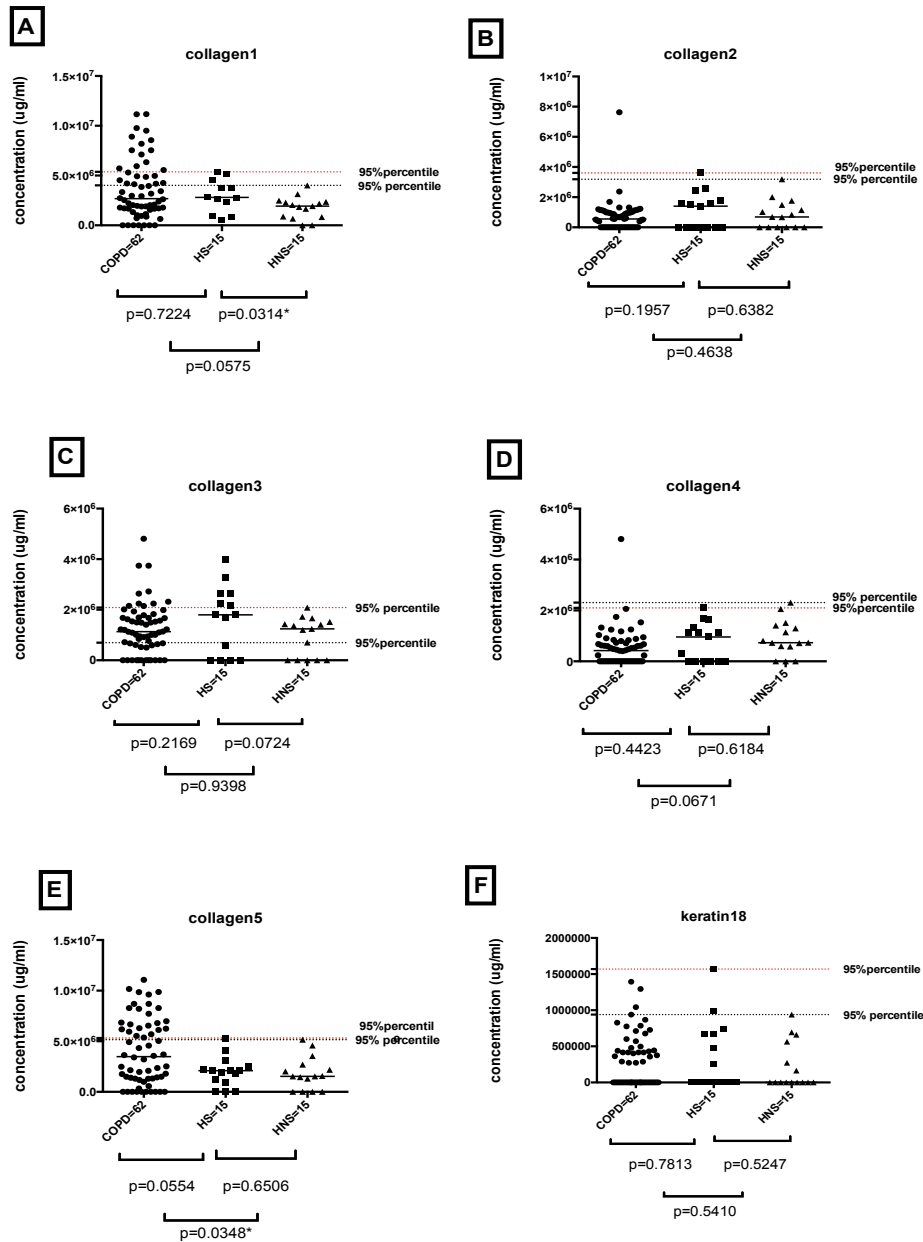


Figure 5. 4: The reactivity of IgG-autoantibodies against different antigens between patients with COPD, healthy non-smokers and healthy smoker controls.

Serum samples from COPD patients (n = 62) and healthy individuals (HS = 15 and HNS = 15) were analysed using antigen microarray for detection of IgG autoantibodies to autoantigens: A) collagen1, B) collagen2, C) collagen3, D) collagen4, E) collagen5 and F) keratin18. Each point represents an individual serum sample, and the lines between the points are the median IgG concentrations of the groups. Black dashed lines are the 95 % percentiles of the healthy non-smokers and red dashed lines are 95%percentile of the healthy smokers. Statistical comparison between groups were performed using the Mann-Whitney U-test and P values < 0.05 were considered as significant.

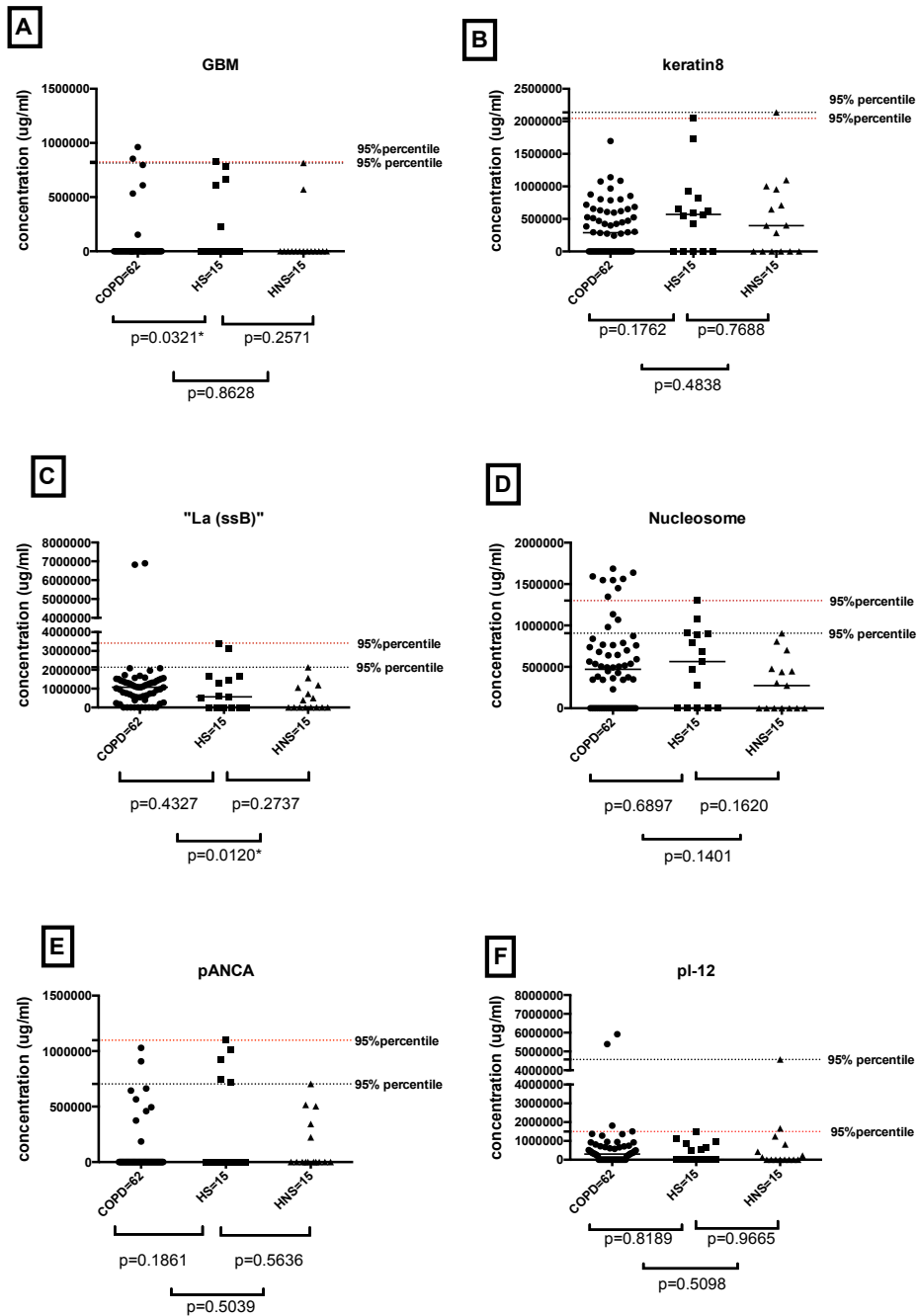


Figure 5. 5: The reactivity of IgG-autoantibodies against different antigens between patients with COPD, healthy non-smokers and healthy smoker controls.

Serum samples from COPD patients ($n = 62$) and healthy individuals ($HS = 15$ and $HNS = 15$) were analysed using antigen microarray for detection of IgG autoantibodies to the autoantigens: A) GBM, B) keratin8, C) La ssb, D) nucleosome, E) pANCA and F) PL-12. Each point represents an individual serum sample, and the lines between the points are the median IgG concentrations of the groups. Black dashed lines are the 95 % percentiles of the healthy non-smokers and red dashed lines are 95% percentile of the healthy smokers. Statistical comparison between groups were performed using the Mann-Whitney U-test and P values < 0.05 were considered as significant.

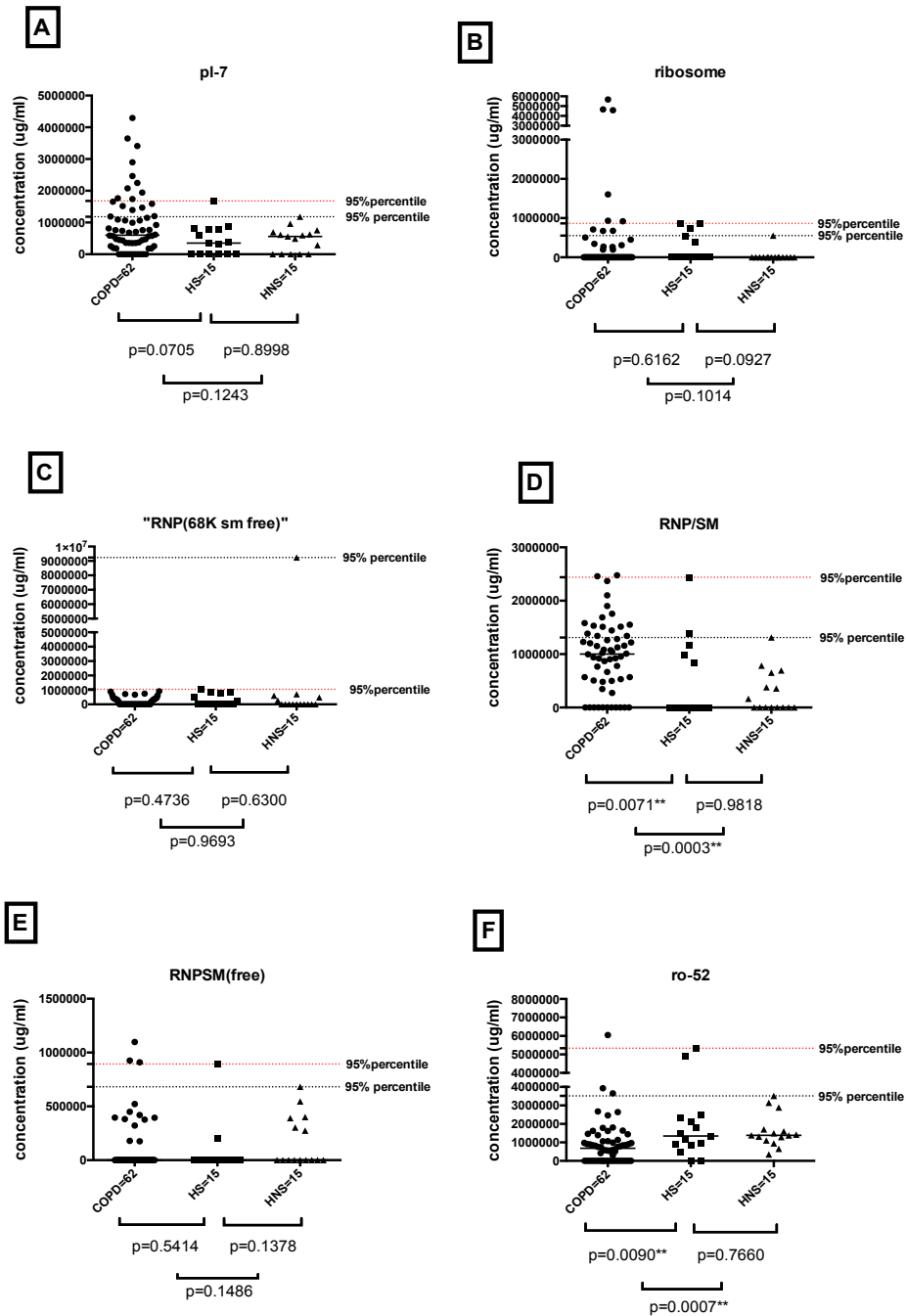


Figure 5. 6: The reactivity of IgG-autoantibodies against different antigens between patients with COPD, healthy non-smokers and healthy smoker controls.

Serum samples from COPD patients (n = 62) and healthy individuals (HS = 15 and HNS = 15) were analysed using antigen microarray for detection of IgG autoantibodies to the autoantigens: A) PL-7, B) ribosome, C) RNP 68k sm free, D) RNP/sm, E) RNP/sm free and F) ro-52. Each point represents an individual serum sample, and the lines between the points are the median IgG concentrations of the groups. Black dashed lines are the 95 % percentiles of the healthy non-smokers and red dashed lines are 95 % percentile of the healthy smokers. Statistical comparison between groups were performed using the Mann-Whitney U-test and P values < 0.05 were considered as significant.

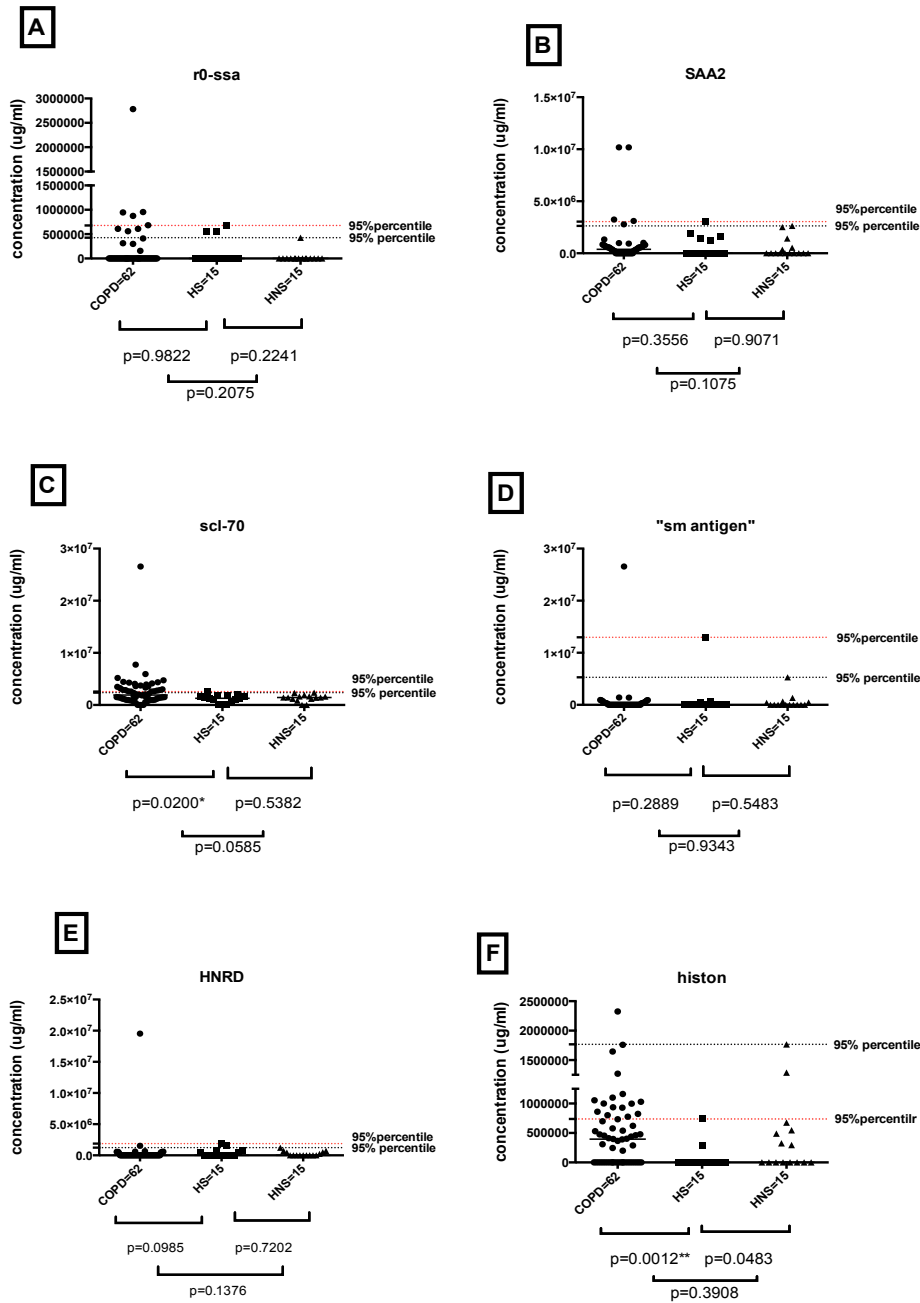


Figure 5. 7: The reactivity of IgG-autoantibodies against different antigens between patients with COPD, healthy non-smokers and healthy smoker controls.

Serum samples from COPD patients ($n = 62$) and healthy individuals ($HS = 15$ and $HNS = 15$) were analysed using antigen microarray for detection of IgG autoantibodies to the autoantigens: A) ro-ssa, B) SAA2, C) SCL-70, D) sm antigen, E) HNRD and F) histone. Each point represents an individual serum sample, and the lines between the points are the median IgG concentrations of the groups. Black dashed lines are the 95 % percentiles of the healthy non-smokers and red dashed lines are the 95% percentile of the healthy smokers. Statistical comparison between groups were performed using the Mann-Whitney U-test and P values < 0.05 were considered as significant.

Table 5. 2: Significant differences of IgG antibodies between study groups.

COPD versus HS	COPD versus HNS	HNS versus HS
Candida*	CENP-B**	cANCA**
citrullinated keratin***	citrullinated fibronectin**	citrullinated fibronectin*
RNP/sm**	collagen1*	collagen1*
ro-52**	Collagen 4	CENP-B**
scl-70*	Collagen 5*	
histone**	La ssb*	
	RNP/sm***	
	ro-52***	

* Antigens in bold indicate the significant increase in COPD group. * = p value < (0.05), ** = p value < (0.005), *** p value < (0.0005)

Table 5. 3: Details of samples and reactivity of IgG antibodies against the examined antigens from COPD patients using the 95 th percentile of the control group as a cutoff.

COPD Number.	Antigen	No. of positive Ags
1	collagen1+candida+CENP-B+PL-7	4
2	ANCA+candida+CENP-B+collagen3+nucleosome+pANCA+PL-7+ribosome	8
3	PL-7+ro-52+rossa	3
4	collagen1+candida+collagen3	3
5		
6	collagen1+candida+cytochrome c+decorin+PL-7+RNP/SM FREE+SCL-70	7
7		
8	cANCA+decorin+PL-7+RNP/sm+collagen2	4
9	collagen1+candida+La ssb+PL-7+ribosome	5
10		
11	Decorin	1
12		
13		
14	collagen5	1
15	collagen1+cANCA+collagen3+ro-ssa	4
16		
17	collagen1+collagen5	2
18	collagen1+candida+collagen5+PL-7+RNP/SM	5
19	collagen1+candida	2
20	candida+RNP/SM+ro-ssa	3
21	candid+collagen5+ribosome	3
22	collagen1+collagen5+ribosome	3
23	cit-collagen5+collagen3+decorin+nucleosome+RNP/SM FREE	5
24	GBM	1
25	CENP-B+cytochrome c+keratin18+RNP/SM FREE+ro-ssa	5
26	CENP-B+cit-collagen2+cytochrome c+keratin18+nucleosome+HNRD	6
27		
28	candida+collagen5	

29	collagen3+collagen5	2
30	collagen3+collagen5	2
31	collagen1+candida+nucleosome+PL-7+RNP/SM+SCL-70	6
32	collagen1+SCL-70	2
33	collagen1+decorin+SCL-70	3
34	collagen1+candida+CENP-B+collagen5+nucleosome+PL-12+PL-7+RNP/SM+SCL-70	9
35	RNP/SM+SCL-70	2
36	collagen1+collagen5+PL-7+SCL-70	2
37	collagen1+candida+collagen5+ribosome+RNP/SM+SCL-70	4
38	collagen1+candida+CENP-B+decorin+PL-7+RNP/SM+histon+SCL-70	8
39	collagen1+decorin+RNP/SM+SCL-70	4
40	collagen1+candida+CENP-+collagen3+keratin18+ribosome+RNP/SM+ro-52+SAA2+SCL-70	9
41	candida+SCL-70	2
42	collagen1+cANCA+candida+CENP-B+collagen3+PL-12+PL-7+RNP/SM+SCL-70	9
43	candida+CENP-B+cit-collagen3+collagen5+pANCA+RNP/SM+SCL-70	7
44	candida+collagen5+cytochrome c	3
45	candida+collagen3+collagen5+RNP/SM	4
46	collagen5+PL-7+ro-52	3
47	collagen5+nucleosome+SCL-70	3
48	collagen1+AGG1+collagen5+decorin+nucleosome+RNP/SM+ro-ssa+SAA2+SCL-70	8
49	collagen1+AGG1+decorin+nucleosome+RNP/SM+ro-ssa+SAA2+SCL-70	8
50	cANCA+collagen5+PL-7+SCL-70	4
51	CENP-B+collagen5+La ssb+nucleosome+PL-7+RNP/SM+SCL-70	7
52	collagen1+candida+decorin+nucleosome+SCL-70	5
53	candida+ro-ssa+SCL-70	3
54	PL-7+SCL-70	2
55	collagen5+SCL-70	2
56	collagen5+ribosomeSCL-70	2
57	AGG1+candida+PL-7+ribosome+SAA2	5
58	cANCA+cit-fibronectin+collagen3+decorin+ribosome+ro-ssa+SCL-70	7
59	collagen5	1
60	cit-keratin+collagen4+GBM+sm antigen	4
61	collagen5+SAA2	2
62	CENP-B+collagen5+decorin	3

* Serum samples from patients were analysed by antigen microarray for the presence of 39 autoantigens. Table represents different antigens that showed values above 95 th percentile of healthy non-smoking control group.

Table 5. 4: Details of samples and reactivity of IgG autoantibodies against the examined antigens from healthy controls.

Serum Number	Antigen above 95 %	No. of positive Ags
HS1	cANCA+cit-collagen2+cit-fibronectin+La ssb+ nucleosome +pANCA+PL-7+collagen3	8
HS2	Lassb+ro-52	2
HS3	AGG1+nucleosome+pANCA+ribosomal p+collagen3	5
HS4	cANCA +cit-collagen4+pANCA+RNP/SM	4
HS5	collagen5+CENP	2
HS6	cANCA+cit-keratin+RNP/SM free+ro-ssa+sm antigen +HNRD	6
HS7	collagen1+cytokeratin18+scl-70	3
HS8	collagen2+pANCA+ribosomal p+RNP/SM+ro-ssa	5
HS9		
HS10	pANCA+HNRD	2
HS11	cANCA+collagen1+ro-ssa+collagen3	4
HS12	ro-52+collagen3	2
HS13		
HS14	cANCA+GBM+cytokeratin18+ribosomal p+collagen3+collagen1	6
HS15	collagen3	1

- HS = healthy smokers. Serum samples from healthy controls were analysed by antigen microarray for the presence of 39 autoantigens. Table represents different antigens that showed values above 95 th percentile of healthy non-smoking control group.

Table 5. 5: Details of samples and reactivity of IgG autoantibodies in COPD patients that are above 95%percentile of healthy smokers control.

COPD Number	Autoantigens	Number of positive autoantigens
1	pl-7,	1
2	collagen3,pl-7,ribosomal p,	3
3	ro-52,	1
4	collagen3	1
5		
6	collagen1,cytochrome c,pl-7,RNP/SMFREE	5
7		4
8	collagen2,pl-7,RNP/SM	4
9	CENP,lassb, ribosomal p,	3
10		
11		
12		
13		
14		
15	collagen3	1
16		
17	collagen1,collagen5	2
18	collagen1,collagen5	2
19	collagen5	1
20	ro-ssa,histone	2
21	collagen5	1
22	collagen1,collagen5	2
23	collagen3,collagen5,nucleosome,RNP/SMFREE	5
24	GBM	1
25	cytochrome c,RNP/SMFREE,ro-ssa	3
26	CENP,cit-collagen2,cytochrome c,HNRD	4
27		
28	collagen5	1
29	collagen3,collagen5	2
30	collagen3,collagen5	2
31	RNP/SM,SCL-70,	2
32	collagen1,SCL-70	2
33	collagen1	2
34	collagen1,collagen5,nucleosom,pl-7,pl-12,SCL-70	6
35	collagen1,histone,SCL-70	3
36	collagen5,PL-7,histone,SCL-70	4
37	collagen1,collagen5,ribosomalp,histone	4
38	collagen1,pl-7,histone,SCL-70	5
39	decorin,histone,SCL-70	3
40	collagen3,ribosomalp,ro-ssa,SCL-70	4
41		
42	collagen3,pl-12,pl-7,histone,SCL-70	5
43	cit-collagen3,collagen5,scl-70	3
44	collagen5,cytochrome c	2
45	collagen3,collagen5	2
46	collagen5,histone	2
47	collagen1,collagen5,nuclusome,histone,scl-70	5
48	collagen1,nucleosome,ro-ssa,scl-70	5
49	collagen1,nucleosome,ro-ssa,scl-70	5
50	cANCA,collagen1,collagen5,scl-70	4

51	CENP,collagen5,lassb,nucleosome,histone,scl-70	6
52	decorin,nucleosome,histone,scl-70	4
53	nucleosome,ro-ssa,scl-70	3
54	pl-7,scl-70	2
55	collagen5	1
56	collagen5,ribosomalp,scl-70	3
57	pl-7,ribosomalp,histone	3
58	cit-fibronectin,collagen3,ro-ssa,scl-70	5
59	collagen5	1
60	collagen4,GBM,sm	3
61	collagen5	1
62	collagen5,histone	3

* Serum samples from patients were analysed by antigen microarray for the presence of 39 autoantigens. Table represents different antigens that showed values above 95% percentile of healthy smoking control group.

5.3.4 The correlation between IgG autoantibodies levels and FEV-1 % in those with COPD

COPD severity is divided into four categories according to international guidelines by the Global Initiative for Chronic Obstructive Lung Disease (GOLD); the stages are known as mild, moderate, severe and very severe, and are based on the forced expiratory volume per second (FEV-1 %). If an individual has a FEV-1 value of 80 % or above, then the pathogenesis of the disease can be classified as being mild. However, if the percentage of FEV-1 drops to 30 % or lower, then the individual has severe COPD[196]. The predicted FEV-1 % was initially evaluated to see if there was a relationship between the FEV-1 % and the concentrations of the different IgG autoantibodies in the COPD group. The correlation between these two variables were analysed by Spearman's Rank correlation, and the results (Figures 5.8 to 5.12) showed that generally there was no significant correlation for any of the autoantibody responses to the 39 autoantigens, the only exception was the antibody responses to ribosomal p antigen, which correlated significantly ($p = 0.0356^*$) with FEV-1 in those with COPD.

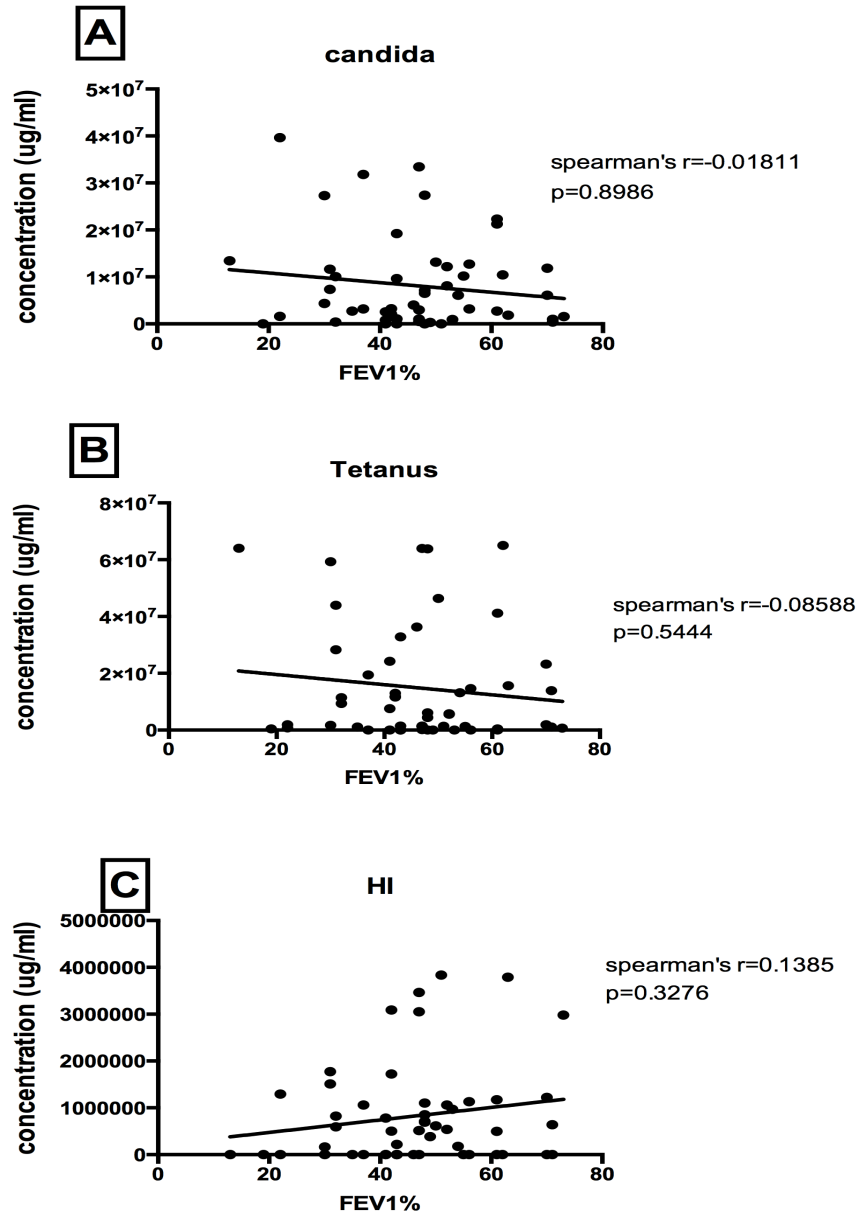


Figure 5. 8: Correlation between predicted FEV-1 and control antibody concentrations for Candida, Tetanus and *H. influenzae*.

Spearman's Rank correlation tests were performed to compare the relationship between the predicted FEV-1 % and the concentration of the respective antibodies to Candida (A), Tetanus (B) and *H. influenzae* (C) in patients with COPD, which showed no significant correlations.

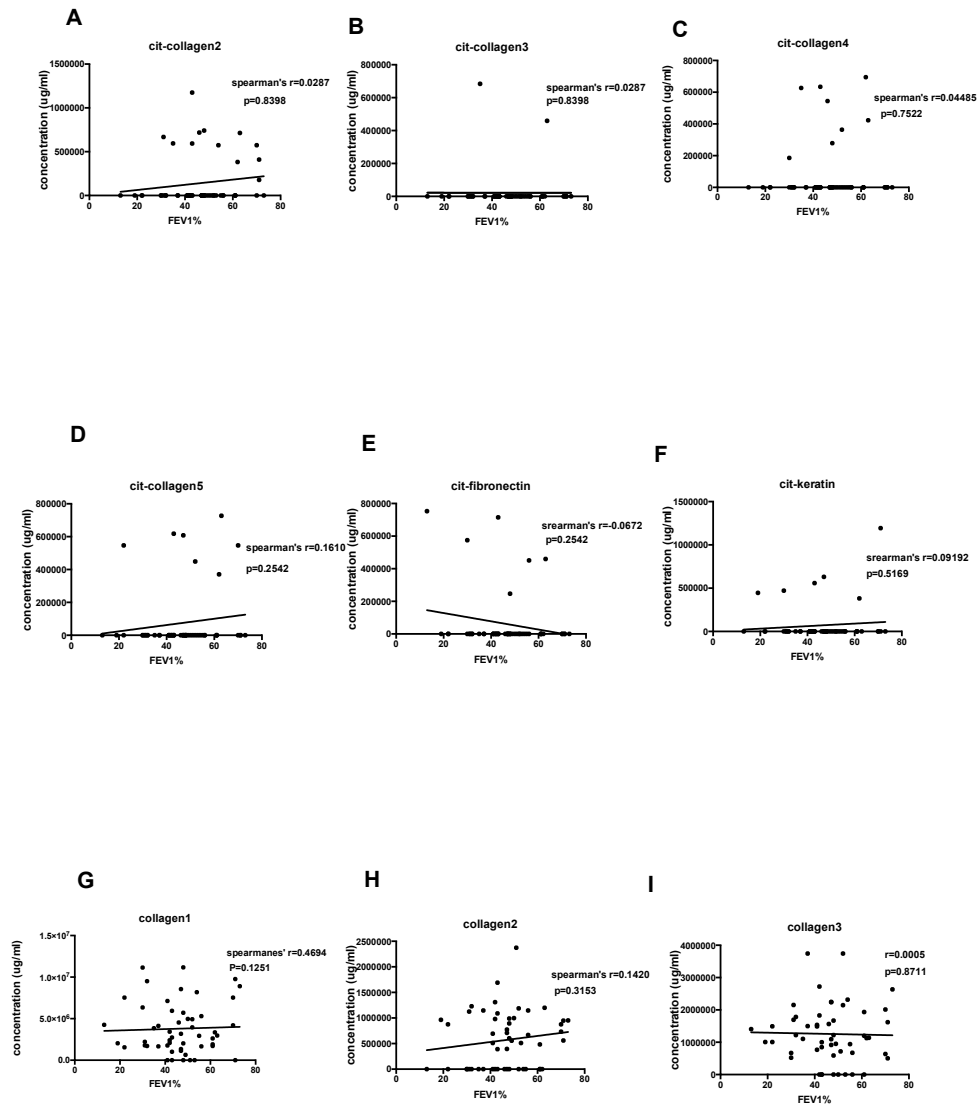


Figure 5. 9: Correlation between predicted FEV-1 and autoantibody concentration: citrullinated forms of collagen2 - collagen5, fibronectin, keratin and collagen1-3 (A-I, respectively).

Spearman's Rank correlation tests were performed to compare the relationship between the predicted FEV-1 % and the concentration of the respective autoantibodies to citrullinated collagen2 (A) - collagen3 (I) in patients with COPD. All above autoantibodies showed negative results in correlation to FEV-1 %.

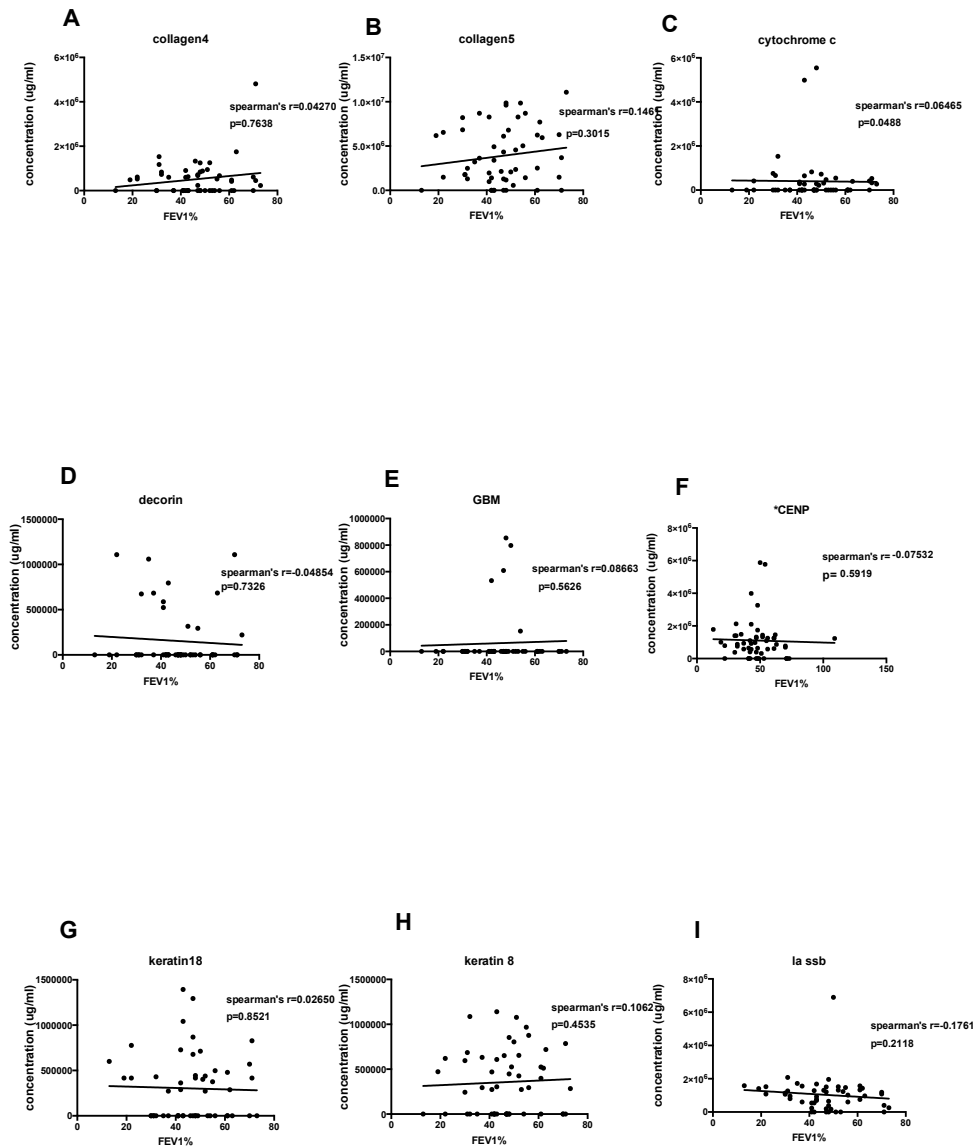


Figure 5. 10: Correlation between predicted FEV-1 and autoantibodies concentration: collagen4, collagen5, cytochrome c, decorin, GBM, CENP-B, keratin18, keratin8 and La ssb.

Spearman's Rank correlation tests were performed to compare the relationship between the predicted FEV-1 % and the concentration of the respective autoantibodies collagen4 (A), collagen5 (B), cytochrome c (C), decorin (D), GBM (E), CENP-B (F), keratin18 (G), keratin8 (H) and La ssb (I) in patients with COPD. All above autoantigens showed negative results in correlation to FEV-1 %.

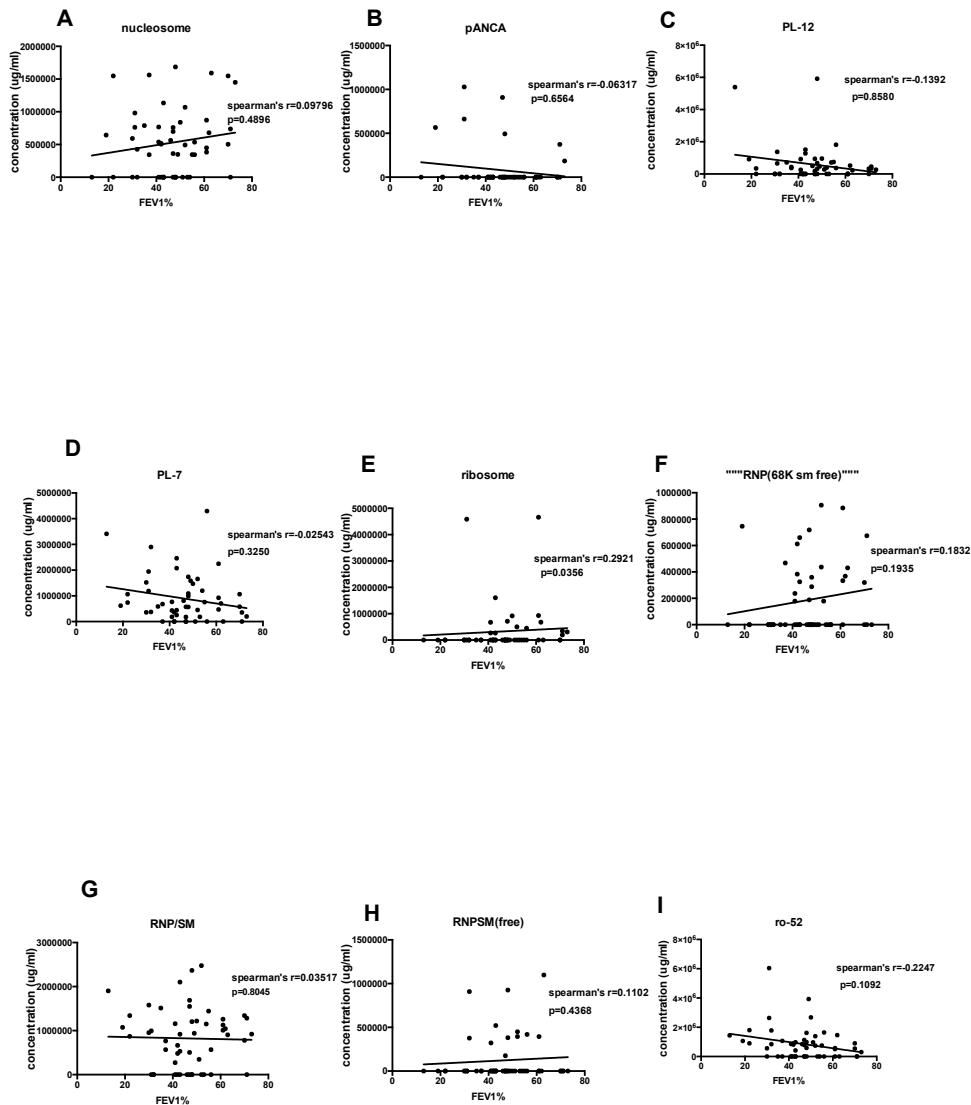


Figure 5. 11: Correlation between predicted FEV-1 and autoantibodies concentration; nucleosome, pANCA, PL-12, PL-7, ribosome, RNP 68k sm free, RNP/sm, RNP/sm free and ro-52.

Spearman's Rank correlation tests were performed to compare the relationship between the predicted FEV-1 % and the concentration of the respective autoantibodies nucleosome (A), pANCA (B), PL-12 (C), PL-7 (D), ribosome (E), RNP68k sm free (F), RNP/sm (G), RNP/sm free (H) and ro-52 (I) in patients with COPD. All above autoantigens showed negative results in correlation to FEV-1 % except ribosomal p which had a p value = 0.0356*.

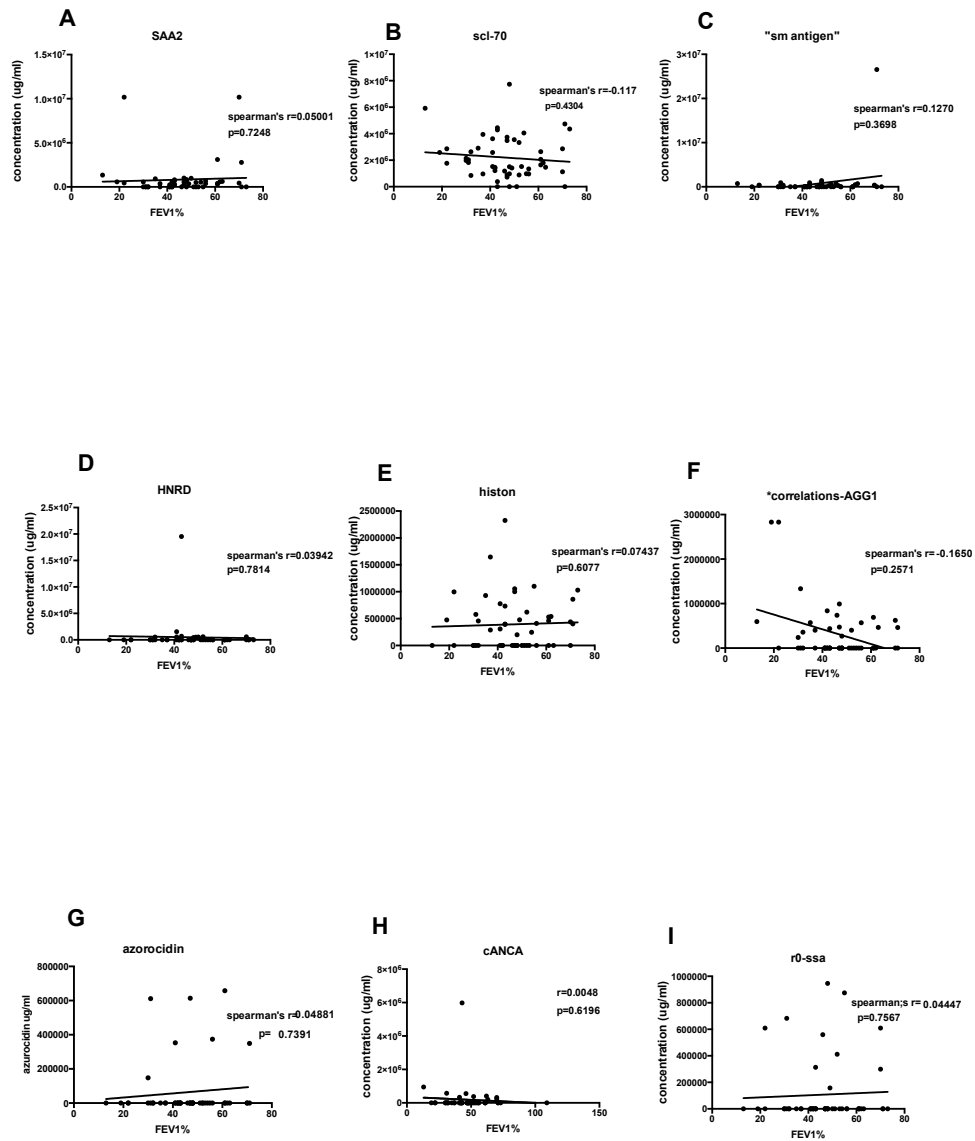


Figure 5. 12: Correlation between predicted FEV-1 and autoantibodies concentration: SAA2, SCL-70, sm antigen, HNRD, histone, AGG1, azorocidin, cANCA and ro-ssa.

Spearman's Rank correlation tests were performed to compare the relationship between the predicted FEV-1 % and the concentration of the respective autoantibodies SAA2 (A), SCL-70 (B), sm antigen (C), HNRD (D), histone (E), AGG1 (F), azorocidin (G), cANCA (H) and ro-ssa (I) in patients with COPD. All above autoantigens showed negative results in correlation to FEV-1 %.

5.3.5 Antigen microarray quality control for IgM antibody responses

The concentration of IgM antibodies in the sera of the different study groups was investigated for three control antigens, Tetanus, Candida, and *H. influenzae*. The results (Figure 5.13) showed there was a significant difference of increased IgM antibody to Candida reactivity in COPD group with $p = 0.0387^*$ and a significant differences of increased antibodies to H.I and Tetanus in non-smoking control group with $p = 0.0006^{***}$, $p = 0.0314^*$ respectively, compared to COPD group (figure 5.13).

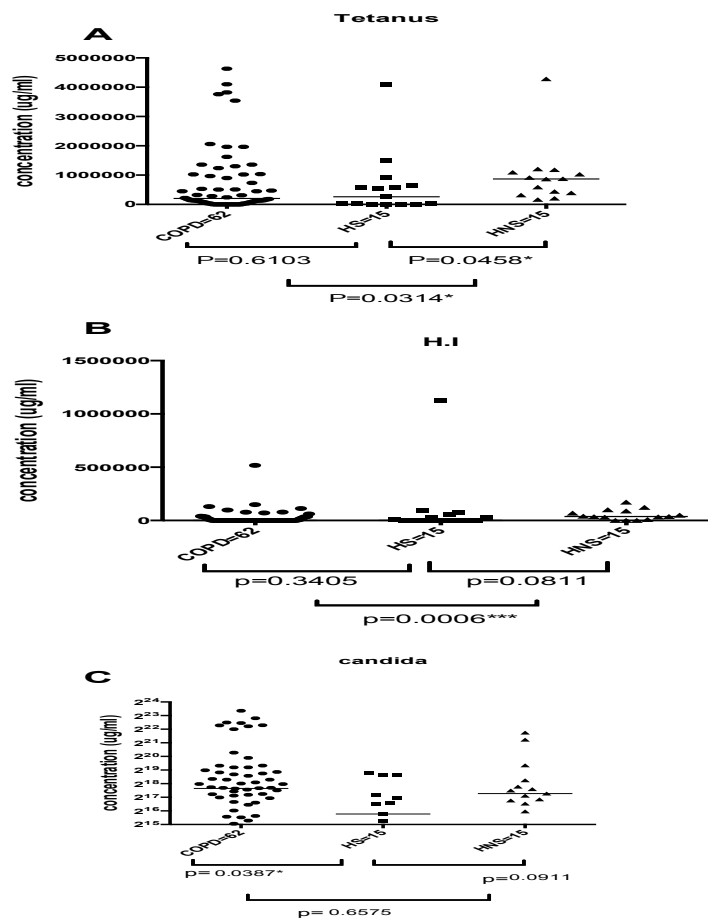


Figure 5. 13: IgM concentration in sera of COPD, healthy smoking and non-smoking controls.

Sera from subjects with COPD, healthy smokers (HS) and healthy non-smokers (HNS) controls were analysed by microarray for total IgM concentrations against: A) Tetanus, B) *H. Influenza* and C) Candida antigens. Each point represents an individual serum sample, and the lines between points are the median IgM µg/ml of the groups. statistical comparisons between all groups were performed using Mann-Whitney test and p values < 0.05 were considered as significant.

5.3.6 The levels of IgM autoantibodies in sera of COPD individuals, non-smoking controls and smoking controls

Sera from COPD individuals, HS and HNS were analysed on the microarray platform for IgM autoantibodies to all the different autoantigens to be investigated (table 5.1). Significant differences between the groups were measured using a Mann-Whitney test. In addition, for all autoantibody results, a line representing the 95 th percentile of the healthy non-smoking group was drawn to allow detection of significantly higher results within the data sets. Furthermore, to ensure a more stringent cut off, the 95 th percentile of the healthy smoking group was also used to determine those patients with higher autoantibody responses to autoantigens.

Autoantibodies that could be associated with a variety of autoimmune diseases namely Aggrecan1, azurite, cANCA, cit-keratin, cit-collagen II, cit-collagen III, cit-collagen IV, cit-collagen V and cit-fibronectin were measured (figure 5.14). Interestingly, no significant differences in IgM autoantibodies against any citrullinated autoantigens were found. IgM autoantibodies to Aggrecan1 and cANCA were significantly higher in HNS compared to COPD and HS with $p = 0.0116^*$, $p = 0.0052^{**}$ and $p = 0.0022^{**}$ respectively. However, autoantibodies against azurocidin were significantly higher in HS with $p = 0.0495^*$ compared to COPD. 7 out of 62 COPD patients had levels of autoantibodies to cit-collagenV higher than 95 th percentile of non-smoking control group, and none of 62 COPD patients had levels of autoantibodies to cit-collagen V higher than 95 th percentile of healthy smoking group.

IgM autoantibodies to collagens, CENP-B, decorin, GBM and cytochrome c were also measured (figure 5.15). Autoantibodies to CENP-B were significantly higher in COPD patients compared to HS and HNS with $p = 0.0063^{**}$ and $p = 0.0318^*$. In addition, autoantibodies to collagen V also were significantly higher in COPD patients compared

to HNS control group with $p = 0.0341^*$. Interestingly, 12 out of 62 COPD patients had levels of autoantibody responses to CENP-B higher than 95 th percentile of the non-smoking group, and 36 out of 62 COPD patients had level of autoantibody responses to CENP-B higher than 95 th percentile of the healthy smoker group. In addition, 18 out of 62 COPD had autoantibody responses to collagen V higher than 95 th percentile of the non-smoking control group, and by using the more stringent cut-off, 17 out of 62 of COPD patients had levels higher than 95 th percentile of the healthy smoker group. Autoantibody responses to histone, HNRPD, keratin 18, keratin 8, La/ssb, nucleosome, pANCA, pl-12 and pl-7 also were measured (figure 5.16). Autoantibodies to histone and La/ssb were significantly higher in COPD patients compared to the non-smoking control group; however, autoantibodies to HNRPD were significantly lower with $p = 0.0040^{**}$ in COPD compared to healthy non-smoking group. Interestingly, 16 out of 62 COPD patients had levels higher than 95 th percentile of the non-smoking group, and no COPD patients had levels of autoantibodies to histone higher than 95 th percentile of the healthy smoker group. Moreover, 12 out of 62 COPD patients had levels of autoantibodies to pl-7 higher than 95 th percentile of the non-smoking group and 10 out of 62 of COPD had level higher than 95 th percentile of the healthy smoker group. With regard to autoantibody responses to ribosomal p, RNP/68 sm free, RNP/sm, RNP/sm free, ro-52, ro-ssa, SAA2, SCL-70 and sm antigen (figure 5.17), autoantibodies to RNP/sm were significantly higher in COPD patients compared to controls with $p = 0.0241^*$. 30 out of 62 COPD patients had levels of autoantibodies to RNP/sm higher than 95 th percentile of the non-smoking group, and 5 out of 62 of patients had levels higher than 95 th percentile of the healthy smoker group. In addition, 6 out of 62 COPD patients had levels of autoantibodies to ribosomal p higher than 95 th percentile of the non-smoking group, and 9 out of 62 had levels of autoantibodies to ribosomal p higher than the 95 th

percentile of the healthy smoker group. 6 out of 62 COPD patients had levels of autoantibodies to RNP/68 sm free higher than 95 th percentile of the non-smoking group and no COPD patients had any autoantibody responses to RNP/68 sm free higher than 95 th percentile of the healthy smoker group. The results show that certain IgM autoantibodies to CENP-B, collagen2, collagen5, histone, La/ssb, PL-7, RNP/sm and SCL-70, showed high levels in the COPD group to be well above the 95 th percentile of the non-smoking group and above the 95 th percentile of the healthy smoking group. The healthy smoker group showed autoantibody responses to most of the examined autoantigens higher than the 95 th percentile of the non-smoking group. We also examined the increase of autoantibody response per COPD patient to determine if all COPD patients had an IgM autoantibody response above 95 th percentile of the control group. The results (Table 5.7) showed that only 12 out of 62 COPD patients had no detectable autoantibody response above the 95 th percentile of the non-smoker group. In addition, the number of IgM autoantibody responses above the 95 th percentile of the healthy smokers group was measured, and this showed that only 9 out of 62 COPD patients had no detectable autoantibody response above the 95 th percentile of the smoker group.

We also examined the autoantibody response of healthy smokers (Table 5.8) and again, most had at least one response above the 95 th percentile of the non-smoker group (12 out of 15).

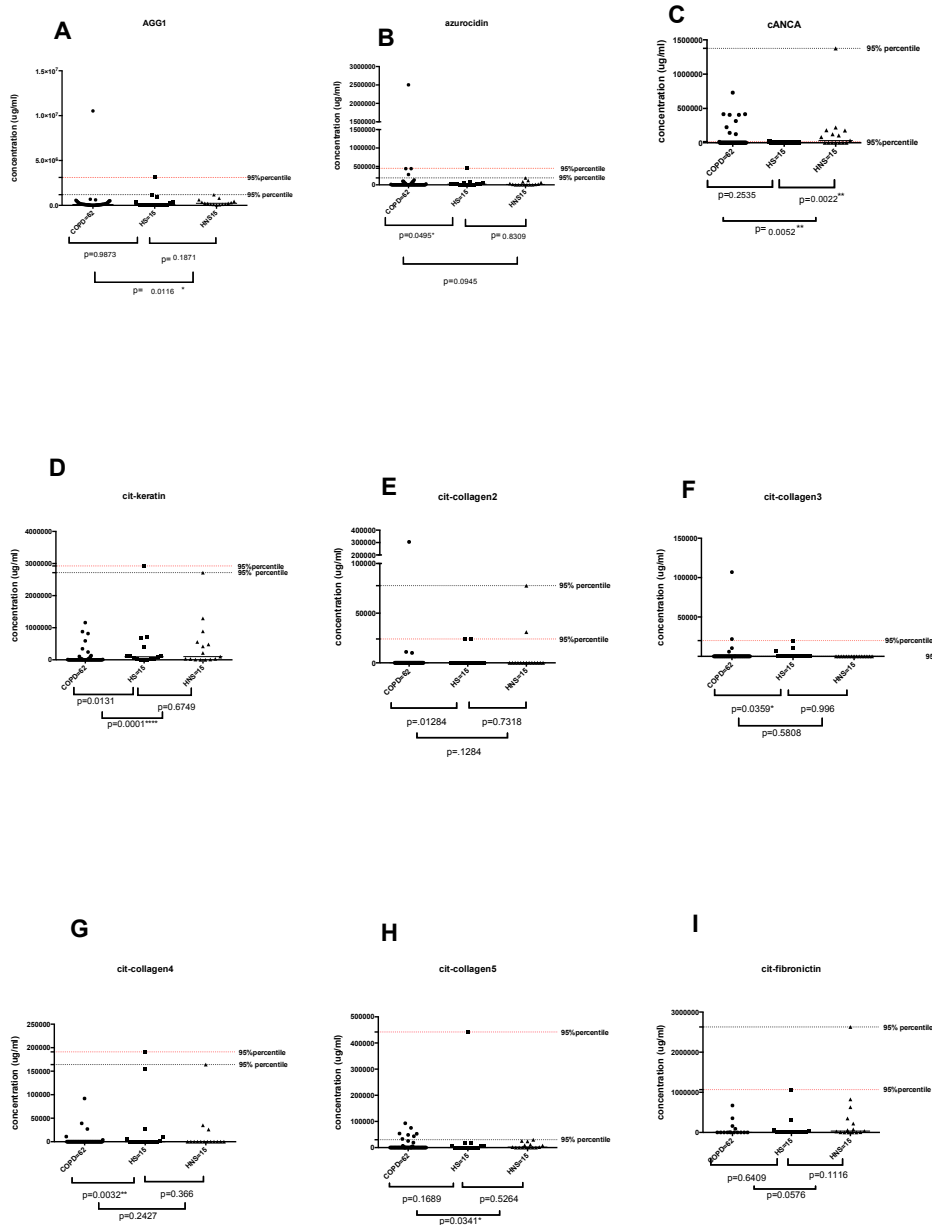


Figure 5. 14: Differences in the concentration of autoantibodies (IgM) against different autoantigens in sera of subjects with COPD, healthy smokers and non-smoker controls.

The difference in IgM concentrations to: A) AGG1, B) azurocidin, C) cANCA, D) citrullinated keratin, E) citrullinated collagen2, and I) citrullinated fibronectin respectively in those with COPD, healthy smokers (HS) and non-smokers (HNS) controls. Each point represents an individual serum sample, and the lines between points are the median IgM µg/ml of the groups. Black dashed lines are the 95 % percentile of the healthy non-smoking control group and red dashed lines are the 95 % percentile of healthy smoker; statistical comparisons between all groups were performed using Mann-Whitney test and p values < 0.05 were considered as significant.

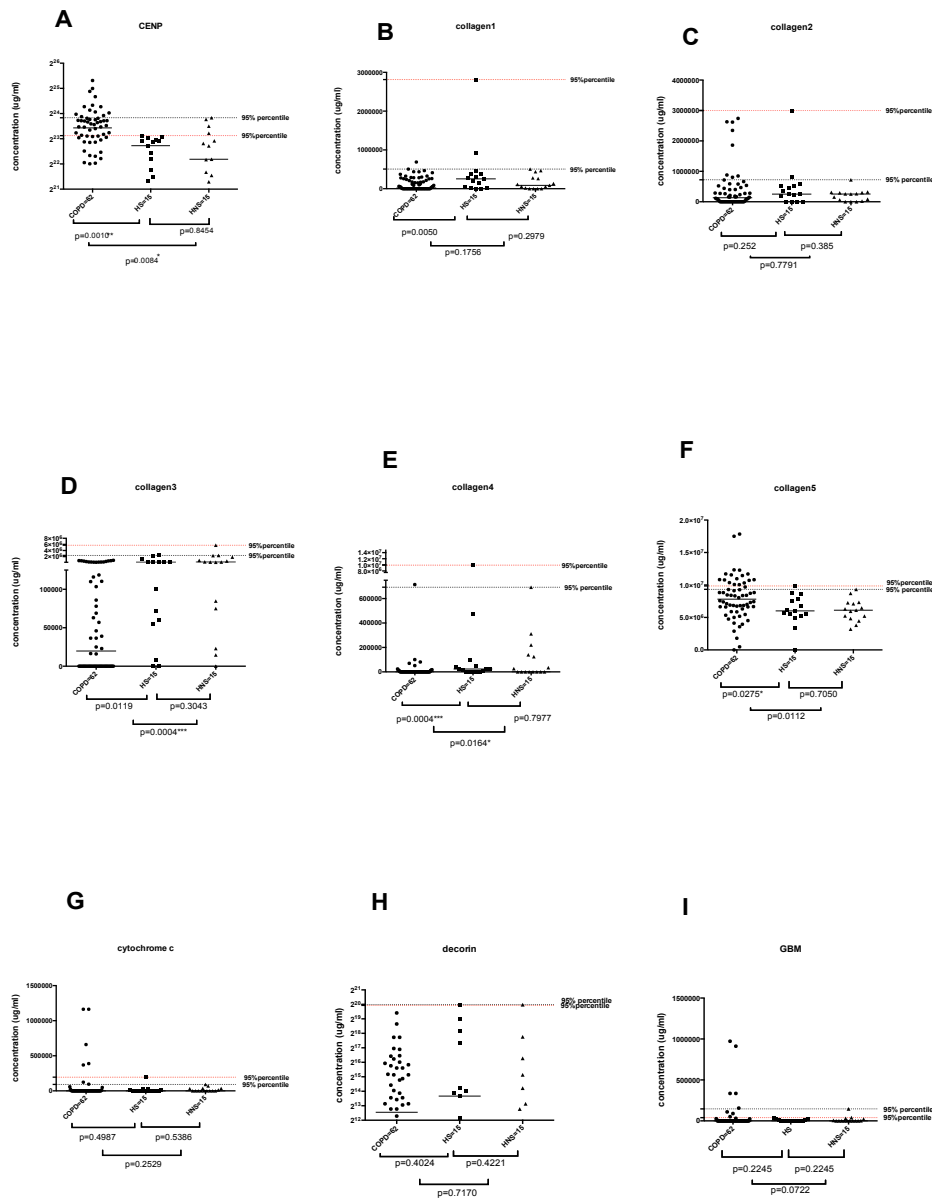


Figure 5. 15: Differences in the concentration of autoantibodies (IgM) against different autoantigens in sera of subjects with COPD, healthy smokers and non-smoker controls.

The difference in autoantibodies (IgM) concentrations to: A) CENP-B, B) collagen1, C) collagen2, D) collagen3, E) collagen4, F) collagen5, G) cytochrome c, H) decorin, I) GBM, respectively, were analysed by Antigen microarray in those with COPD, healthy smokers (HS) and non-smokers (HNS) controls. Each point represents an individual serum sample, and the lines between points are the median IgM µg/ml of the groups. Black dashed lines are the 95% percentile of the healthy non-smoking control group and red dashed lines are the 95%percentile of healthy smokers group; statistical comparisons between all groups were performed using Mann-Whitney test and p values < 0.05 were considered as significant.

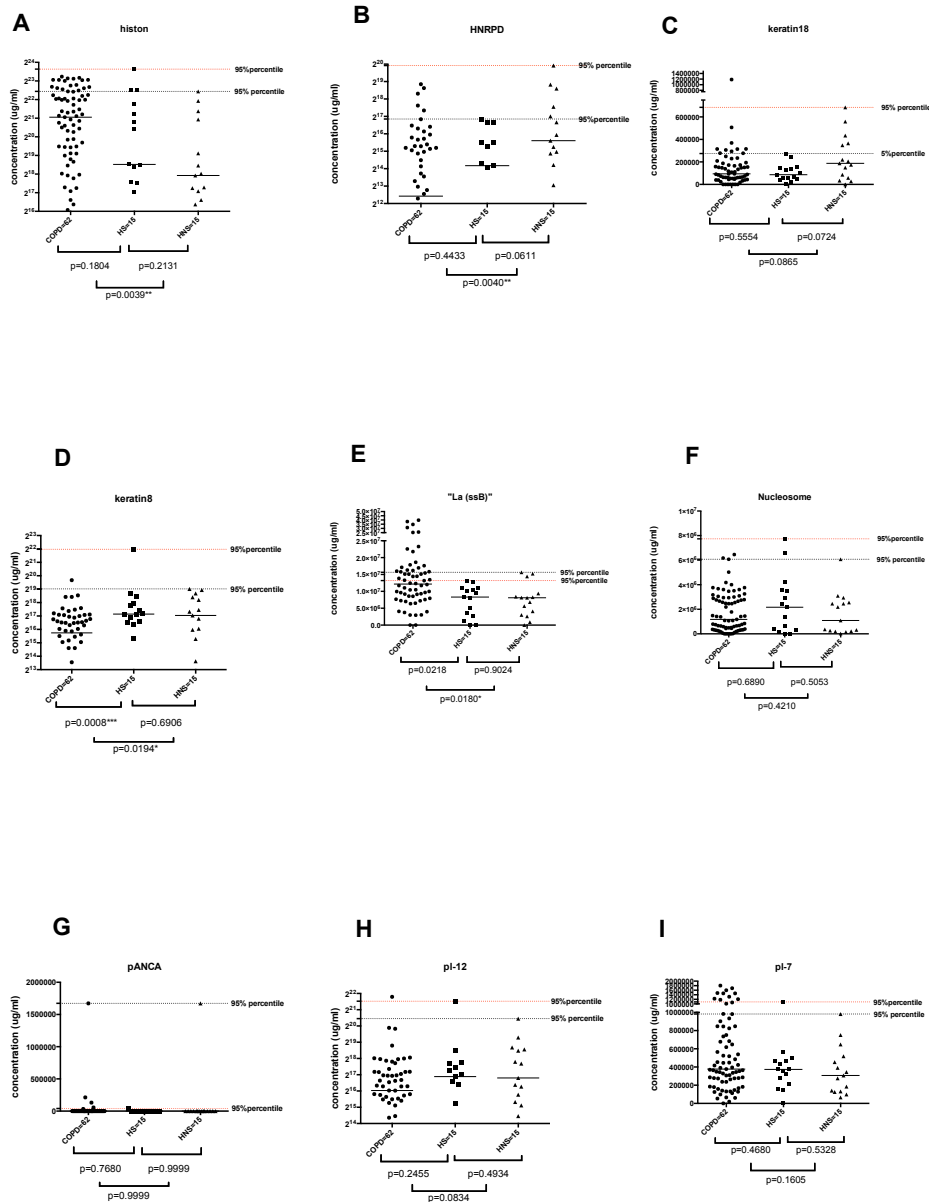


Figure 5. 16: Differences in the concentration of autoantibodies (IgM) against different autoantigens in sera of subjects with COPD, healthy smokers and non-smoker controls.

The difference in autoantibodies (IgM) concentrations to: A) histone, B) HNRD, C) keratin18, D) keratin8, E) La ssb, F) nucleosome, G) pANCA, H) PL-12, I) PL-7 respectively, were analysed by Antigen microarray in those with COPD, healthy smokers (HS) and non-smokers (HNS) controls. Each point represents an individual serum sample, and the lines between points are the median IgM $\mu\text{g/ml}$ of the groups. Black dashed lines are the 95% percentile of the healthy non-smoking control group and red dashed lines are the 95%percentile of healthy smokers control; statistical comparisons between all groups were performed using Mann-Whitney test and p values < 0.05 were considered as significant.

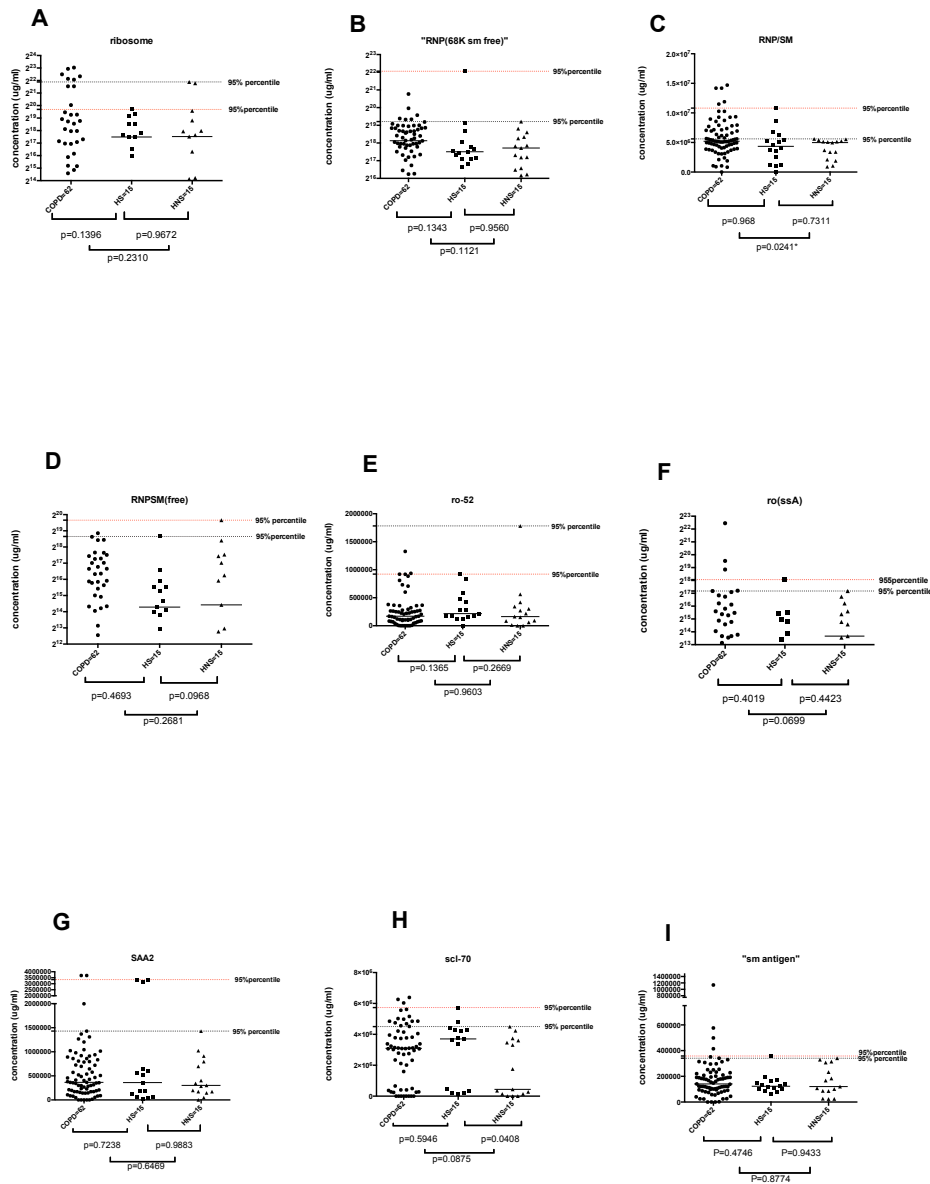


Figure 5. 17: Differences in the reactivity of autoantibodies (IgM) against different autoantigens in sera of subjects with COPD, healthy smokers and non-smokers controls.

The difference in autoantibodies (IgM) concentrations to: A) ribosome, B) RNP 68ksm free, C) RNP/sm, D) RNP/sm free, E) ro-52, F) ro-ssa, G) SAA2, H) SCL-70, I) sm antigen, respectively, were analysed by Antigen microarray in those with COPD, healthy smokers (HS) and non-smokers (HNS) controls. Each point represents an individual serum sample, and the lines between points are the median IgM µg/ml of the groups. Black dashed lines are the 955 percentile of the healthy non-smoking control group and red dashed lines are the 95%percentile of healthy smokers control; statistical comparisons between all groups were performed using Mann-Whitney test and p values < 0.05 were considered as significant.

Table 5. 6: Significant differences between IgM antibodies between the study groups.

COPD versus HS	COPD versus HNS	HNS versus HS
azorocidin*	AGG1*	SCL-70*
Candida*	cANCA**	cANCA*
CENP-B**	CENP-B*	Tetanus*
citrellenated collagen3*	citrellenated collagen5*	
citrellenated collagen4**	citrellenated keratin***	
citrellenated keratin*	collagen3***	
collagen1**	keratin8*	
collagen3*	collagen5*	
	H.Influenza***	
collagen5*	histon**	
keratin8***	HNRD**	
La ssb*	La ssb*	
	RNP/sm*	
	Tetanus*	
	cANCA**	

* Listed above are the specific autoantigens that have significantly different reactions between the study groups. Statistical significance was calculated using unpaired Mann-Whitney test. All listed are $p < 0.05$. Antigen in bold indicate the significant increase in COPD group.

* Antigens in bold indicate the significant increase in COPD group. * = p value $< (0.05)$, ** = p value $< (0.005)$, *** p value $< (0.0005)$

Table 5. 7: Details of samples and reactivity of IgM autoantibodies against the examined autoantigens from COPD.

COPD Number	Antigen above 95 th percentile	No. of positive Ags
1		
2	ribosome	1
3	histone+RNP/SM	2
4		
5	RNP/SM	1
6	ro-ssa	1
7	collagen5+histone+nucleosome+RNP/SM+SCL-70	5
8	histone+RNP/SM+SCL-70	3
9	cytochrome c+histone+RNP/SM+SAA2+SCL-70	5
10	cytochrome c+histone+RNP/SM+SAA2+SCL-70	5
11	collagen2	1
12	collagen2	1
13		
14		
15	collagen2+collagen5	2
16	collagen2+histone+RNP/SM	3
17	collagen5+histone+RNP/SM	3
18	collagen2+histone+La ssb+RNP/SM+SAA2	5
19	collagen2+PL-7+RNP/SM	3
20	CENP-B+collagen5+histone+PL-7+RNP/68k sm	6

	free+RNP/SM	
21	CENP-B+cit-collagen5+collagen2+PL-7	4
22	cit-collagen5+collagen2+collagen5+RNP/SM	4
23	PL-7+SCL-70	2
24	collagen5+histone+PL-7+RNP/SM+SCL-70	5
25	PL-7	1
26	CENP-B+collagen5+histone+La ssb+PL-7+ribosome+RNP/SM+ro-ssa+SCL-70+sm antigen	10
27	cit-collagen5+La ssb+PL-7	3
28	cit-collagen5+GBM+histone+PL-7	3
29	collagen5+RNP/68k sm free+RNP/SM	3
30	CENP-B+cit-collagen5+La ssb+RNP/SM	4
31		
32	histone+SCL-70+RNP/SM	3
33	cytochrome c+RNP/SM	2
34	PL-12+RNP/68k sm free+SCL-70	3
35	CENP-B+collagen5+La ssb+SCL-70+RNP/SM	5
36	collagen5+SCL-70+sm antigen+RNP/SM	4
37	CENP-B+collagen5+La ssb+PL-7+SCL-70+RNP/SM	6
38	cit-collagen5+collagen5+RNP/SM	3
39		
40	PL-7+SCL-70+sm antigen	3
41	CENP-B+La ssb	2
42		
43		
44		
45	CENP-B+cit-collagen5+cytochrome c+GBM+keratin18+keratin8+La ssb+PL-7+ribosome+RNP/68k sm free+ro-ssa+sm antigen+RNP/SM	13
46	cit-collagen2+PL-7	2
47	CENP-B+La ssb+ribosome+RNP/SM	4
48	histone+La ssb+RNP/68k sm free+RNP/SM	4
49	La ssb+RNP/68k sm free+RNP/SM	3
50	collagen5+histone+La ssb+RNP/SM	4
51	sm antigen+RNP/SM	2
52	histone+La ssb+RNP/SM	3
53	La ssb	1
54	La ssb+ribosome+RNP/SM	3
55	La ssb	1
56	cytochrome c+SCL-70	2
57	CENP-B	1
58	CENP-B+cytochrome c+GBM+ribosome	4
59		
60		
61	collagen5	1
62	CENP-B+collagen1+collagen4	3

* Serum samples from patients were analysed by antigen microarray for the presence of 39 autoantigens. Table represents different antigens that showed values above 95 th percentile of healthy non-smoking control.

Table 5. 8: Details of samples and reactivity of IgM autoantibodies against the examined antigens from healthy smokers and healthy non-smoker controls.

Serum. Number	Antigen above 95 th percentile	No. of positive Ags
HS1	Nucleosome	1
HS2	Histone+RNP/SM	2
HS3	cit-collagen5+ro-ssa	2
HS4	cytochrome c	1
HS5	AGG1+cit-keratin+SSA2	3
HS6	SSA2\+RNP/SM	2
HS7	histone+RNP/SM	2
HS8	PL-12+PL-7+RNP/SM+SCL-70	4
HS9	azorocidin+cit-histone+nucleosome+SCL-70+sm+cit-collagen4+cit-collagen3	7
HS10	Cit-collagen3	1
HS11	collagen2+collagen4+cytokeratin8+RNP/68k sm free	4
HS12	collagen5	1
HS13	collagen1+collagen2	2
HS14	Cit-collagen3	1
HS15	SSA2+AGG1	2

HS= healthy smokers and HNS= healthy non-smokers serum samples from healthy controls were analysed by antigen microarray for the presence of 39 autoantigens. Table represents different antigens that showed values above 95 th percentile of HNS.

Table 5. 9: Details of samples and reactivity of IgM autoantibodies in COPD patients that are above 95 % percentile of healthy smokers control.

COPD Number	Autoantigens	Number of positive ags
1		
2	ribosomalp,ro-52	2
3	scl-70	1
4		
5		
6	CENP-B,ro-ssa	2
7	CENP-B,collagen5,lassb,ribosomalp,RNP/SM,scl-70	6
8	CENP-B,RNP/SM	2
9	cytochrome c,GBM,RNP/SM,SAA2	4
10	cytochrome c,GBM,RNP/SM,SAA2	4
11	collagen5,GBM	2
12	collagen5	1
13		
14	GBM	1

15	collagen5	1
16		
17	collagen5	1
18	Lassb	1
19		
20	CENP-B,collagen5,lassb,pl-7	3
21	CENP-B,lassb,pl-7	3
22	CENP-B,collagen5	2
23	pl-7	1
24	collagen5,pl-7	2
25	pl-7	1
26	CENP-B,collagen5,lassb,pl-7,ribosome	5
27	CENP-B,lassb,pl-7	3
28	CENP-B,GBM,PL-7	3
29	collagen5	1
30	CENP-B,collagen5,lassb	3
31		
32	RNP/sm	1
33		
34	CENP-B,pl-12,lassb,	3
35	CENP-B,collagen5,lassb	3
36	collagen5,sm	2
37	CENP-B,collagen5,GBM,lassb,scl-70	5
38	CENP-B,collagen5	2
39	CENP-B	1
40	CENP-B,lassb	2
41	CENP-B,lassb	2
42	CENP-B,lassb,ribosomal p	3
43	CENP-B,lassb,ribosomal p	3
44	CENP-B,lassb	2
45	CENP-B,cit-collagen3,cytochrome c,GBM,keratin18,lassb,pl-7,ribosomal p,ro-ssa,sm	10
46	CENP-B,cit-collagen2,lassb,pl-7	4
47	CENP-B,lassb,ribosomal p	3
48	CENP-B,lassb	2
49	CENP-B,lassb	2
50	CENP-B,lassb	2
51	lassb,sm	2
52	CENP-B,lassb	2
53	CENP-B,lassb,collagen5	3
54	CENP-B,lassb,ribosomal p	3
55	CENP-B, lassb	2
56	CENP-B,cytochrome c,lassb	3
57	CENP-B	1
58	CENP-B,cytochrome c,GBM,ribosomal p	4

59		
60	CENP-B	1
61	CENP-B,cit-collagen3,collagen5	3
62	Aggrecan,azurocidin,CENP-B,ro-ssa	4

Serum samples from patients were analysed by antigen microarray for the presence of 39 autoantigens. Table represents different antigens that showed values above 95 % percentile of healthy smoking control.

5.3.7 The correlation between IgM autoantibody concentrations and FEV-1 % in those with COPD

The predicted FEV-1 % was initially evaluated to see if there was a relationship between the FEV-1 % and the concentrations of IgM autoantibodies for the specific autoantigens investigated in COPD group. The correlation between these two variables was analysed by Spearman's Rank correlation, and the results (Figure 5.18 to 5.22) showed that there were no significant correlations for any of the 39 autoantigens.

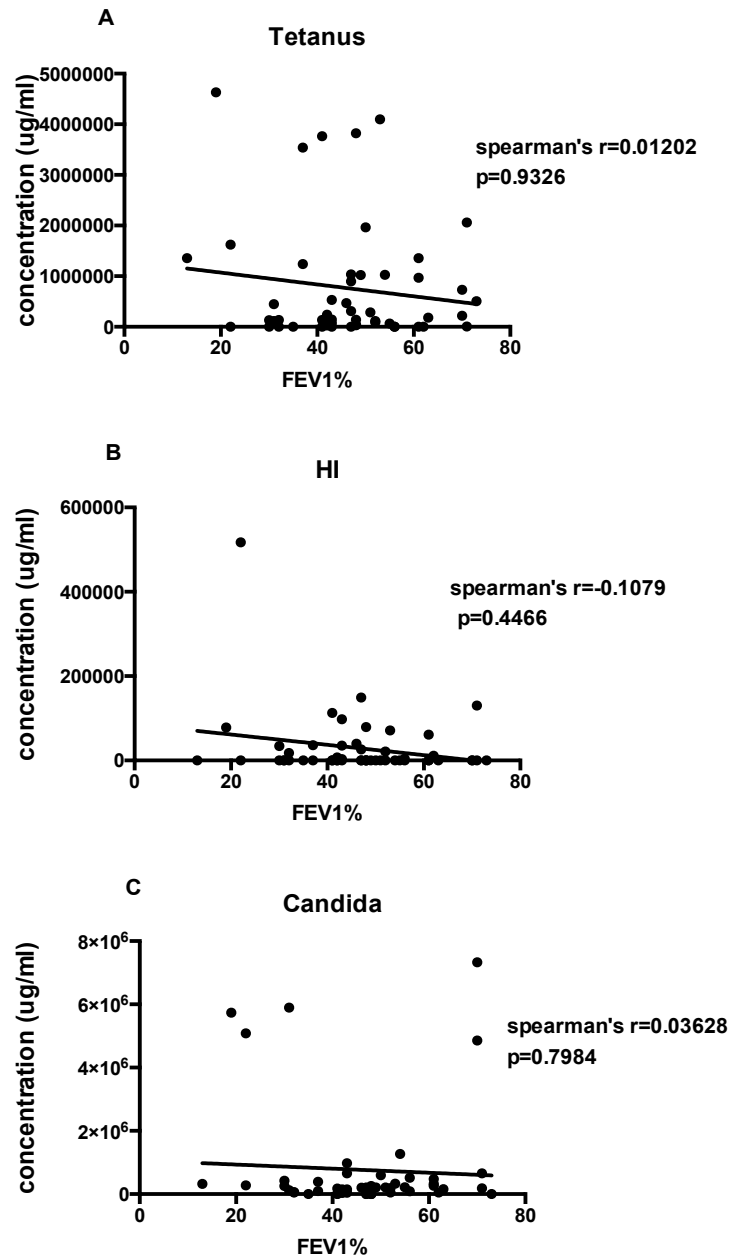


Figure 5. 18: Correlation between predicted FEV-1 % and IgM antibody concentration for the specific-control antigen: Candida, Tetanus and *H. Influenza*.

Spearman's Rank correlation tests were performed to compare the relationship between the FEV-1 % predicted against the concentration of the antigens Candida (A), Tetanus (B) and *H. influenza* (C) in patients with COPD, which showed no significant correlations.

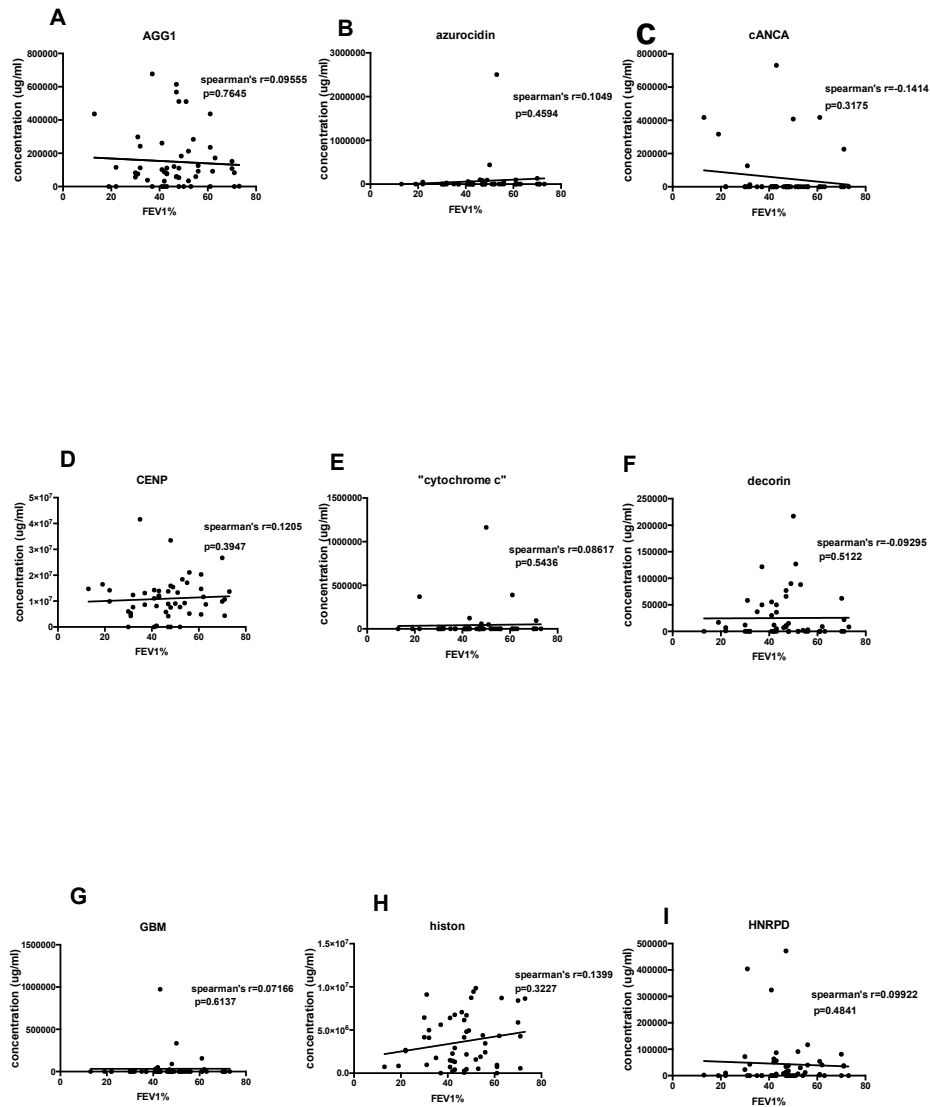


Figure 5. 19: Correlation between predicted FEV-1 % and IgM autoantibody concentrations of the specific- autoantigens: AGG1, azorocidin, cANCA, CENP-B, cytochrome c, decorin, GBM, histone and HNRD.

Spearman's Rank correlation tests were performed to compare the relationship between the FEV-1 % predicted against the concentration of the antigens A) AGG1, B) azorocidin, C) cANCA, D) CENP-B, E) cytochrome c, F) decorin, G) GBM, H) histone and I) HNRD, respectively, in patients with COPD, which showed no significant correlations.

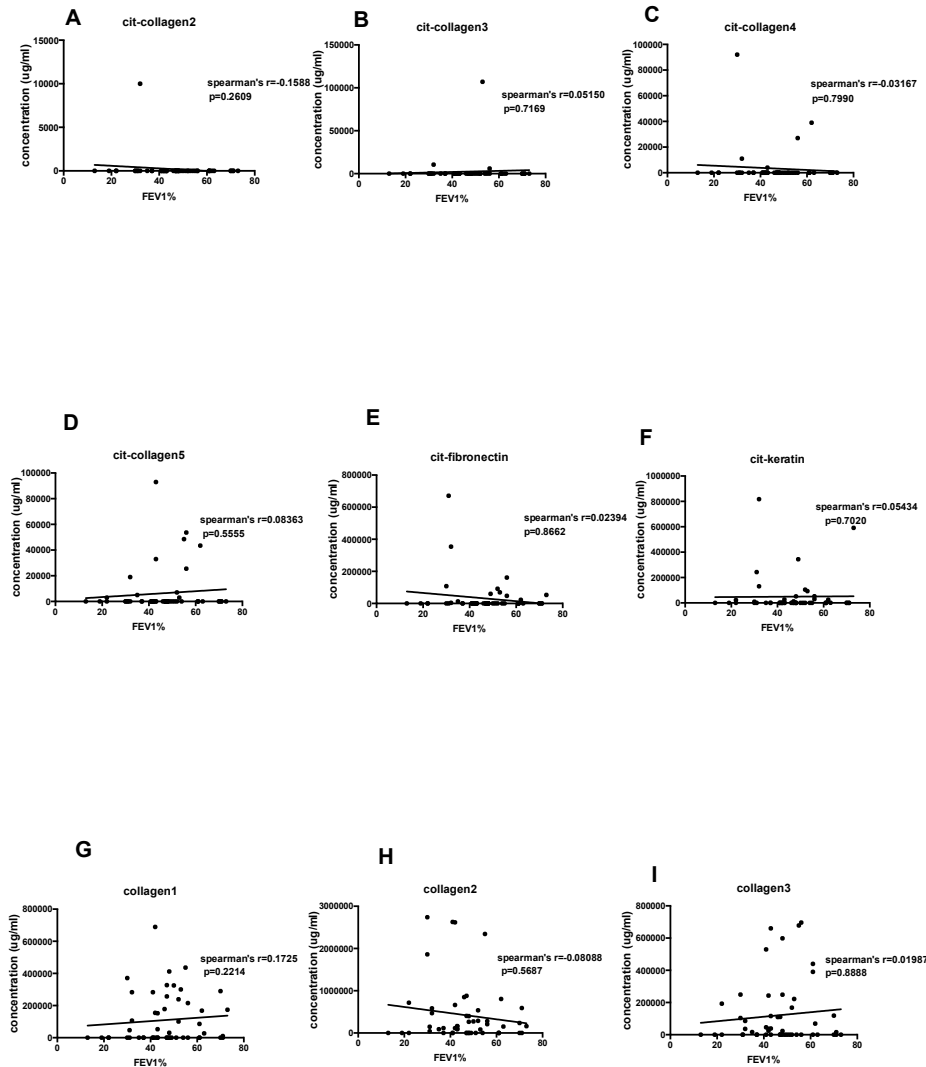


Figure 5. 20: Correlation between predicted FEV-1 % and IgM autoantibody concentrations for the specific- autoantigens: citrullinated collagen2, citrullinated collagen3, citrullinated collagen4, citrullinated collagen5, citrullinated fibronectin, citrullinated keratin, collagen1, collagen2 and collagen3.

Spearman's Rank correlation tests were performed to compare the relationship between the FEV-1 % predicted against the concentration of the antigens A) cit-collagen2, B) cit-collagen3, C) cit-collagen4, D) cit-collagen5, E) cit-fibronectin, F) cit-keratin, G) collagen1, H) collagen2 and I) collagen3 respectively, in patients with COPD, which showed no significant correlations.

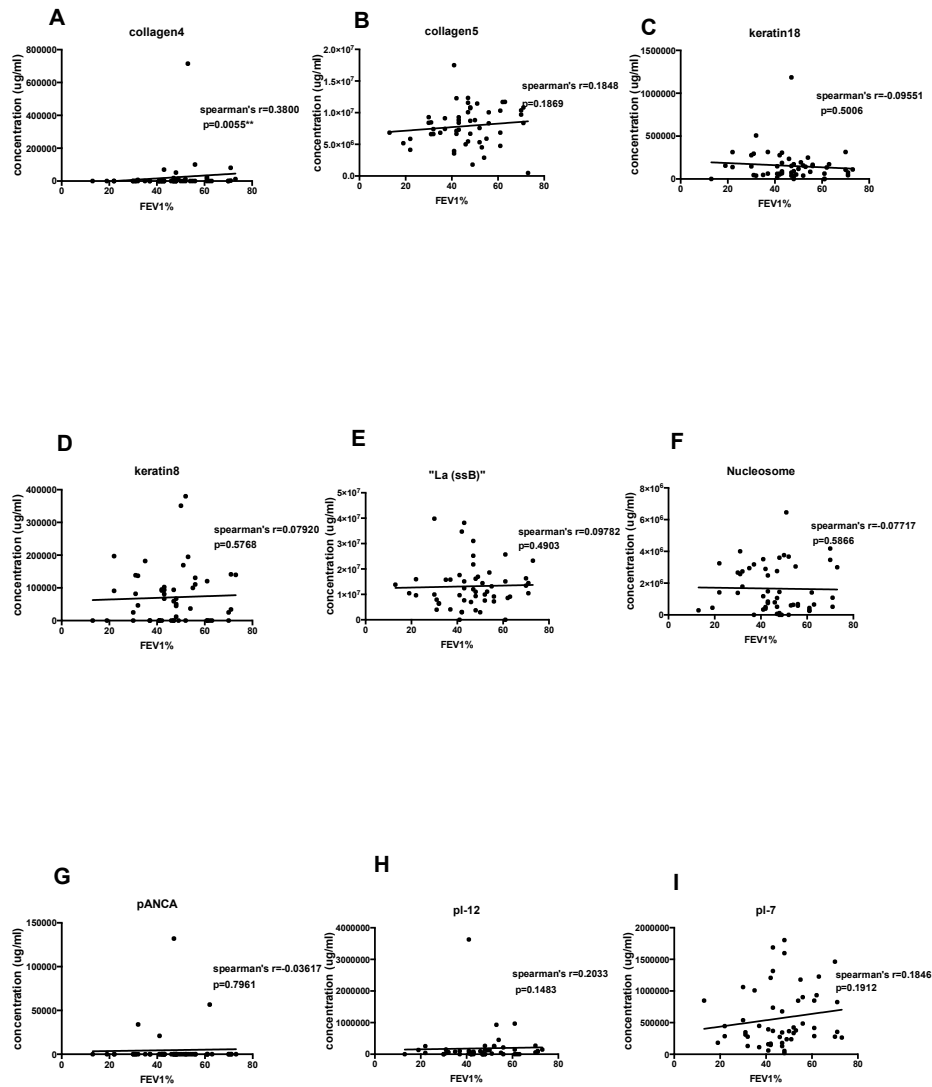


Figure 5. 21: Correlation between predicted FEV-1 % and IgM autoantibody concentrations of the specific- autoantigens: collagen4, collagen5, keratin18, keratin8, La ssb, nucleosome, pANCA, PL-12 and pl-7.

Spearman's Rank correlation tests were performed to compare the relationship between the FEV-1 % predicted against the concentration of the antigens A) collagen4, B) collagen5, C) keratin18, D) keratin8, E) La ssb, F) nucleosome, G) pANCA, H) PL-12 and I) PL-7, respectively, in patients with COPD, which showed no significant correlations.

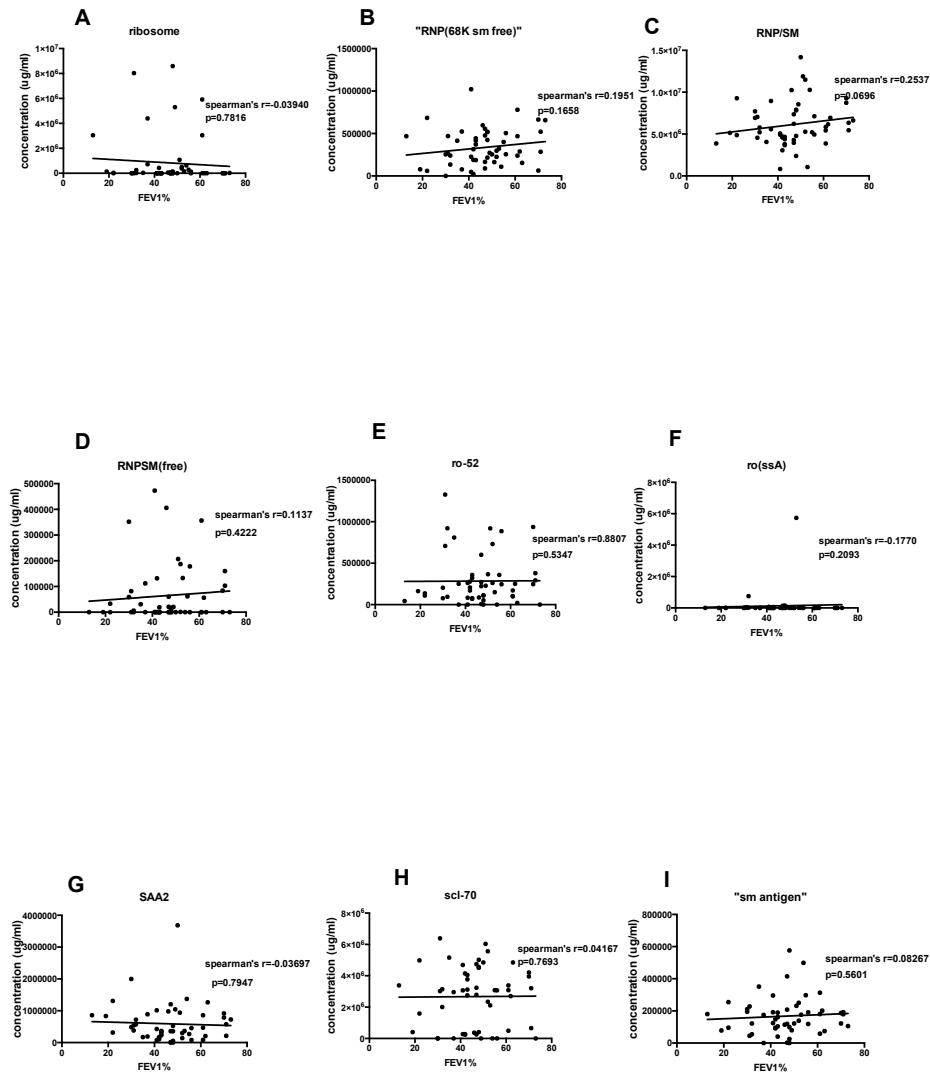


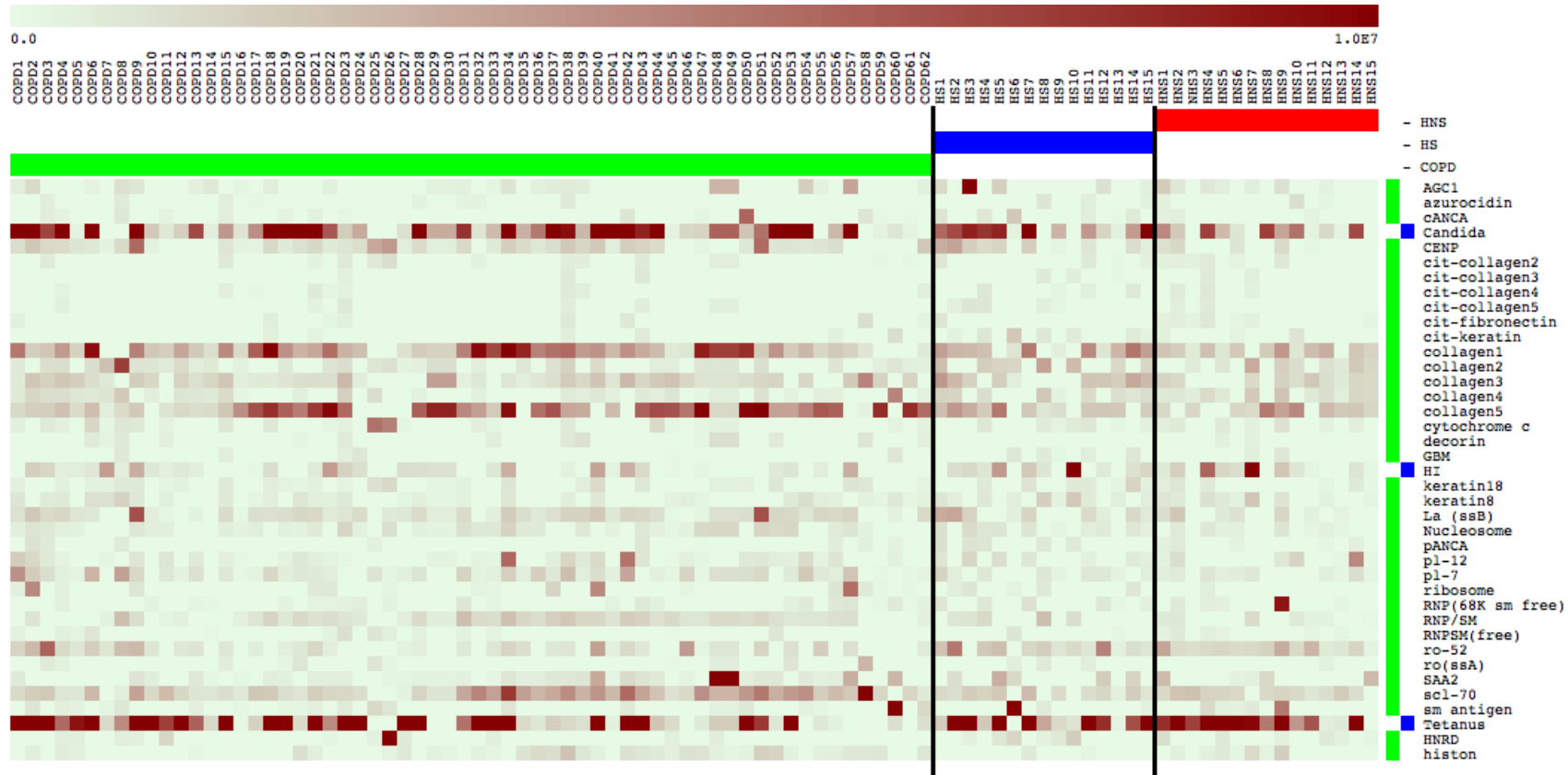
Figure 5. 22: Correlation between predicted FEV-1 % and IgM autoantibody concentrations of the specific- autoantigens: ribosome, RNP/sm, RNP/sm free, ro-52, ro-ssa, scl-70 and sm antigen.

Spearman's Rank correlation tests were performed to compare the relationship between the FEV-1 % predicted against the concentration of the autoantigens A) ribosome, B) RNP 68k sm free, C) RNP/sm, D) RNP/sm free, E) ro-52, F) ro-ssa, G) Saa2, H) scl-70 and I) sm antigen respectively, in patients with COPD, which showed no significant correlations.

5.3.8 Investigation of potential autoantibodies associations and disease states within the microarray data

In order to visualize the large data set (due to the big sample size and the 39 autoantigens used in this study) in an easy to compare format, the Venter Institute MEV Java tool was used for further analysis of the data. This software handles complex proteomic data sets and supports a range of analytical methods, including hierarchical clustering; it was therefore used to examine if there were any correlations or significant differences that were not obvious in the graphical representations of individual autoantibody responses previously presented in this chapter. In addition, the whole data set can be represented as just one projection in a Heat-map format, where samples are columns and responses to specific antigens are rows. Heat-maps were generated for the antigen specific-IgG autoantibodies (Figure 5.23) to visualise the differences between all three-study groups.

The heat-maps (Figure 5-23 A and B) show that an exclusion of response data below the 95 th percentile of the HNS population removed low level autoantibody signals and revealed IgG antibody responses to multiple antigens. This included the *Candida albicans* antigen preparation, which was included as a standardized control and showed a biased positivity among the smoker and COPD samples (Figure 5.23B). In addition, Figure 5.23B reveals that IgG antibody responses to collagen 5, collagen 1 and scl-70 are also particularly elevated amongst the COPD samples. There was also lower elevation of IgG antibodies in both COPD patients and healthy smokers, compared to the healthy non-smokers, for the antibodies to several other antigens, including CENP, collagen 3 and RNP/Sm.



A

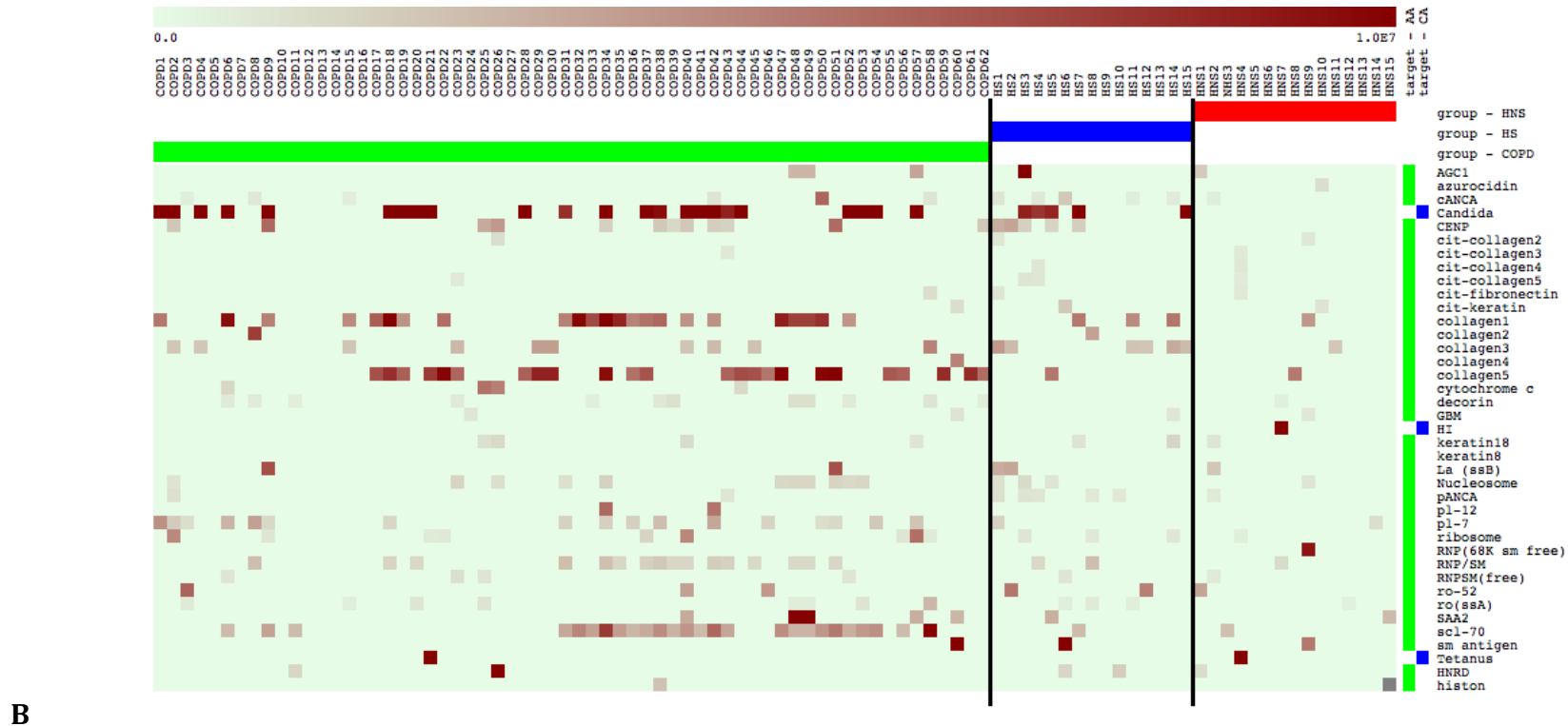
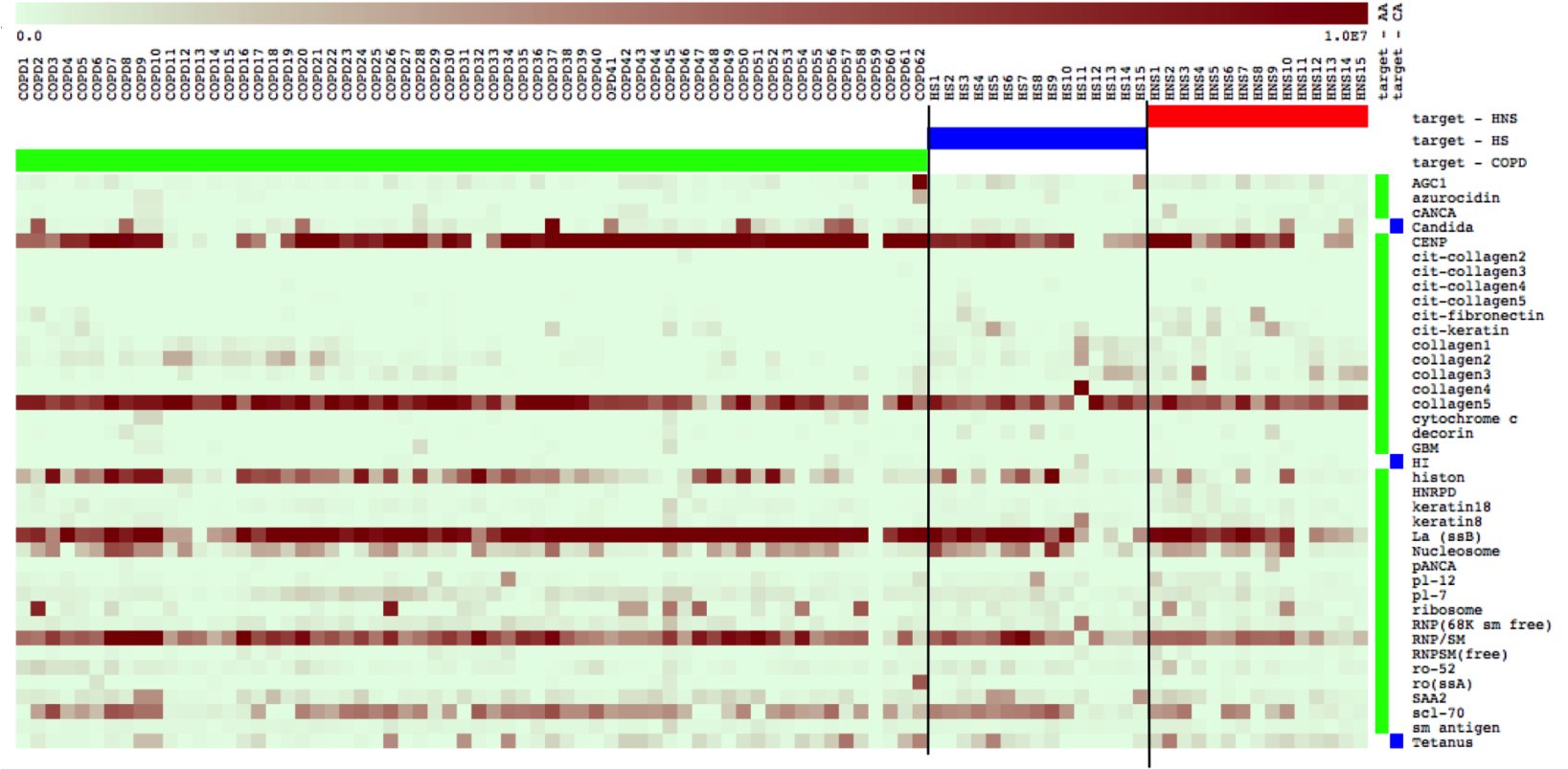


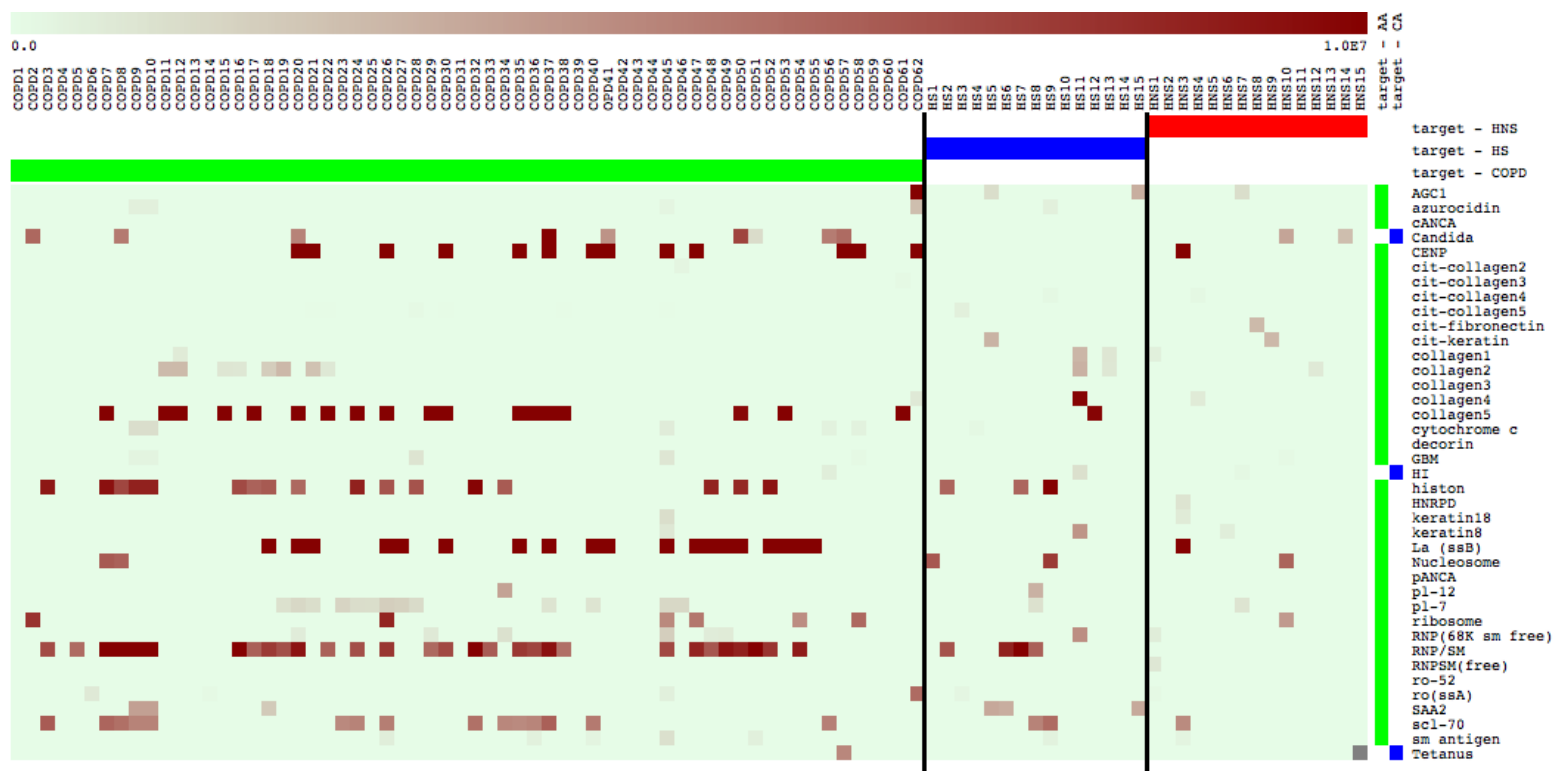
Figure 5. 23: Heat map of IgG autoantibodies

(A) Heat-map to show the screening of IgG autoantibodies in serum samples from COPD, healthy smokers and healthy non-smokers controls. (B) Heat-map of IgG autoantibodies detected in serum samples after filtering to exclude signals below the 95 th percentile derived from healthy non-smokers controls signals for each antigen respectively. The heat-map represents clustering by similarity of antigen-associated autoantibody signals for the presence of IgG autoantibodies against 39 autoantigens in sera of patients with COPD (green colour coding across the top of the plot), healthy smokers (HS; blue block across top of plot) and healthy non-smokers (HNS; red block). All sample derived signals are presented, without any pre-filtering to remove signals below that found in the healthy non-smokers. The relative degree of autoantibody reactivity in the sera is indicated by dark red for high reactivity and light green for low reactivity. The colour scale is presented at the extreme top of the plot.

Heat-maps were also generated to show antigen specific-IgM autoantibodies across the sample groups (figure 5.24 A and B). The heat map presents a colour-coded representation of the autoantibody signal detected from each target antigen, with darker colours indicating higher levels of autoantibody being detected. Again exclusion of response data below the 95th percentile of the healthy non-smoker population removed low level autoantibody signals yet revealed that IgM antibody responses to multiple antigens, including Collagen 5, CENP and La (ssB) in COPD and RNP/SM, histone and scl-70 in the COPD and healthy smoker groups. There were also lower IgM reactivities to collagen-1 and pI-7.



A



B

Figure 5. 24: Heat-map of IgM autoantibodies

(A) Heat-map to show the screening of IgM autoantibodies in serum samples from COPD, healthy smokers and healthy non-smoker controls. (B) Heat-map of IgM autoantibodies detected in serum samples after filtering to exclude signals below the 95 th percentile derived from healthy non-smokers controls signals for each antigen respectively. The heat-map represents clustering by similarity of antigen-associated autoantibody signals for the presence of IgM autoantibodies against 39 autoantigens in sera of patients with COPD (green colour coding across the top of the plot), healthy smokers (HS; blue block across top of plot) and healthy non-smokers (HNS; red block). All sample derived signals are presented, without any pre-filtering to remove signals below that found in the healthy non-smokers. The relative degree of autoantibody reactivity in the sera is indicated by dark red for high reactivity and light green for low reactivity. The colour scale is presented at the extreme top of the plot.

Furthermore, hierarchical clustering by both antigen and sample distance measures (ie most similar sample patterns are close to each other) reveals that there are subgroups of samples with particular IgG autoantibody responses. The results (Figure 5.25) indicate there is are multiple subgroups of patients with similar autoantibodies being detected, including major groupings associated with antibodies to Collagen 5, *Candida albicans* and Collagen 1. Interestingly, the larger collagen 5 cluster does contain one healthy non-smoker, however existing clinical data did not allow further examination of this sample origin. Lesser clusters include samples with SCL-70 and CENP.

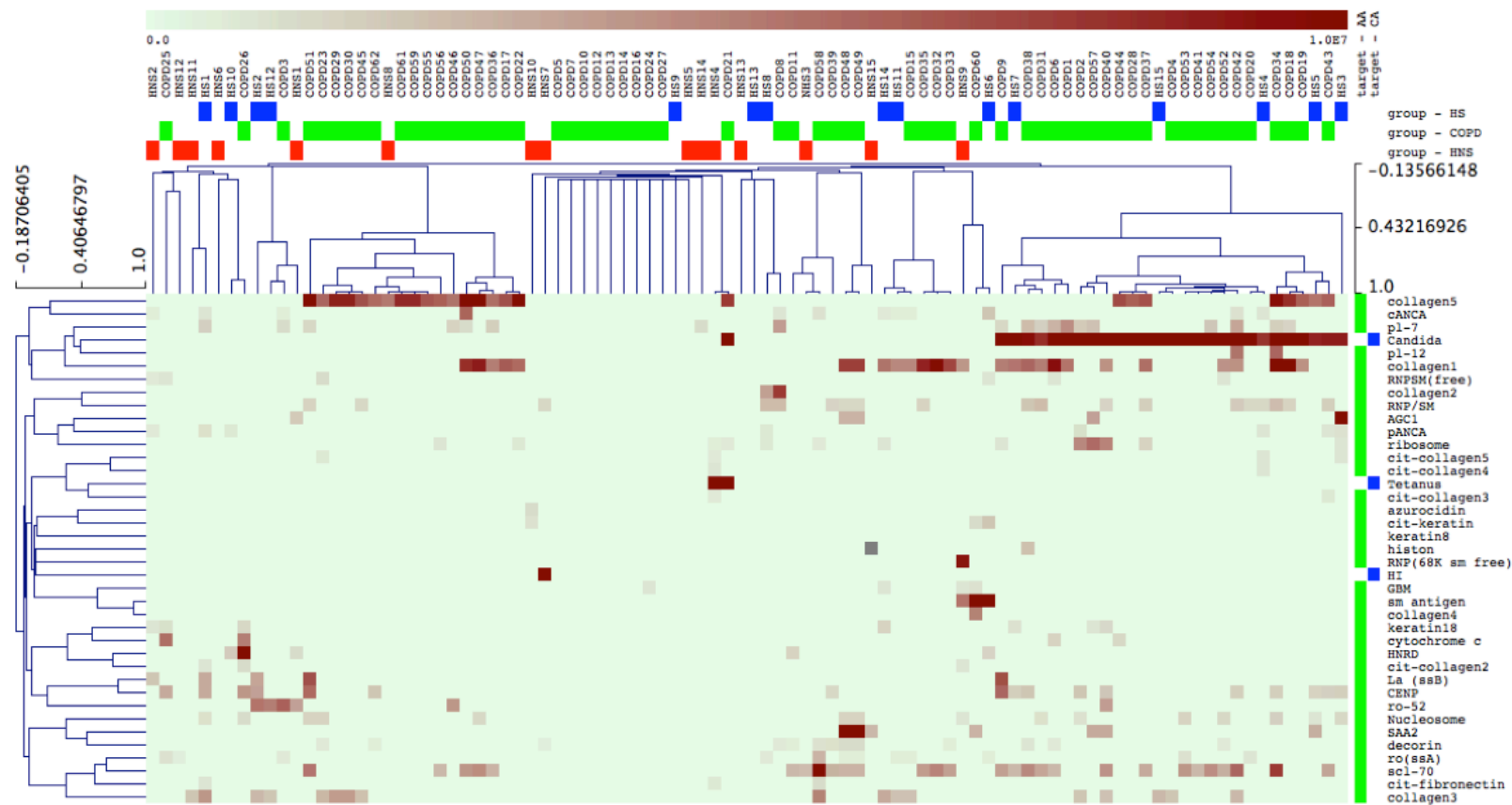


Figure 5.25: Hierarchical clustering of IgG autoantibody measurements using both antigen and sample distance measures.

Clustering by both antigen and sample distance measures (ie most similar sample patterns are close to each other) reveals that there are subgroups of samples with particular autoantibody responses.

Similarly, clustering of the IgM autoantibody data by both sample and antigen reveals multiple clusters with similarity of responses. The results (Figure 5.26) show the clustering and distance measures associated with the IgM responses: defined clusters, with some overlap of antigens recognized are seen for antigens including collagen 5, p1-7, RNP/SM, Histone and Scl-70. These results also show that the clustering patterns are clearly different for IgM and IgG autoantibodies.

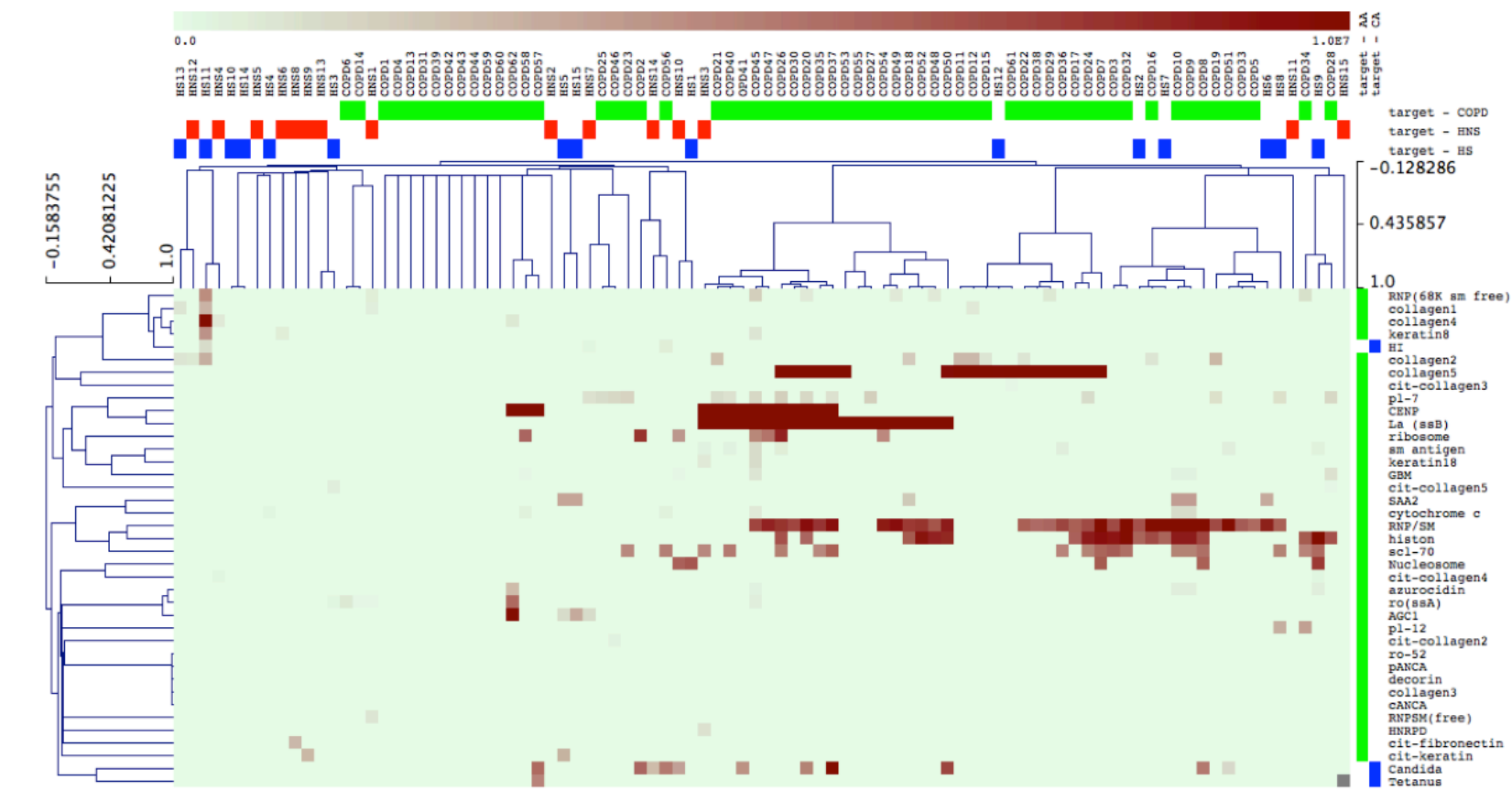


Figure 5. 26: Hierarchical clustering of IgM autoantibody measurements using both antigen and sample distance measures.

Clustering by both antigen and sample distance measures (ie most similar sample patterns are close to each other) reveals that there are subgroups of samples with particular autoantibody response.

5.4 Discussion:

This study investigated the occurrence of autoantibodies to 39 antigens associated with many autoimmune diseases in COPD patients, by identifying the reactivity and concentrations in the subjects' sera using a microarray. We applied our optimized and validated antigen microarray platform to the sera from COPD patients, healthy smokers (HS) and healthy non-smokers (HNS) as control groups, to assess the reactivity of IgG and IgM autoantibodies against these specific autoantigens. Overall the results of this chapter showed that autoantibodies to none of the 39 autoantigens completely correlated to all of the patient demographics and spirometric measurements (age, gender and FEV-1 %), except for ribosomal p, which showed a significant correlation ($P = 0.03$) between the lung function FEV-1 % for COPD patients and anti-ribosomal p concentration in their serum (decreasing the lung function associated with an increase of ribosomal p antigen in the serum).

However, the results highlighted a group of antigens (RNP/sm, ro-52, SCL-70, histone, CENP-B, collagen5 and La/ssb) that showed significant differences in autoantibody levels between the COPD group and the HS control group; while another set of antigens (Candida, CENP-B, collagen5, La/ssb and RNP/sm) were significantly different in autoantibody levels between the COPD and the HNS groups, despite there being no significant correlation with FEV-1 %. Hence anti-RNP/sm may be an important biomarker in distinguishing between those that have COPD, and those who are HS or HNS as it had a significantly higher concentration in COPD patients than in smokers and non-smokers. The higher

prevalence of antibodies to *Candida* in COPD patients may be indicative of more frequent infections or colonisation by *Candida* in these patients.

Apart from anti-collagen-5, all the autoantibodies that showed a significant increase in the COPD group when compared to the controls, were specific for extractable nuclear antigens (ENA) and thus, the occurrence of ANA in some COPD patients was indicated by high levels of serum IgG antibodies specific to CENP-B, La/ssb, Ro-52, SCL-70, histone and RNP/sm. Within the literature there are few publications that have shown the prevalence of ANA in the serum of COPD patients compared to the controls, and one such study also demonstrated that there was no significant association with age, gender and smoking status, which agreed with our study[107, 197].

IgG antibodies to collagen-5 were raised significantly in the serum of COPD patients when compared to the control groups, and this finding is consistent with a previous study that showed an increase in levels of serum IgG antibodies to collagen-5 in COPD patients, detected by enzyme-linked immunosorbent assay (ELISA)[109]. In our study we expanded the panel of examined antigens to include all collagen types in order to investigate if there were any differences in specific autoantibody concentrations in COPD sera, as well as investigating other extracellular matrix proteins in the lung such as decorin, cytokeratin 18 and cytokeratin 8[198]. There is also a B cell component, which is shown by the presence of B cell lymphoid follicles in COPD lung tissue, with increasing numbers corresponding to a higher disease severity. By analysing the genes associated with the increased numbers of B cells, studies have shown there were somatic hypermutations and oligoclonality, suggesting the B cell response in COPD is antigen specific. Currently it is not clear which antigens cause the

response, but the suggested sources of antigens include auto-antigens from extracellular matrix degradation products[199].

This immune involvement had been further demonstrated by studies that have shown that neutrophils can be activated by cigarette smoke extract. Once activated the neutrophils can cause collagen to be broken down to N-ac-PGP, which in itself can activate neutrophils, and this can lead to a self-propagating cycle of activation, which may result in chronic inflammation in the lung and emphysema[200].

One of the processes that can play a role in healthy and disease progression is citrullination; this is the post-translational modification of proteins which used peptidylarginine deiminases (PAD) to enzymatically convert arginine to citrulline, and it occurs in a large range of conditions and tissues[201, 202]. Studies have shown that a sub-set of rheumatoid arthritis (RA) patients have distinctive antibodies to citrullinated proteins; other studies have investigated the effect of lung inflammation on protein citrullination in COPD patients, and found there was a potential link between RA and airway inflammation[203, 204]. With this study, the results showed some IgG autoantibodies against citrullinated proteins were detected in the serum of some COPD patients and healthy controls, but their levels were not significantly different between groups.

Autoantibodies to citrullinated antigens such as cit-fibronectin and cytokeratin were significantly higher in both HNS and HS control groups. A possible explanation for this finding is that citrullinated antigens were recruited to the site of inflammation and thus, they can act as indicators for development of autoimmune diseases or COPD, which has been demonstrated in many publications[205-207], irrespective of the inflammation triggered by smoking or

other genetic or environmental risk factors, as seen in the non-smoker cases.

Most of the antibodies to autoantigens investigated (Table 5.4) had concentrations in COPD serum samples above the 95 th percentile of the HNS, which produced some significant differences between the groups compared, such as Candida, RNP/sm, ro-52, SCL-70, histone, CENP-B, collagen5 and La/ssb. A study by Packard *et al.* showed a table that agreed with our results as most of the antigens in common had antibody concentrations that were increased above the baseline, or significantly differed between the groups when compared to COPD patients[133]. However, 6 out of the 62 serum samples for COPD patients did not show any response to any of the antigens investigated. In addition, Tetanus, H.I and HNRD did not show any values above the 95 th percentile in any of the COPD samples (HNRD, Tetanus and *H. influenza*). In terms of the presence of antibodies to Tetanus antigens, this may be due to the variability in the vaccination coverage between individuals. Interestingly, many of the healthy smoking group in this study had positive results for IgG autoantibodies against the same antigens that were raised in the COPD patient samples, which suggests that these individuals may have had an unknown infection or an inflammatory reaction that might make them more susceptible to developing COPD at a later date[208].

The IgM autoantibodies in COPD patients' sera were also investigated in this study against the same panel of 39 candidate antigens. The results showed that, as with the IgG autoantibodies, the reactivity of IgM autoantibodies to most of examined antigens were detected above 95 th percentile. Some IgM autoantibodies to specific antigens were significantly higher in the COPD group compared to controls, which are were also significantly higher for the IgG antibodies as well (Candida, CENP-B, scl-70, collagen 5, La/ssb, RNP/sm and

histone), whereas antibodies to SCL-70 and ro-52, were significantly higher for IgM only.

The healthy smokers also showed a positive response to most of the antigens to which autoantibodies were increased in the COPD group, and this may be due to the effect of smoking, which could stimulate inflammation, making them more susceptible to developing COPD.

The investigation of the concentration of IgM antibodies to citrullinated antigens showed significantly higher levels in healthy samples when compared to COPD. The majority of the IgM autoantibodies for the specific antigens investigated did not correlate to the FEV-1 %, of the COPD patients, only autoantibodies to collagen-4 showed a significant correlation between the decrease in lung function and increase in its levels in the serum of COPD patients (Figure 5.19 A).

IgM antibodies appear early in the course of an infection and usually reappear, to a lesser extent, after further exposure. IgM antibodies do not pass across the human placenta (only isotype IgG does), and these two biological properties make it useful in the diagnosis of infectious diseases. Detecting IgM antibodies in a patient's serum indicates recent infection or, more generally, it demonstrates activation of naïve B cells that have not undergone class switching as a consequence of previous activation. Therefore, the detection of IgM autoantibodies is indicative of a recent activation of naïve autoreactive B cells, which are distinct from the IgG autoantibodies that result from the stimulation of autoreactive memory cells that have undergone class switching. The results from the heat-maps of the IgG and IgM autoantibody responses show that differences were observed between these isotypes; indicating there were differences in the profiles of autoantigens recognized by IgM and IgG autoantibodies, as discussed

above. For particular antigens, some patients showed positivity for both IgM and IgG autoantibodies, whereas others expressed just one isotype or the other.

The effect of gender and age between the groups in this study was investigated statistically by using a Fisher's exact test, and the results showed there was no significant differences found for gender between the study groups. There were no significant differences between the ages of the COPD and smokers (Mann-Whitney non-parametric test) but there were significant differences between the COPD patients and the healthy non-smokers. It would have been better to ensure the groups were matched for age to negate the possibility of differences in autoantibody levels related to age rather than disease status. However, as there was no significant difference between the ages of the COPD group and healthy smokers, the 95th percentile of the healthy smokers was used to determine the occurrence of actual disease-associated autoantibodies in the COPD patients.

6. General Discussion, future work and conclusions

6.1 General Discussion

COPD can be defined as a persistent, and usually progressive, airflow limitation, which can be associated with a chronic inflammatory response to gases and noxious particles in the lungs. There are two distinct aspects of COPD that frequently co-exist, which are emphysema (or parenchymal destruction) and small airway abnormalities[209]. One of the major causes of COPD is smoking cigarettes, as in industrial countries, this accounts for 95% or more of the cases, whereas in developing countries a greater proportion of the incidence is due to other environmental factors [210]. Recent studies have highlighted the importance of autoimmune mechanisms in the progression of COPD; it can explain how the inflammatory process can continue after smoking cessation, as the initial environmental and inflammatory insults in the lungs trigger an immune response that creates epitopes for the autoimmune response[126, 211].

Previous studies using a traditional immunoassay method (ELISA) have shown that there is a significant increase in the levels of autoantibodies to specific-antigens in the serum of COPD patients such as cytokeratin-18, collagen 5 and histone[212] [109] [213]. However, ELISA assays are limited by their ability to measure one autoantigen in one sample at any one time, which makes the process of investigating multiple antigens slow. Within the field of microarrays, recent technological advances have led to the production of protein-based microarrays, and more specifically antigen microarrays allow the antigen-antibody reaction to be investigated. As with all microarrays, the technology allows interactions to be investigated in small sample size and in a highly multiplexed format.

The aim of this thesis was to develop a microarray platform that would allow multiple biomarkers to be measured. Our antigen microarray platform was optimized and validated to ensure it could be accurate and reproducible (Chapter 3 and 4), then it was applied to 62 COPD serum samples and 30 healthy controls of smokers and non-smokers (Chapter 5). The optimization process showed the amino-silane-coated arrays combined with I-Block buffer, Dako Antibody Diluent Buffer, and the UltraAmp amplification method (Gensphere) with the optimal dilution of 1:100, gave the best quality performance. This combination produced low slide noise, high assay sensitivity, good spot size and morphology, good reproducibility, and low spot background. Within microarray studies there are several different slide chemistries to choose from, and each can offer different advantages. These slides are positively charged, which allows them to interact with the surface of the proteins on the slide, helping to hold them in place, but the interaction will vary depending on the surface charge of the protein (some will bind more than others). For use in ELISA microarrays, studies have shown that poly-l-lysine, aldehyde silane-coated, and amino-silane-coated (either untreated or activated with homo-bifunctional cross linker) slides are superior to the other slide types. This is due to the fact they allow low slide noise, high assay sensitivity, good spot size and morphology, good reproducibility, and low spot background. Among the slide surfaces chemistries examined, amino-silane-coated arrays showed an accepted quality of performance, and these characteristics were seen for all of the 23 antibody assays evaluated [151] [214][140].

The validation chapter showed this assay was accurate and reproducible, with a low intra assay variability (CV = 9 %), and all antigens had an acceptable inter assay variability (CV = 15 %). As microarray methods are still new and being developed, the acceptable criteria tend to be defined by the group using it. For example, the antibody microarray developed by Urbanoswa *et al.* fit in with the FDA analytical method validation at the time, as it had an accuracy level of between 70-130 %, and the precision level was variable and reached as high as 30 %[215]. The FDA parameters have been revised in recent years, they are now more strict as the accuracy has to be between 80-120 %, and the precision has to be below 20 %[188]. The LOD was lower than the lowest dilution of the standard curve and thus, it was not chosen to be the LOD for measuring protein levels in our serum samples, and no cross-reactivity was observed with the optimal dilution (1:20000) for all the three detection antibodies without amplification. The comparison between ELISA and this microarray showed significant correlations for three of the control antigens tested, and the microarray produced a more sensitive performance with a greater dynamic range.

The last stage of our study (Chapter 5) used the optimized microarray to screen for autoantibodies directed against a panel of 39 autoantigens in the serum of COPD patients, healthy smokers (HS) and non-smokers (HNS) as controls. The aim was to use these detectable levels of IgG and IgM-autoantibodies to 39 autoantigen biomarkers as diagnostic tool for the detection of COPD at the early stage of the disease.

The results of this study showed that for both IgG and IgM, most autoantibodies were not statistically significantly up-regulated in the COPD group compared to the other two control groups, but individual patients within the COPD group

showed antibody levels above the 95 th percentile of the HS or HNS, and higher than the healthy groups. In terms of the reactivity of the IgG-antibodies, only those specific to Candida, CENP-B, collagen5, RNP/sm, La/ssb, histone, ro-52 and SCL-70 showed significant differences between the three groups, suggesting these may be key biomarkers for tracking the identification of the disease. The results for the correlation between the autoantibody levels in COPD patients and lung function (FEV- 1 %) demonstrated that only ribosomal p (IgG) and collagen4 (IgM) produced a significant correlation with the FEV-1 %, which suggests these could be used to monitor lung function. Interestingly, a number of HS produced positive IgG and IgM-autoantibodies against particular antigens, most of which were also present in COPD sera, and the correlation with lung function (FEV-1 %) showed only 5 out of 39 antigens for IgG and IgM-autoantibodies produced a significant correlation. These findings might be indicative of an ongoing inflammation that may make them susceptible to becoming COPD patients in the future, and again supports the use of these autoantibodies in detecting COPD progression.

These new and interesting findings demonstrate the sensitivity of microarray, how it can potentially be used to shed light on the early stages of COPD progression, and could be used to diagnose COPD earlier, particularly in healthy smokers, by undertaking screening studies which monitor these biomarkers in their serum over the time. In addition, our findings highlight autoantibodies that could potentially be used as biomarkers to identify patients at higher risk of disease progression, allowing these patients to be more closely monitored and different treatment options considered. These biomarkers could also help to identify a subset of patients who may need other treatments alongside the traditional treatments used

for patients with COPD. Currently diagnosis is based on clinical evaluation and spirometry tests, and the COPD treatments include the use of LABA, LAMA and corticosteroids. The use of this test could therefore allow an earlier diagnosis to be carried out in order to determine a specific course of treatment, and then be used in monitoring the success of these therapeutic interventions, which would provide benefits to the patient.

To further extend the possibility of using this type of microarray to detect the potential to develop COPD in healthy smokers and the overall progression of the disease, future studies should utilize these approaches to assess the level of auto-reactivity to an expanded set of lung antigens, as this will allow any other changes in the patients' autoimmune response to be detected and so treatment plans can be designed accordingly. Future studies should also include an increase in the number of serum samples investigated, and recruitment of patients from different cohorts of COPD groups, which will enable the study to evaluate if these biomarkers are truly related to the disease and disease progression.

The results from this type of microarray study could also have an effect on the treatment regime used to treat COPD in the future; instead of using the most common treatment (corticosteroids), the changes in the biomarkers observed could provide insight into new treatment options, such as combatting the autoantibodies that are prevalent in the COPD patients by destroying them, or perhaps by regulating B cell formation in the early stages to prevent the production of these antibodies. The use of intra-venous immunoglobulin therapy could even be investigated, as has been successful in certain other settings of autoimmunity. This change in treatment could help to slow the progression of the disease at an earlier stage, giving the patient a better quality of life.

The results of our study also showed there was an increased level of antibodies against *Candida* in the COPD group, which suggests this technique can also be useful in detecting potential infection threats and therefore would allow infection to be prevented in the early stages by application of vaccines and antibiotics before the patients become exacerbated.

The use of this type of microarray platform is not limited to determine the progression of COPD, it has the potential to be used for detecting the progression of other diseases with an autoimmune component, such as RA. If a suitable set of biomarkers can be determined, then this technology could be used to provide insight into disease progression and highlight potential treatments for other diseases in a similar manner to COPD.

This study has added support to the concept of autoimmunity as a process within the complex pathology of COPD. However, it also raises many questions about the meaning and implications of these findings. For example, is autoimmunity a primary or secondary phenomenon within the development of COPD, and does autoimmunity help to drive the pathology and tissue damage, or is it an epiphenomenon that serves as a marker of the disease process without actually being pathogenic? Further studies are clearly required to address these questions; for example, prospectively profiling the development of autoantibody production in healthy smokers should help to determine whether autoimmunity precedes, or follows, the development of COPD.

Overall, our results in this study were largely positive, we have proved that this microarray platform can detect differences between COPD patients and healthy controls, and the results have suggested some potential biomarkers that could be

taken in account to for the diagnosis of COPD in the future, or could be used in research to monitor the disease development.

6.2 Future work & conclusions

The results of this thesis guide us in several interesting directions in which could enrich this study in the future:

* **Demographic information of patients:** this study included three variables only as a tool for analysis, which were gender, FEV-1 % and age. It would be useful in the future to extend these variables to include more aspects of the patients' demographic data such as: BODE index, smoking pack-year history and smoking status (ex-smokers and current-smokers) for further correlations with the autoantigen data.

* **Stages of COPD:** our study included only two stages of the disease severity (moderate and severe) based on the FEV-1 %, however, including all four disease stages could expand the knowledge about the levels of autoantibody-specific antigens in each stage, and in particular the autoantigens which were the most prominent of all the 39 biomarkers (collagen5, Lassb, CENP-B, RNP/sm, Candida, histone, ro-52 and scl-70).

* **Antigen microarray capacity:** Our developed antigen microarray is not only designed for the 39 autoantigens used in this study, it is possible to investigate further and include many more autoantigens thought to be involved in the pathogenesis of COPD.

* **Data analysis:** analysis of the data generated from the microarrays takes a long time, and this also depends on the number of samples and antigens

investigated, therefore a higher sample number or antigen selection would then take longer to analyze. Overall this suggests it would be beneficial to develop and introduce a centralized computer program to allow the data to be processed faster, enabling a wider clinical audience to undertake investigations using this microarray technology.

* **Serum samples;** it would be good in the future if this study was performed with purified IgG and IgM from serum samples.

* **Autoantibody isotypes;** this study investigated the reactivity of two antibodies IgG and IgM. However, this can be extending to include all types of antibodies or perhaps subclasses of IgG the most abundant type in the blood.

***Application to other inflammatory lung diseases;** autoantibodies have been detected in a variety of inflammatory lung diseases, but the application of the microarray technology used in this thesis could expand and consolidate these findings, as well as being used to explore other disease settings for evidence of autoimmunity – e.g. certain non-atopic asthma endotypes.

6.2.1 Concluding remarks

In conclusion, this thesis has shown that an in-house antigen microarray platform has been optimised and validated by testing many parameters that allows for accurate and precise detection of up to 39 autoantigens thought to be implicated in the pathogenesis of COPD. The application using the antigen-microarray technology on the clinical serum samples of patients with COPD have shown that numerous autoantibodies could potentially be used as biomarkers of COPD in sera. Further future optimisation and validation would allow for more autoantigens to be tested on this antigen microarray that would

allow this platform to be a useful diagnostic tool. This would enable this microarray system to be used in any disease setting.

7. References

1. Mannino, D.M., *Chronic obstructive pulmonary disease: definition and epidemiology*. Respiratory care, 2003. **48**(12): p. 1185-91; discussion 1191-3.
2. Bartoli, M.L., et al., *Biological markers in induced sputum of patients with different phenotypes of chronic airway obstruction*. Respiration; international review of thoracic diseases, 2009. **77**(3): p. 265-72.
3. Hill, A.T., et al., *Airways inflammation in chronic bronchitis: the effects of smoking and alpha1-antitrypsin deficiency*. The European respiratory journal, 2000. **15**(5): p. 886-90.
4. <http://www.thinkcopdifferently.com/en/About-COPD/What-is-COPD/Pathophysiology-of-COPD>. 2012.
5. Decramer, M., W. Janssens, and M. Miravitlles, *Chronic obstructive pulmonary disease*. Lancet, 2012.
6. Decramer, M., W. Janssens, and M. Miravitlles, *Chronic obstructive pulmonary disease*. Lancet, 2012. **379**(9823): p. 1341-51.
7. Blanc, P.D., et al., *Occupational exposures and the risk of COPD: dusty trades revisited*. Thorax, 2009. **64**(1): p. 6-12.
8. Trupin, L., et al., *The occupational burden of chronic obstructive pulmonary disease*. The European respiratory journal, 2003. **22**(3): p. 462-9.
9. Wan, E.S. and E.K. Silverman, *Genetics of COPD and emphysema*. Chest, 2009. **136**(3): p. 859-66.
10. Blanchard, V., et al., *N-glycosylation and biological activity of recombinant human alpha1-antitrypsin expressed in a novel human neuronal cell line*. Biotechnology and bioengineering, 2011. **108**(9): p. 2118-28.
11. Tudor, R.M., S.M. Janciauskiene, and I. Petrache, *Lung disease associated with alpha1-antitrypsin deficiency*. Proceedings of the American Thoracic Society, 2010. **7**(6): p. 381-6.
12. Soler Artigas, M., L.V. Wain, and M.D. Tobin, *Genome-wide association studies in lung disease*. Thorax, 2012. **67**(3): p. 271-3, 280.
13. Cho, M.H., et al., *Risk loci for chronic obstructive pulmonary disease: a genome-wide association study and meta-analysis*. The Lancet. Respiratory medicine, 2014. **2**(3): p. 214-25.
14. Agusti, A., J. Gea, and R. Faner, *Biomarkers, the control panel and personalized COPD medicine*. Respirology, 2016. **21**(1): p. 24-33.
15. Ziolkowska-Suchanek, I., et al., *Susceptibility loci in lung cancer and COPD: association of IREB2 and FAM13A with pulmonary diseases*. Scientific reports, 2015. **5**: p. 13502.
16. Xie, J., et al., *Gene susceptibility identification in a longitudinal study confirms new loci in the development of chronic obstructive pulmonary disease and influences lung function decline*. Respiratory research, 2015. **16**: p. 49.

17. Kim, W.J. and S.D. Lee, *Candidate genes for COPD: current evidence and research*. International journal of chronic obstructive pulmonary disease, 2015. **10**: p. 2249-55.
18. Shapiro, S.D. and R.M. Senior, *Matrix metalloproteinases. Matrix degradation and more*. American journal of respiratory cell and molecular biology, 1999. **20**(6): p. 1100-2.
19. Arinir, U., et al., [*The genetics of chronic obstructive pulmonary disease*]. Pneumologie, 2009. **63**(1): p. 41-8.
20. Roth, M., *Pathogenesis of COPD. Part III. Inflammation in COPD*. The international journal of tuberculosis and lung disease : the official journal of the International Union against Tuberculosis and Lung Disease, 2008. **12**(4): p. 375-80.
21. Wood, A.M. and R.A. Stockley, *The genetics of chronic obstructive pulmonary disease*. Respiratory research, 2006. **7**: p. 130.
22. Bergren, D.R., *Environmental tobacco smoke exposure and airway hyperresponsiveness*. Inflammation & allergy drug targets, 2009. **8**(5): p. 340-7.
23. Churg, A., M. Cosio, and J.L. Wright, *Mechanisms of cigarette smoke-induced COPD: insights from animal models*. American journal of physiology. Lung cellular and molecular physiology, 2008. **294**(4): p. L612-31.
24. Zaher, C., et al., *Smoking-related diseases: the importance of COPD*. The international journal of tuberculosis and lung disease : the official journal of the International Union against Tuberculosis and Lung Disease, 2004. **8**(12): p. 1423-8.
25. Briggs, D.D., Jr., *Chronic obstructive pulmonary disease overview: prevalence, pathogenesis, and treatment*. Journal of managed care pharmacy : JMCP, 2004. **10**(4 Suppl): p. S3-10.
26. Hoenderdos, K. and A. Condliffe, *The neutrophil in chronic obstructive pulmonary disease*. American journal of respiratory cell and molecular biology, 2013. **48**(5): p. 531-9.
27. Thorley, A.J. and T.D. Tetley, *Pulmonary epithelium, cigarette smoke, and chronic obstructive pulmonary disease*. International journal of chronic obstructive pulmonary disease, 2007. **2**(4): p. 409-28.
28. Rahman, I., *The role of oxidative stress in the pathogenesis of COPD: implications for therapy*. Treatments in respiratory medicine, 2005. **4**(3): p. 175-200.
29. Rahman, I., *Oxidative stress in pathogenesis of chronic obstructive pulmonary disease: cellular and molecular mechanisms*. Cell biochemistry and biophysics, 2005. **43**(1): p. 167-88.
30. Pride, N.B., *Smoking cessation: effects on symptoms, spirometry and future trends in COPD*. Thorax, 2001. **56 Suppl 2**: p. ii7-10.
31. Tashkin, D.P. and R.P. Murray, *Smoking cessation in chronic obstructive pulmonary disease*. Respiratory medicine, 2009. **103**(7): p. 963-74.
32. Tantucci, C. and D. Modena, *Lung function decline in COPD*. International journal of chronic obstructive pulmonary disease, 2012. **7**: p. 95-9.

33. Fletcher, C. and R. Peto, *The natural history of chronic airflow obstruction*. British medical journal, 1977. **1**(6077): p. 1645-8.
34. Celli, B.R. and W. MacNee, *Standards for the diagnosis and treatment of patients with COPD: a summary of the ATS/ERS position paper*. The European respiratory journal, 2004. **23**(6): p. 932-46.
35. Donohue, J.F., *Combination therapy for chronic obstructive pulmonary disease: clinical aspects*. Proceedings of the American Thoracic Society, 2005. **2**(4): p. 272-81; discussion 290-1.
36. Barnes, P.J., *Future treatments for chronic obstructive pulmonary disease and its comorbidities*. Proceedings of the American Thoracic Society, 2008. **5**(8): p. 857-64.
37. Barnes, P.J., *Novel approaches and targets for treatment of chronic obstructive pulmonary disease*. American journal of respiratory and critical care medicine, 1999. **160**(5 Pt 2): p. S72-9.
38. Suissa, S., *Effectiveness of inhaled corticosteroids in chronic obstructive pulmonary disease: immortal time bias in observational studies*. American journal of respiratory and critical care medicine, 2003. **168**(1): p. 49-53.
39. Wouters, E.F., E.C. Creutzberg, and A.M. Schols, *Systemic effects in COPD*. Chest, 2002. **121**(5 Suppl): p. 127S-130S.
40. Huiart, L., P. Ernst, and S. Suissa, *Cardiovascular morbidity and mortality in COPD*. Chest, 2005. **128**(4): p. 2640-6.
41. Hunninghake, D.B., *Cardiovascular disease in chronic obstructive pulmonary disease*. Proceedings of the American Thoracic Society, 2005. **2**(1): p. 44-9.
42. Agusti, A., *Systemic effects of COPD: just the tip of the Iceberg*. COPD, 2008. **5**(4): p. 205-6.
43. Naik, D., et al., *Chronic obstructive pulmonary disease and the metabolic syndrome: Consequences of a dual threat*. Indian journal of endocrinology and metabolism, 2014. **18**(5): p. 608-16.
44. Mantovani, A., et al., *Neutrophils in the activation and regulation of innate and adaptive immunity*. Nature reviews. Immunology, 2011. **11**(8): p. 519-31.
45. Rovina, N., A. Koutsoukou, and N.G. Koulouris, *Inflammation and immune response in COPD: where do we stand? Mediators of inflammation*, 2013. **2013**: p. 413735.
46. Bals, R. and P.S. Hiemstra, *Innate immunity in the lung: how epithelial cells fight against respiratory pathogens*. The European respiratory journal, 2004. **23**(2): p. 327-33.
47. Comer, D.M., et al., *Airway epithelial cell apoptosis and inflammation in COPD, smokers and nonsmokers*. The European respiratory journal, 2013. **41**(5): p. 1058-67.
48. Mills, P.R., R.J. Davies, and J.L. Devalia, *Airway epithelial cells, cytokines, and pollutants*. American journal of respiratory and critical care medicine, 1999. **160**(5 Pt 2): p. S38-43.
49. Busse, W.W. and J.B. Sedgwick, *Eosinophils in asthma*. Annals of allergy, 1992. **68**(3): p. 286-90.
50. Siva, R., et al., *Eosinophilic airway inflammation and exacerbations of COPD: a randomised controlled trial*. The European respiratory

- journal : official journal of the European Society for Clinical Respiratory Physiology, 2007. **29**(5): p. 906-13.
51. Saha, S. and C.E. Brightling, *Eosinophilic airway inflammation in COPD*. International journal of chronic obstructive pulmonary disease, 2006. **1**(1): p. 39-47.
 52. Hiemstra, P.S., S. van Wetering, and J. Stolk, *Neutrophil serine proteinases and defensins in chronic obstructive pulmonary disease: effects on pulmonary epithelium*. The European respiratory journal, 1998. **12**(5): p. 1200-8.
 53. Williams, T.J. and P.J. Jose, *Neutrophils in chronic obstructive pulmonary disease*. Novartis Foundation symposium, 2001. **234**: p. 136-41; discussion 141-8.
 54. Tetley, T.D., *Macrophages and the pathogenesis of COPD*. Chest, 2002. **121**(5 Suppl): p. 156S-159S.
 55. Hiemstra, P.S., S. van Wetering, and J. Stolk, *Neutrophil serine proteinases and defensins in chronic obstructive pulmonary disease: effects on pulmonary epithelium*. The European respiratory journal : official journal of the European Society for Clinical Respiratory Physiology, 1998. **12**(5): p. 1200-8.
 56. Yoshikawa, T., et al., *Impaired neutrophil chemotaxis in chronic obstructive pulmonary disease*. American journal of respiratory and critical care medicine, 2007. **175**(5): p. 473-9.
 57. Suzaki, I., et al., *Suppression of IL-8 production from airway cells by tiotropium bromide in vitro*. International journal of chronic obstructive pulmonary disease, 2011. **6**: p. 439-48.
 58. Caram, L.M., et al., *Serum Vitamin A and Inflammatory Markers in Individuals with and without Chronic Obstructive Pulmonary Disease*. Mediators of inflammation, 2015. **2015**: p. 862086.
 59. Yamamoto, C., et al., *Airway inflammation in COPD assessed by sputum levels of interleukin-8*. Chest, 1997. **112**(2): p. 505-10.
 60. Fujimoto, K., et al., *Airway inflammation during stable and acutely exacerbated chronic obstructive pulmonary disease*. The European respiratory journal : official journal of the European Society for Clinical Respiratory Physiology, 2005. **25**(4): p. 640-6.
 61. Martinez, F.O. and S. Gordon, *The M1 and M2 paradigm of macrophage activation: time for reassessment*. F1000prime reports, 2014. **6**: p. 13.
 62. Byers, D.E. and M.J. Holtzman, *Alternatively activated macrophages and airway disease*. Chest, 2011. **140**(3): p. 768-74.
 63. Culpitt, S.V., et al., *Inhibition by red wine extract, resveratrol, of cytokine release by alveolar macrophages in COPD*. Thorax, 2003. **58**(11): p. 942-6.
 64. Beck-Schimmer, B., et al., *Alveolar macrophages regulate neutrophil recruitment in endotoxin-induced lung injury*. Respiratory research, 2005. **6**: p. 61.
 65. Jacobs, R., et al., *CD16- CD56+ natural killer cells after bone marrow transplantation*. Blood, 1992. **79**(12): p. 3239-44.
 66. Fairclough, L., et al., *Killer cells in chronic obstructive pulmonary disease*. Clinical science, 2008. **114**(8): p. 533-41.

67. Tang, Y., et al., *Increased numbers of NK cells, NKT-like cells, and NK inhibitory receptors in peripheral blood of patients with chronic obstructive pulmonary disease*. Clinical & developmental immunology, 2013. **2013**: p. 721782.
68. Urbanowicz, R.A., et al., *Enhanced effector function of cytotoxic cells in the induced sputum of COPD patients*. Respiratory research, 2010. **11**: p. 76.
69. Tsoumakidou, M., et al., *Dendritic cells in chronic obstructive pulmonary disease: new players in an old game*. American journal of respiratory and critical care medicine, 2008. **177**(11): p. 1180-6.
70. Robbins, C.S., et al., *Cigarette smoke exposure impairs dendritic cell maturation and T cell proliferation in thoracic lymph nodes of mice*. Journal of immunology, 2008. **180**(10): p. 6623-8.
71. Givi, M.E., et al., *Dendritic cells in pathogenesis of COPD*. Current pharmaceutical design, 2012. **18**(16): p. 2329-35.
72. Van Pottelberge, G.R., et al., *The role of dendritic cells in the pathogenesis of COPD: liaison officers in the front line*. COPD, 2009. **6**(4): p. 284-90.
73. Freeman, C.M., et al., *Cytotoxic potential of lung CD8(+) T cells increases with chronic obstructive pulmonary disease severity and with in vitro stimulation by IL-18 or IL-15*. Journal of immunology, 2010. **184**(11): p. 6504-13.
74. Majo, J., H. Ghezzi, and M.G. Cosio, *Lymphocyte population and apoptosis in the lungs of smokers and their relation to emphysema*. The European respiratory journal : official journal of the European Society for Clinical Respiratory Physiology, 2001. **17**(5): p. 946-53.
75. Maeno, T., et al., *CD8+ T Cells are required for inflammation and destruction in cigarette smoke-induced emphysema in mice*. Journal of immunology, 2007. **178**(12): p. 8090-6.
76. Urbanowicz, R.A., et al., *Altered effector function of peripheral cytotoxic cells in COPD*. Respiratory research, 2009. **10**: p. 53.
77. Tubby, C., et al., *Immunological basis of reversible and fixed airways disease*. Clinical science, 2011. **121**(7): p. 285-96.
78. Gadgil, A. and S.R. Duncan, *Role of T-lymphocytes and pro-inflammatory mediators in the pathogenesis of chronic obstructive pulmonary disease*. International journal of chronic obstructive pulmonary disease, 2008. **3**(4): p. 531-41.
79. Cosio, M.G. and J. Majo, *Inflammation of the airways and lung parenchyma in COPD: role of T cells*. Chest, 2002. **121**(5 Suppl): p. 160S-165S.
80. Vargas-Rojas, M.I., et al., *Increase of Th17 cells in peripheral blood of patients with chronic obstructive pulmonary disease*. Respiratory medicine, 2011. **105**(11): p. 1648-54.
81. Hong, S.C. and S.H. Lee, *Role of th17 cell and autoimmunity in chronic obstructive pulmonary disease*. Immune network, 2010. **10**(4): p. 109-14.
82. Stumhofer, J.S., J. Silver, and C.A. Hunter, *Negative regulation of Th17 responses*. Seminars in immunology, 2007. **19**(6): p. 394-9.

83. Lane, N., et al., *Regulation in chronic obstructive pulmonary disease: the role of regulatory T-cells and Th17 cells*. *Clinical science*, 2010. **119**(2): p. 75-86.
84. Delgoffe, G.M., et al., *Stability and function of regulatory T cells is maintained by a neuropilin-1-semaphorin-4a axis*. *Nature*, 2013. **501**(7466): p. 252-6.
85. Dancer, R. and D.M. Sansom, *Regulatory T cells and COPD*. *Thorax*, 2013. **68**(12): p. 1176-8.
86. Tan, D.B., et al., *Impaired function of regulatory T-cells in patients with chronic obstructive pulmonary disease (COPD)*. *Immunobiology*, 2014. **219**(12): p. 975-9.
87. Kalathil, S.G., et al., *T-regulatory cells and programmed death 1+ T cells contribute to effector T-cell dysfunction in patients with chronic obstructive pulmonary disease*. *American journal of respiratory and critical care medicine*, 2014. **190**(1): p. 40-50.
88. Drolet, J.P., et al., *B lymphocytes in inflammatory airway diseases*. *Clinical and experimental allergy : journal of the British Society for Allergy and Clinical Immunology*, 2010. **40**(6): p. 841-9.
89. Kasaian, M.T. and P. Casali, *Autoimmunity-prone B-1 (CD5 B) cells, natural antibodies and self recognition*. *Autoimmunity*, 1993. **15**(4): p. 315-29.
90. Spiegelberg, H.L., *Biological role of different antibody classes*. *International archives of allergy and applied immunology*, 1989. **90 Suppl 1**: p. 22-7.
91. Brandsma, C.A., et al., *Differential switching to IgG and IgA in active smoking COPD patients and healthy controls*. *The European respiratory journal : official journal of the European Society for Clinical Respiratory Physiology*, 2012.
92. Seiler, F.R., *[Structure and function of immunoglobulins]*. *Beitrage zu Infusionstherapie und klinische Ernährung*, 1982. **9**: p. 1-15.
93. Qvarfordt, I., et al., *IgG subclasses in smokers with chronic bronchitis and recurrent exacerbations*. *Thorax*, 2001. **56**(6): p. 445-9.
94. Gosman, M.M., et al., *Increased number of B-cells in bronchial biopsies in COPD*. *The European respiratory journal : official journal of the European Society for Clinical Respiratory Physiology*, 2006. **27**(1): p. 60-4.
95. Leidinger, P., et al., *Novel autoantigens immunogenic in COPD patients*. *Respiratory research*, 2009. **10**: p. 20.
96. Feghali-Bostwick, C.A., et al., *Autoantibodies in patients with chronic obstructive pulmonary disease*. *American journal of respiratory and critical care medicine*, 2008. **177**(2): p. 156-63.
97. Mannie, M.D., *Autoimmunity and asthma: The dirt on the hygiene hypothesis*. *Self/nonsel*, 2010. **1**(2): p. 123-128.
98. Agusti, A., et al., *Hypothesis: does COPD have an autoimmune component?* *Thorax*, 2003. **58**(10): p. 832-4.
99. Stefanska, A.M. and P.T. Walsh, *Chronic obstructive pulmonary disease: evidence for an autoimmune component*. *Cellular & molecular immunology*, 2009. **6**(2): p. 81-6.

100. Shen, T.C., et al., *Increased risk of chronic obstructive pulmonary disease in patients with rheumatoid arthritis: a population-based cohort study*. QJM : monthly journal of the Association of Physicians, 2014. **107**(7): p. 537-43.
101. Shen, T.C., et al., *Increased risk of chronic obstructive pulmonary disease in patients with systemic lupus erythematosus: a population-based cohort study*. PloS one, 2014. **9**(3): p. e91821.
102. Vossenaar, E.R. and W.J. van Venrooij, *Citrullinated proteins: sparks that may ignite the fire in rheumatoid arthritis*. Arthritis research & therapy, 2004. **6**(3): p. 107-11.
103. Ruiz-Esquide, V., et al., *Anti-citrullinated peptide antibodies in the serum of heavy smokers without rheumatoid arthritis. A differential effect of chronic obstructive pulmonary disease?* Clinical rheumatology, 2012. **31**(7): p. 1047-50.
104. Schellekens, G.A., et al., *The diagnostic properties of rheumatoid arthritis antibodies recognizing a cyclic citrullinated peptide*. Arthritis and rheumatism, 2000. **43**(1): p. 155-63.
105. Catrina, A.I., et al., *Lungs, joints and immunity against citrullinated proteins in rheumatoid arthritis*. Nature reviews. Rheumatology, 2014. **10**(11): p. 645-53.
106. Wegner, N., et al., *Autoimmunity to specific citrullinated proteins gives the first clues to the etiology of rheumatoid arthritis*. Immunological reviews, 2010. **233**(1): p. 34-54.
107. Nunez, B., et al., *Anti-tissue antibodies are related to lung function in chronic obstructive pulmonary disease*. American journal of respiratory and critical care medicine, 2011. **183**(8): p. 1025-31.
108. Kirkham, P.A., et al., *Oxidative stress-induced antibodies to carbonyl-modified protein correlate with severity of chronic obstructive pulmonary disease*. American journal of respiratory and critical care medicine, 2011. **184**(7): p. 796-802.
109. Daffa, N.I., et al., *Natural and disease-specific autoantibodies in chronic obstructive pulmonary disease*. Clinical and experimental immunology, 2015. **180**(1): p. 155-63.
110. Pfeiffer, C., et al., *Selective activation of Th1- and Th2-like cells in vivo--response to human collagen IV*. Immunological reviews, 1991. **123**: p. 65-84.
111. Harju, T., et al., *Variability in the precursor proteins of collagen I and III in different stages of COPD*. Respiratory research, 2010. **11**: p. 165.
112. van der Rest, M. and R. Garrone, *Collagen family of proteins*. FASEB journal : official publication of the Federation of American Societies for Experimental Biology, 1991. **5**(13): p. 2814-23.
113. Ricard-Blum, S., *The collagen family*. Cold Spring Harbor perspectives in biology, 2011. **3**(1): p. a004978.
114. Terato, K., et al., *Induction of arthritis with monoclonal antibodies to collagen*. Journal of immunology, 1992. **148**(7): p. 2103-8.
115. Stuart, J.M., A.S. Townes, and A.H. Kang, *Collagen autoimmune arthritis*. Annual review of immunology, 1984. **2**: p. 199-218.

116. Morgan, K., et al., *Incidence of antibodies to native and denatured cartilage collagens (types II, IX, and XI) and to type I collagen in rheumatoid arthritis*. *Annals of the rheumatic diseases*, 1987. **46**(12): p. 902-7.
117. Brandsma, C.A., et al., *The search for autoantibodies against elastin, collagen and decorin in COPD*. *The European respiratory journal*, 2011. **37**(5): p. 1289-92.
118. Cottin, V., et al., *Combined pulmonary fibrosis and emphysema: a distinct underrecognised entity*. *The European respiratory journal*, 2005. **26**(4): p. 586-93.
119. Betsuyaku, T., et al., *Elastin-derived peptides and neutrophil elastase in bronchoalveolar lavage fluid*. *American journal of respiratory and critical care medicine*, 1996. **154**(3 Pt 1): p. 720-4.
120. van der Woude, F.J., et al., *Autoantibodies against neutrophils and monocytes: tool for diagnosis and marker of disease activity in Wegener's granulomatosis*. *Lancet*, 1985. **1**(8426): p. 425-9.
121. Roozendaal, C. and C.G. Kallenberg, *Are anti-neutrophil cytoplasmic antibodies (ANCA) clinically useful in inflammatory bowel disease (IBD)?* *Clinical and experimental immunology*, 1999. **116**(2): p. 206-13.
122. Harper, L., et al., *Neutrophil priming and apoptosis in anti-neutrophil cytoplasmic autoantibody-associated vasculitis*. *Kidney international*, 2001. **59**(5): p. 1729-38.
123. Yang, J.J., et al., *Target antigens for anti-neutrophil cytoplasmic autoantibodies (ANCA) are on the surface of primed and apoptotic but not unstimulated neutrophils*. *Clinical and experimental immunology*, 2000. **121**(1): p. 165-72.
124. Mayadas, T.N., X. Cullere, and C.A. Lowell, *The multifaceted functions of neutrophils*. *Annual review of pathology*, 2014. **9**: p. 181-218.
125. Amulic, B., et al., *Neutrophil function: from mechanisms to disease*. *Annual review of immunology*, 2012. **30**: p. 459-89.
126. Bagdonas, E., et al., *Novel aspects of pathogenesis and regeneration mechanisms in COPD*. *International journal of chronic obstructive pulmonary disease*, 2015. **10**: p. 995-1013.
127. Hietarinta, M. and O. Lassila, *Clinical significance of antinuclear antibodies in systemic rheumatic diseases*. *Annals of medicine*, 1996. **28**(4): p. 283-91.
128. Bozinovski, S., et al., *Serum amyloid a is a biomarker of acute exacerbations of chronic obstructive pulmonary disease*. *American journal of respiratory and critical care medicine*, 2008. **177**(3): p. 269-78.
129. Anthony, D., et al., *Serum amyloid A promotes lung neutrophilia by increasing IL-17A levels in the mucosa and gammadelta T cells*. *American journal of respiratory and critical care medicine*, 2013. **188**(2): p. 179-86.
130. Noordhoek, J.A., et al., *Different modulation of decorin production by lung fibroblasts from patients with mild and severe emphysema*. *COPD*, 2005. **2**(1): p. 17-25.

131. Puente-Maestu, L., et al., *Abnormal transition pore kinetics and cytochrome C release in muscle mitochondria of patients with chronic obstructive pulmonary disease*. American journal of respiratory cell and molecular biology, 2009. **40**(6): p. 746-50.
132. Mundlos, S., et al., *Distribution of cartilage proteoglycan (aggrecan) core protein and link protein gene expression during human skeletal development*. Matrix, 1991. **11**(5): p. 339-46.
133. Packard, T.A., et al., *COPD is associated with production of autoantibodies to a broad spectrum of self-antigens, correlative with disease phenotype*. Immunologic research, 2013. **55**(1-3): p. 48-57.
134. Crowther, J.R., *The ELISA guidebook*. Methods in molecular biology, 2000. **149**: p. III-IV, 1-413.
135. Gan, S.D. and K.R. Patel, *Enzyme immunoassay and enzyme-linked immunosorbent assay*. The Journal of investigative dermatology, 2013. **133**(9): p. e12.
136. Leng, S.X., et al., *ELISA and multiplex technologies for cytokine measurement in inflammation and aging research*. The journals of gerontology. Series A, Biological sciences and medical sciences, 2008. **63**(8): p. 879-84.
137. Feng, Y., et al., *Parallel detection of autoantibodies with microarrays in rheumatoid diseases*. Clinical chemistry, 2004. **50**(2): p. 416-22.
138. Schweitzer, B. and S.F. Kingsmore, *Measuring proteins on microarrays*. Current opinion in biotechnology, 2002. **13**(1): p. 14-9.
139. Haab, B.B., M.J. Dunham, and P.O. Brown, *Protein microarrays for highly parallel detection and quantitation of specific proteins and antibodies in complex solutions*. Genome biology, 2001. **2**(2): p. RESEARCH0004.
140. Kusnezow, W., et al., *Antibody microarrays: an evaluation of production parameters*. Proteomics, 2003. **3**(3): p. 254-64.
141. Sears, H.F., et al., *Monoclonal antibody detection of a circulating tumor-associated antigen. II. A longitudinal evaluation of patients with colorectal cancer*. Journal of clinical immunology, 1982. **2**(2): p. 141-9.
142. Quintana, F.J., et al., *Antigen microarrays identify unique serum autoantibody signatures in clinical and pathologic subtypes of multiple sclerosis*. Proceedings of the National Academy of Sciences of the United States of America, 2008. **105**(48): p. 18889-94.
143. Anderson, K.S., et al., *Application of protein microarrays for multiplexed detection of antibodies to tumor antigens in breast cancer*. Journal of proteome research, 2008. **7**(4): p. 1490-9.
144. Pinto-Plata, V., et al., *Profiling serum biomarkers in patients with COPD: associations with clinical parameters*. Thorax, 2007. **62**(7): p. 595-601.
145. Kumble, K.D., *Protein microarrays: new tools for pharmaceutical development*. Analytical and bioanalytical chemistry, 2003. **377**(5): p. 812-9.

146. Ramachandran, N., S. Srivastava, and J. Labaer, *Applications of protein microarrays for biomarker discovery*. Proteomics. Clinical applications, 2008. **2**(10-11): p. 1444-59.
147. Haab, B.B., *Applications of antibody array platforms*. Current opinion in biotechnology, 2006. **17**(4): p. 415-21.
148. Sobek, J., C. Aquino, and R. Schlapbach, *Quality considerations and selection of surface chemistry for glass-based DNA, peptide, antibody, carbohydrate, and small molecule microarrays*. Methods in molecular biology, 2007. **382**: p. 17-31.
149. Taylor, S., et al., *Impact of surface chemistry and blocking strategies on DNA microarrays*. Nucleic acids research, 2003. **31**(16): p. e87.
150. Olle, E.W., et al., *Comparison of antibody array substrates and the use of glycerol to normalize spot morphology*. Experimental and molecular pathology, 2005. **79**(3): p. 206-9.
151. Seurnyck-Servoss, S.L., et al., *Evaluation of surface chemistries for antibody microarrays*. Analytical biochemistry, 2007. **371**(1): p. 105-15.
152. Dandy, D.S., P. Wu, and D.W. Grainger, *Array feature size influences nucleic acid surface capture in DNA microarrays*. Proceedings of the National Academy of Sciences of the United States of America, 2007. **104**(20): p. 8223-8.
153. Shin, D., et al., *Advances in fluorescence imaging techniques to detect oral cancer and its precursors*. Future oncology, 2010. **6**(7): p. 1143-54.
154. Barron, A.R., *Fluorescence Characterization and its Application in DNA Detection*. 2010.
155. Espina, V., et al., *Protein microarray detection strategies: focus on direct detection technologies*. Journal of immunological methods, 2004. **290**(1-2): p. 121-33.
156. Haab, B.B., *Methods and applications of antibody microarrays in cancer research*. Proteomics, 2003. **3**(11): p. 2116-22.
157. Lesaicherre, M.L., et al., *Antibody-based fluorescence detection of kinase activity on a peptide array*. Bioorganic & medicinal chemistry letters, 2002. **12**(16): p. 2085-8.
158. Ranasinghe, R.T. and T. Brown, *Ultrasensitive fluorescence-based methods for nucleic acid detection: towards amplification-free genetic analysis*. Chemical communications, 2011. **47**(13): p. 3717-35.
159. Buick, A.R., et al., *Method validation in the bioanalytical laboratory*. Journal of pharmaceutical and biomedical analysis, 1990. **8**(8-12): p. 629-37.
160. Lang, J.R. and S. Bolton, *A comprehensive method validation strategy for bioanalytical applications in the pharmaceutical industry--1. Experimental considerations*. Journal of pharmaceutical and biomedical analysis, 1991. **9**(5): p. 357-61.
161. Tiwari, G. and R. Tiwari, *Bioanalytical method validation: An updated review*. Pharmaceutical methods, 2010. **1**(1): p. 25-38.

162. Shah, V.P., et al., *Bioanalytical method validation--a revisit with a decade of progress*. *Pharmaceutical research*, 2000. **17**(12): p. 1551-7.
163. Wang, X., S. Ghosh, and S.W. Guo, *Quantitative quality control in microarray image processing and data acquisition*. *Nucleic acids research*, 2001. **29**(15): p. E75-5.
164. Papp, K. and J. Prechl, *The use of antigen microarrays in antibody profiling*. *Methods in molecular biology*, 2012. **815**: p. 175-85.
165. Szkola, A., et al., *Automated, high performance, flow-through chemiluminescence microarray for the multiplexed detection of phycotoxins*. *Analytica chimica acta*, 2013. **787**: p. 211-8.
166. Holt, L.J., et al., *By-passing selection: direct screening for antibody-antigen interactions using protein arrays*. *Nucleic acids research*, 2000. **28**(15): p. E72.
167. Moran-Mirabal, J.M., et al., *Controlling microarray spot morphology with polymer liftoff arrays*. *Analytical chemistry*, 2007. **79**(3): p. 1109-14.
168. Negm, O.H., et al., *Profiling Humoral Immune Responses to Clostridium difficile-Specific Antigens by Protein Microarray Analysis*. *Clinical and vaccine immunology : CVI*, 2015. **22**(9): p. 1033-9.
169. Selvarajah, S., et al., *Development and validation of protein microarray technology for simultaneous inflammatory mediator detection in human sera*. *Mediators of inflammation*, 2014. **2014**: p. 820304.
170. Chapman, C., et al., *Autoantibodies in breast cancer: their use as an aid to early diagnosis*. *Annals of oncology : official journal of the European Society for Medical Oncology / ESMO*, 2007. **18**(5): p. 868-73.
171. Sobek, J., et al., *Drop drying on surfaces determines chemical reactivity - the specific case of immobilization of oligonucleotides on microarrays*. *BMC biophysics*, 2013. **6**: p. 8.
172. Guilleaume, B., et al., *Systematic comparison of surface coatings for protein microarrays*. *Proteomics*, 2005. **5**(18): p. 4705-12.
173. Liu, Y., et al., *Optimization of printing buffer for protein microarrays based on aldehyde-modified glass slides*. *Frontiers in bioscience : a journal and virtual library*, 2007. **12**: p. 3768-73.
174. Snappyan, M., et al., *Dissecting DNA-protein and protein-protein interactions involved in bacterial transcriptional regulation by a sensitive protein array method combining a near-infrared fluorescence detection*. *Proteomics*, 2003. **3**(5): p. 647-57.
175. Stears, R.L., R.C. Getts, and S.R. Gullans, *A novel, sensitive detection system for high-density microarrays using dendrimer technology*. *Physiological genomics*, 2000. **3**(2): p. 93-9.
176. Administration, F.a.D., *Guidance for industry: Bioanalytical Method Validation*. <http://www.fda.gov/downloads/Drugs/.../Guidances/ucm070107.pdf>, 2001. 2001.
177. Bastarache, J.A., et al., *Accuracy and reproducibility of a multiplex immunoassay platform: a validation study*. *Journal of immunological methods*, 2011. **367**(1-2): p. 33-9.

178. Iwaki, K. and Y. Hayashi, [*Method for estimating the precision and detection limit for ELISA*]. *Nihon yakurigaku zasshi. Folia pharmacologica Japonica*, 2009. **134**(4): p. 207-11.
179. Armbruster, D.A. and T. Pry, *Limit of blank, limit of detection and limit of quantitation*. *The Clinical biochemist. Reviews / Australian Association of Clinical Biochemists*, 2008. **29 Suppl 1**: p. S49-52.
180. Choi, D.H., et al., *Validation of a method for predicting the precision, limit of detection and range of quantitation in competitive ELISA*. *Analytical sciences : the international journal of the Japan Society for Analytical Chemistry*, 2007. **23**(2): p. 215-8.
181. Longford, N.T., *Handling the limit of detection by extrapolation*. *Statistics in medicine*, 2012. **31**(26): p. 3133-46.
182. Bergstrand, M. and M.O. Karlsson, *Handling data below the limit of quantification in mixed effect models*. *The AAPS journal*, 2009. **11**(2): p. 371-80.
183. Fang, L., et al., *Estimating area under the curve and relative exposure in a pharmacokinetic study with data below quantification limit*. *Journal of biopharmaceutical statistics*, 2011. **21**(1): p. 66-76.
184. Tate, J. and G. Ward, *Interferences in immunoassay*. *The Clinical biochemist. Reviews / Australian Association of Clinical Biochemists*, 2004. **25**(2): p. 105-20.
185. Pflieger, C., N. Schloot, and F. ter Veld, *Effect of serum content and diluent selection on assay sensitivity and signal intensity in multiplex bead-based immunoassays*. *Journal of immunological methods*, 2008. **329**(1-2): p. 214-8.
186. Valentin, M.A., et al., *Validation of immunoassay for protein biomarkers: bioanalytical study plan implementation to support pre-clinical and clinical studies*. *Journal of pharmaceutical and biomedical analysis*, 2011. **55**(5): p. 869-77.
187. Ellington, A.A., et al., *Measurement and quality control issues in multiplex protein assays: a case study*. *Clinical chemistry*, 2009. **55**(6): p. 1092-9.
188. Administration, F.A.D., *Guidance for Industry: Bioanalytical Method Validation*. 2001.
189. Lee, J.S., et al., *Assessing the detection capacity of microarrays as bio/nanosensing platforms*. *BioMed research international*, 2013. **2013**: p. 310461.
190. Elshal, M.F. and J.P. McCoy, *Multiplex bead array assays: performance evaluation and comparison of sensitivity to ELISA*. *Methods*, 2006. **38**(4): p. 317-23.
191. Espinosa de los Monteros, M.J., et al., *Variability of respiratory symptoms in severe COPD*. *Archivos de bronconeumologia*, 2012. **48**(1): p. 3-7.
192. Tashkin, D.P., et al., *Lung function and respiratory symptoms in a 1-year randomized smoking cessation trial of varenicline in COPD patients*. *Respiratory medicine*, 2011. **105**(11): p. 1682-90.
193. Riario Sforza, G.G. and C. Incorvaia, *Change in FEV1 over time in COPD*. *The New England journal of medicine*, 2011. **365**(26): p. 2540; author reply 2541.

194. Celli, B.R., et al., *Predictors of Survival in COPD: more than just the FEV1*. Respiratory medicine, 2008. **102 Suppl 1**: p. S27-35.
195. Burtscher, M., et al., *Intermittent hypoxia increases exercise tolerance in patients at risk for or with mild COPD*. Respiratory physiology & neurobiology, 2009. **165**(1): p. 97-103.
196. Shavelle, R.M., et al., *Life expectancy and years of life lost in chronic obstructive pulmonary disease: findings from the NHANES III Follow-up Study*. International journal of chronic obstructive pulmonary disease, 2009. **4**: p. 137-48.
197. Bonarius, H.P., et al., *Antinuclear autoantibodies are more prevalent in COPD in association with low body mass index but not with smoking history*. Thorax, 2011. **66**(2): p. 101-7.
198. Sullivan, A.K., et al., *Oligoclonal CD4+ T cells in the lungs of patients with severe emphysema*. American journal of respiratory and critical care medicine, 2005. **172**(5): p. 590-6.
199. Brandsma, C.A., et al., *Induction of autoantibodies against lung matrix proteins and smoke-induced inflammation in mice*. BMC pulmonary medicine, 2010. **10**: p. 64.
200. Overbeek, S.A., et al., *Cigarette smoke-induced collagen destruction; key to chronic neutrophilic airway inflammation?* PloS one, 2013. **8**(1): p. e55612.
201. Valesini, G., et al., *Citrullination and autoimmunity*. Autoimmunity reviews, 2015. **14**(6): p. 490-7.
202. Pruijn, G.J., *Citrullination and carbamylation in the pathophysiology of rheumatoid arthritis*. Frontiers in immunology, 2015. **6**: p. 192.
203. Klareskog, L. and A.I. Catrina, *Autoimmunity: lungs and citrullination*. Nature reviews. Rheumatology, 2015. **11**(5): p. 261-2.
204. Bieber, V., et al., *Autoimmune smoke and fire--coexisting rheumatoid arthritis and chronic obstructive pulmonary disease: a cross-sectional analysis*. Immunologic research, 2013. **56**(2-3): p. 261-6.
205. Khandpur, R., et al., *NETs are a source of citrullinated autoantigens and stimulate inflammatory responses in rheumatoid arthritis*. Science translational medicine, 2013. **5**(178): p. 178ra40.
206. Sohn, D.H., et al., *Local Joint Inflammation and Histone Citrullination in a Murine Model of the Transition From Preclinical Autoimmunity to Inflammatory Arthritis*. Arthritis & rheumatology, 2015. **67**(11): p. 2877-87.
207. Wigerblad, G., et al., *Autoantibodies to citrullinated proteins induce joint pain independent of inflammation via a chemokine-dependent mechanism*. Annals of the rheumatic diseases, 2015.
208. Hoonhorst, S.J., et al., *Increased activation of blood neutrophils after cigarette smoking in young individuals susceptible to COPD*. Respiratory research, 2014. **15**: p. 121.
209. Baraldo, S., G. Turato, and M. Saetta, *Pathophysiology of the small airways in chronic obstructive pulmonary disease*. Respiration; international review of thoracic diseases, 2012. **84**(2): p. 89-97.
210. Vlahos, R. and S. Bozinovski, *Recent advances in pre-clinical mouse models of COPD*. Clinical science, 2014. **126**(4): p. 253-65.

211. Hemminki, K., et al., *Subsequent COPD and lung cancer in patients with autoimmune disease*. The European respiratory journal, 2011. **37**(2): p. 463-5.
212. Hacker, S., et al., *Increased soluble serum markers caspase-cleaved cytokeratin-18, histones, and ST2 indicate apoptotic turnover and chronic immune response in COPD*. Journal of clinical laboratory analysis, 2009. **23**(6): p. 372-9.
213. Yang, C.L., et al., *Autoantibodies to cartilage collagens in relapsing polychondritis*. Archives of dermatological research, 1993. **285**(5): p. 245-9.
214. Xu, Q. and K.S. Lam, *Protein and Chemical Microarrays-Powerful Tools for Proteomics*. Journal of biomedicine & biotechnology, 2003. **2003**(5): p. 257-266.
215. Urbanowska, T., et al., *Protein microarray platform for the multiplex analysis of biomarkers in human sera*. Journal of immunological methods, 2006. **316**(1-2): p. 1-7.

